

AD-A078 624

COLORADO STATE UNIV FORT COLLINS

F/G 4/2

TROPICAL CYCLONE ORIGIN, MOVEMENT, AND INTENSITY CHARACTERISTIC--ETC(U)

AUG 79 W M GRAY

N00228-76-C-2129

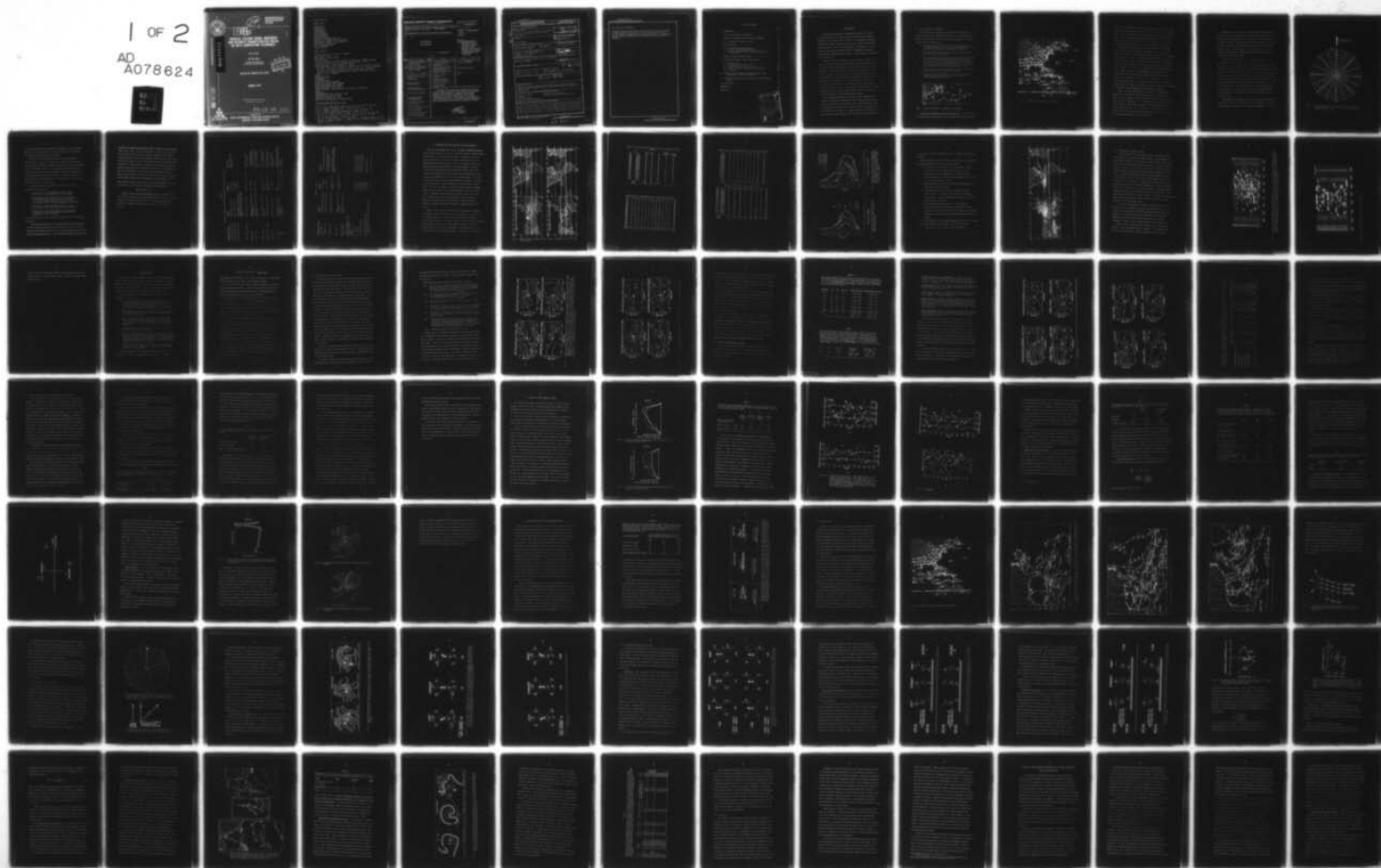
UNCLASSIFIED

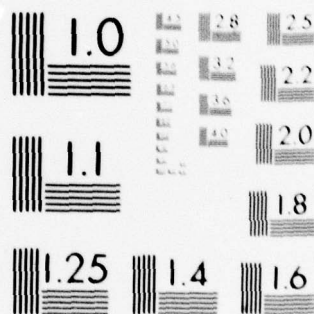
NEPRF-CR-79-06

NL

1 OF 2

AD
A078624





MICROCOPY RESOLUTION TEST CHART
NATIONAL BUREAU OF STANDARDS-1963-A



NAVENVPREDRSCHFAC CR 79-06

ADA 078624

12

NAVENVPREDRSCHFAC
CONTRACTOR REPORT
CR 79-06

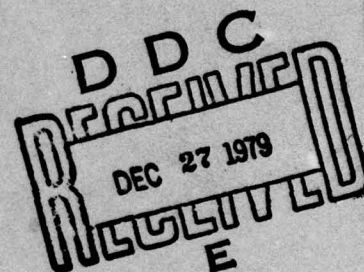
LEVEL II

TROPICAL CYCLONE ORIGIN, MOVEMENT AND INTENSITY CHARACTERISTICS BASED ON DATA COMPOSITING TECHNIQUES

Prepared By:

W. M. Gray

Colorado State University
Fort Collins, Colorado 80523



Contract No. N00228-76-C-2129

AUGUST 1979

APPROVED FOR PUBLIC RELEASE
DISTRIBUTION UNLIMITED

79-12 27 120

Prepared For:

NAVAL ENVIRONMENTAL PREDICTION RESEARCH FACILITY
MONTEREY, CALIFORNIA 93940



DDC FILE COPY

Distribution:

SNDL, Part 1

CINCLANTFLT
CINCPACFLT
COMSECONDFLT
COMTHIRDFLT
COMSEVENTHFLT
COMPHIBGRUPAC
COMPHIBGRULANT
AIRCRAFT CARRIER LANT/PAC
AMPHIBIOUS COMMAND SHIP LANT/PAC
AMPHIBIOUS ASSAULT SHIP LANT/PAC
DESTROYER TENDER LANT
MISC. COMMAND SHIP
CINCPAC (J37)

SNDL, Part 2

Special Asst. to the Asst. SECNAV
CNR (Code 734)
ONR (Codes, 100B1, 465)
CNO (OP-952)
Special Agencies, Staffs, Board, & Committees (NMCC-Weather
Element, Dep. Dir. for Operations for Env. Serv.)
Naval Personnel at DOD Agencies (NOAA)
NAVOCEANCOMDET (Guam, Asheville, Barbers Pt., Beeville, Atsugi,
Bermuda, Charleston, Corpus Christi, Cubi Pt., Guantanamo Bay,
Key West, Kingsville, Mayport, Milton, Midway, Misasa,
New Orleans, Offutt AFB, Roosevelt Roads, Virginia Beach,
Diego Garcia, Kadena)
NORDA
COMNAVOCEANCOM
NAVOCEANO
FLENUMOCEANCEN
NAVEASTOCEANCEN NORFOLK
NAVWESTOCEANCEN PEARL HARBOR
NAVPOlarOCEANCEN SUITLAND
NAVOCEANCOMCEN (Guam, Rota)
NAVOCEANCOMFAC (Jacksonville, San Diego, Yokosuka)
USNA
NAVWARCOL
NAVAIRSYSCOM (Air-954, Air-370)
PACMISTESTCEN (Code 3250)
NAVPGSCOL (Codes 63, 68)
MCAS (Okinawa, Iwakuni, Kaneohe Bay)

NAVENVPREDRSCHFAC Master List

List 3, U.S. Air Force: Items 1, 4, 12, 13, 14, 15, 16, 17.
List 5, Other DOD Agencies: Items 1, 2, 5.
List 7, NOAA: Items 1, 2, 3, 7, 8, 9, 11, 14, 16, 18.
List 8, Other Government Agencies: Items 1, 2, 4.
List 9, U.S. Universities: Items 1, 3, 4, 5, 6, 7, 8, 9, 10,
11, 12, 13, 15, 17, 18, 19, 20, 22, 24, 26, 27, 30, 48.
List 11, Miscellaneous: Items 1, 2, 4.
List 12, Foreign Addresses: Items AUS-2, 3; CAN-1; ENG-1, 2, 11;
GER-1, 2; HGKG-1; IND-1, 4; JAP-1, 2, 4, 7; NZEA-1; PHI-1, 2, 4;
TAI-1, 2, 3.

ROUTINE REPLY, ENDORSEMENT, TRANSMITTAL OR INFORMATION SHEET
OPNAV 5216/158 (Rev. 1 77)

A WINDOW ENVELOPE MAY BE USED
Formerly NAVJAGS 1989

CLASSIFICATION (UNCLASSIFIED when detached from enclosures, unless otherwise indicated)

UNCLASSIFIED

FROM (Show telephone number in addition to address)

Commanding Officer, Naval Environmental Prediction Research
Facility, Monterey, CA 93940 AVN 878-2837

DATE

14 NOV 1979

SUBJECT

NAVENVPREDRSCHFAC technical publication; forwarding of

SERIAL OR FILE NO

5600

NEPRF/SBB:sb

Ser: 500

REFERENCE

Distribution
(on reverse)

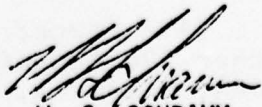
ENCLOSURE

(1) NAVENVPREDRSCHFAC
Contractor Report
CR 79-06: Tropical
Cyclone Origin,
Movement and Intensity
Characteristics based
on Data Compositing
Techniques

VIA:

ENDORSEMENT ON

☒ FORWARDED ☐ RETURNED ☐ FOLLOW-UP, OR TRACER ☐ REQUEST ☐ SUBMIT ☐ CERTIFY ☐ MAIL ☐ FILE

GENERAL ADMINISTRATION		CONTRACT ADMINISTRATION		PERSONNEL	
FOR APPROPRIATE ACTION		NAME & LOCATION OF SUPPLIER OF SUBJECT ITEMS		REPORTED TO THIS COMMAND:	
UNDER YOUR COGNIZANCE		SUBCONTRACT NO. OF SUBJECT ITEM			
<input checked="" type="checkbox"/> INFORMATION & retention		APPROPRIATION SYMBOL, SUBHEAD, AND CHARGEABLE ACTIVITY		DETACHED FROM THIS COMMAND	
APPROVAL RECOMMENDED <input type="checkbox"/> YES <input type="checkbox"/> NO		SHIPPING AT GOVERNMENT EXPENSE <input type="checkbox"/> YES <input type="checkbox"/> NO		OTHER	
<input type="checkbox"/> APPROVED <input type="checkbox"/> DISAPPROVED		A CERTIFICATE, VICE BILL OF LADING			
COMMENT AND/OR CONCURRENCE		COPIES OF CHANGE ORDERS, AMENDMENT OR MODIFICATION			
CONCUR		CHANGE NOTICE TO SUPPLIER			
LOANED, RETURN BY:		STATUS OF MATERIAL ON PURCHASE DOCUMENT			
SIGN RECEIPT & RETURN		REMARKS (Continue on reverse)			
REPLY TO THE ABOVE BY:					
REFERENCE NOT RECEIVED					
SUBJECT DOCUMENT FORWARDED TO:					
SUBJECT DOCUMENT RETURNED FOR:					
SUBJECT DOCUMENT HAS BEEN REQUESTED, AND WILL BE FORWARDED WHEN RECEIVED					
COPY OF THIS CORRESPONDENCE WITH YOUR REPLY					
ENCLOSURE NOT RECEIVED					
ENCLOSURE FORWARDED AS REQUESTED		 W. G. SCHRAMM			
ENCLOSURE RETURNED FOR CORRECTION AS INDICATED					
CORRECTED ENCLOSURE AS REQUESTED					
REMOVE FROM DISTRIBUTION LIST REDUCE DISTRIBUTION AMOUNT TO					

COPY TO

CLASSIFICATION (UNCLASSIFIED when detached from enclosures, unless otherwise indicated)

UNCLASSIFIED

UNCLASSIFIED

SECURITY CLASSIFICATION OF THIS PAGE (When Data Entered)

REPORT DOCUMENTATION PAGE		READ INSTRUCTIONS BEFORE COMPLETING FORM
1. REPORT NUMBER NAVENVPREDRSCHFAC Contractor Report CR 79-06	2. GOVT ACCESSION NO.	3. RECIPIENT'S CATALOG NUMBER
4. TITLE (and Subtitle) 6 Tropical Cyclone Origin, Movement, and Intensity Characteristics Based on Data Compositing Techniques	5. TYPE OF REPORT & PERIOD COVERED 9 Final rept.	
7. AUTHOR(s) 10 William M. Gray	8. CONTRACT OR GRANT NUMBER(s) 15 N00228-76-C-2129 NEPRF WU 6.2-14	
9. PERFORMING ORGANIZATION NAME AND ADDRESS Colorado State University Fort Collins, CO 80523 12 128	10. PROGRAM ELEMENT, PROJECT, TASK AREA & WORK UNIT NUMBERS PE 62759N PN WF52551792	
11. CONTROLLING OFFICE NAME AND ADDRESS Commander, Naval Air Systems Command Department of the Navy Washington, DC 20361 088 300	12. REPORT DATE 11 Aug 79	
14. MONITORING AGENCY NAME & ADDRESS (if different from Controlling Office) Naval Environmental Prediction Research Facility Monterey, CA 93940	13. NUMBER OF PAGES 26	
15. SECURITY CLASS. (of this report) UNCLASSIFIED		18 NEPRF
16. DISTRIBUTION STATEMENT (of this Report) Approved for public release; distribution unlimited. 16 F52551 17 WF52551792		
17. DISTRIBUTION STATEMENT (of the abstract entered in Block 20, if different from Report) 19 CR-79-06		
18. SUPPLEMENTARY NOTES Additional funding for the research reported herein was supplied by the National Science Foundation and the National Oceanographic and Atmospheric Administration.		
19. KEY WORDS (Continue on reverse side if necessary and identify by block number) Tropical cyclones Typhoons Data compositing Tropical cyclone forecasting Tropical cyclone modeling Tropical cyclone observational studies		
20. ABSTRACT (Continue on reverse side if necessary and identify by block number) Up-to-date results of recent tropical cyclone research at Colorado State University are presented. Particular attention is paid to new findings which impact on tropical cyclone analysis and forecasting efforts. Observational studies using large amounts of composited rawinsonde, satellite, and aircraft flight data have been performed to analyze global aspects of tropical cyclone occurrences, physical processes of tropical cyclone genesis, tropical cyclone		

DD FORM 1473
1 JAN 73EDITION OF 1 NOV 65 IS OBSOLETE
S/N 0102-014-6601

UNCLASSIFIED

SECURITY CLASSIFICATION OF THIS PAGE (When Data Entered)

088 300

set

UNCLASSIFIED

SECURITY CLASSIFICATION OF THIS PAGE(When Data Entered)

20. Abstract (Continued)

Cont → intensity change, environmental factors influencing tropical cyclone turning motion 24-36 hours before the turn takes place, tropical cyclone intensity determination from upper tropospheric reconnaissance, and the diurnal variations of vertical motion in tropical weather systems. ↗

UNCLASSIFIED

SECURITY CLASSIFICATION OF THIS PAGE(When Data Entered)

TABLE OF CONTENTS

	Page
1. INTRODUCTION	1
1.1 Data and Analysis Techniques	2
2. STATISTICS ON GLOBAL TROPICAL CYCLONE OCCURRENCE	11
2.1 Clustering of Cyclones in Time.	18
3. CYCLONE GENESIS.	22
3.1 Individual Day Cyclone Genesis	24
3.2 Atlantic Non-developing Systems	28
3.3 Pacific Pretyphoon Versus Non-developing Cloud Clusters	35
4. TROPICAL CYCLONE INTENSITY CHANGE	40
5. FORECASTING TROPICAL CYCLONE TURNING MOTION	54
5.1 Composite Data.	57
5.2 Surrounding Flow at Turn Time	63
5.3 Surrounding Flow Before Turn Time	69
5.4 Study of Satellite Temperature Sounding Data	76
5.5 Discussion	84
6. TROPICAL CYCLONE INTENSITY DETERMINATION FROM UPPER TROPOSPHERIC AIRCRAFT RECONNAISSANCE	87
7. DIURNAL VARIATIONS OF VERTICAL MOTION IN TROPICAL WEATHER SYSTEMS	100
ACKNOWLEDGEMENTS	112
BIBLIOGRAPHY	113
APPENDIX A	119

Accession For	
NTIS	<input checked="" type="checkbox"/>
DDC TAB	<input type="checkbox"/>
Unannounced	<input type="checkbox"/>
Justification	
By	
Distribution/	
Availability Codes	
Dist	Avail and/or special
A	

1. INTRODUCTION

The author has undertaken a comprehensive study of the origins and characteristics of tropical cyclones. Many of these results are believed to be relevant to the U.S. Navy for forecasting and numerical simulations of these storms, and this report is issued to disseminate this information. This is the third report on this subject. Previous reports by Gray and Frank (1977, 1978) give additional information. This research includes composite studies of large amounts of rawinsonde and satellite data.

Section 2 presents information on global tropical cyclone occurrence. Section 3 discusses current research on cyclone genesis and a suggested parameter which might be used to operationally forecast this phenomena. Section 4 gives new information on the intensity change of tropical cyclones. Section 5 discusses tropical cyclone motion and gives information on how cyclone turning motion can be anticipated from surrounding flow parameters 24 to 36 hours before it takes place. Section 6 discusses new ways to determine tropical cyclone intensity. The last section discusses the large diurnal variations which are being observed in tropical weather system vertical motion. Other tropical cyclone information is also presented and discussed.

More detailed information is contained in the Colorado State University Department of Atmospheric Science tropical cyclone project reports of Gray, 1975a, 1975b; George, 1975; Frank, 1976; Zehr, 1976; S. Erickson, 1977; Arnold, 1977; and other papers by Frank, 1977a, b, c; Gray, 1975a, b; Gray, 1977a, b, c; Núñez and Gray, 1977; McBride and Gray, 1978; Gray, 1979; McBride, 1979; and Chan, Gray and Kidder, 1979.

1.1 Data and Analysis Techniques

The information in this paper is taken from various studies of tropical cyclones using composited rawinsonde data, climatological information, NOAA flight data and DMSP satellite photographs. The data sources used are listed below:

- 1) Fourteen years (1957-1970) of N.W. Pacific rawinsonde data ($\sim 18,000$ soundings) from 30 stations as shown in Fig. 1. This data sample is currently being expanded to 20 years.
- 2) Twenty-two years (1956-1977) of N. Atlantic rawinsonde data from the stations shown in Fig. 2.
- 3) Five years (1971-1975) of direct read-out satellite photographs from Guam Defense Meteorological Satellite Program (DMSP) of tropical cyclones and cloud clusters in the N.W. Pacific. This $1/3$ nautical mile resolution data has been digitized and composited to perform quantitative analyses of the convection associated with West Pacific tropical weather systems.
- 4) All of the Joint Typhoon Warning Center (JTWC), Guam typhoon summaries for the 32-year period of 1946-1977.
- 5) Seasonal sea-surface temperature and thermocline data in 5° mardsen squares for the whole Pacific as furnished by the Navy Oceanographic Office.

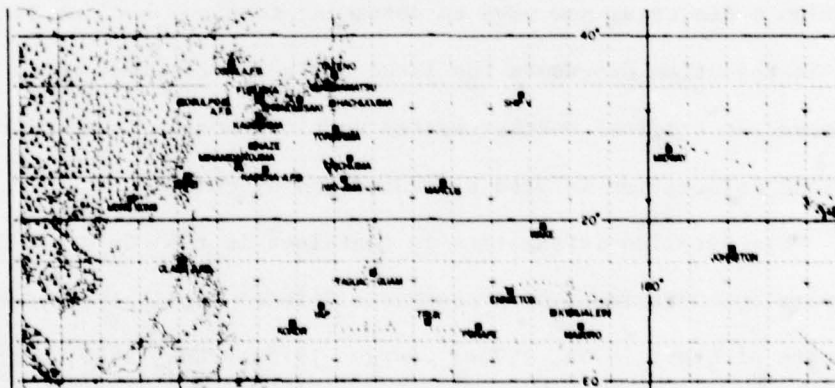


Fig. 1. Western North Pacific rawinsonde data network.

Rawinsonde Compositing Philosophy and Technique. Tropical cyclones and cloud clusters spend most of their lifetimes over the warm tropical

Fig. 2. North Atlantic Rawinsonde Data Network.

oceans. Traditional data sources are very sparse in such regions, and daily tropical weather analyses are notoriously unreliable. The severe winds found in tropical cyclones further reduce the availability of such data. It is not possible to obtain enough rawinsonde data or surface observations around any individual storm or cluster at one time period to permit quantitative analysis of structure, dynamics or energetics.

Aircraft data have provided the best information concerning the activities in the intense central core regions of tropical cyclones. There are a number of case studies of individual storms based on Northwest Atlantic hurricane flight data (Riehl and Malkus, 1961; Miller, 1962; Gray, 1962, 1967; LaSeur and Hawkins, 1963; Sheets, 1967a, 1967b, 1968; Hawkins and Rubsam, 1968; Hawkins and Imbembo, 1976) and also statistical treatments of the flight data (Shea and Gray, 1973; Gray and Shea, 1973). However, logistical considerations have limited the ability of aircraft to provide information concerning the outer convective regions of the storm and its broader scale environment. Aircraft data also have been limited to a few flight levels per storm time period due to the usually low number of available aircraft, maximum aircraft ceilings of 200 mb or less, and dangerous low level flight conditions.

None of the above data sources can produce an accurate vertical profile of the radial wind pattern around a system. Without such a profile it is impossible to compute meaningful budgets of energy, water vapor, momentum, vorticity, etc. In addition, vertical profiles of the other dynamic and thermodynamic variables cannot be determined fully over the mesoscale area. It is necessary to composite very large amounts of data from many similar weather systems at many time periods to obtain meaningful quantitative measurements.

Although the extreme variabilities and individual asymmetries of tropical cyclones and cloud clusters are well known, the nature of the basic dynamic and energetic processes which govern these systems must be largely invariant. Compositing allows quantitative analyses of these features. Any compositing system smoothes out many of the individual characteristics of single systems, but a great deal of information concerning asymmetrical or "eddy" qualities can be deduced by the use of proper data handling techniques.

Compositing was performed on a 15° latitude radius cylindrical grid extending from sea level to 50 mb. The system circulation center was located at each time period using JTWC and NOAA Miami reports and/or satellite photographs, and the grid was positioned with the system at grid center of the lowest level. Whenever available rawinsonde soundings fell on the grid at a given time period for a given storm, each sounding was located relative to the storm center in cylindrical coordinates. Figure 3 shows the grid and the number of soundings per grid space for a typical stratification. All of the parameters to be composited, whether directly measured or computed from the directly measured parameters, were determined at the observation station locations at 21 vertical pressure levels.

The geographical alignment of the grid varied with the coordinate system used. After all parameters were either measured or computed for each sounding, the value of each parameter was assigned to a point at

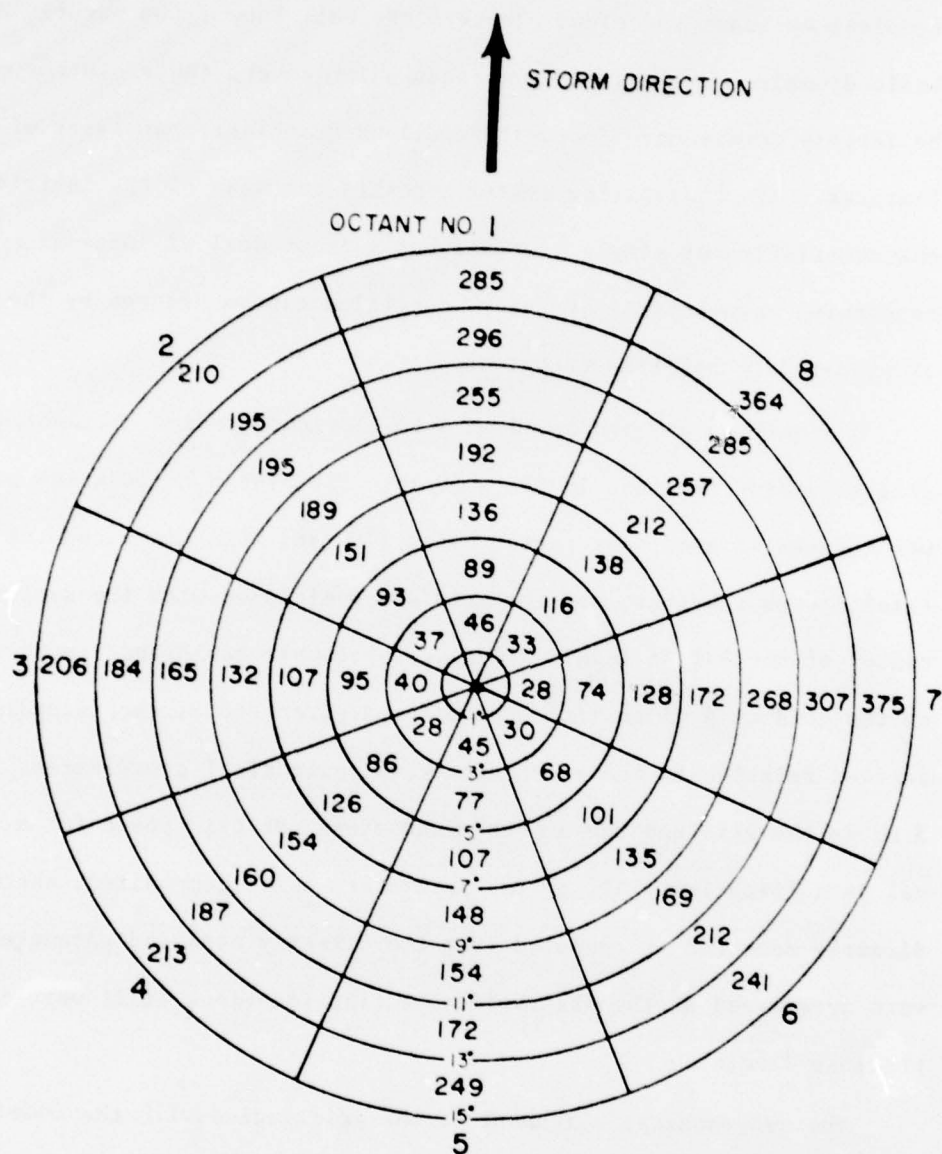


Fig. 3. Compositing grid (15° latitude radius) with the number of rawinsonde reports in each octant and each 2° radial band for a typical stratification.

the center of the grid box in which the sounding fell. All soundings which fell in that grid space for the particular group of storms and time periods being analyzed were composited.

The data set was sufficiently large to allow compositing of various subsets. Data could be grouped according to any characteristics observed in individual systems such as location, season, intensity, motion, or intensity tendency. By comparing the composites of different types of systems it was possible to quantitatively analyze the persistent differences between the groups. It was also possible to remove obviously atypical systems or time periods from a data group to improve the quality of the data set.

Rawinsonde compositing procedures involve the use of four separate reference frames:

- 1) With respect to the instantaneously fixed cyclone center in a N-S or geographical coordinate system.
- 2) With respect to the cyclone center in a geographical coordinate system with the cyclone motion subtracted out of all the winds (portrayal of data relative to the moving cyclone center in geographical coordinates).
- 3) With respect to the instantaneously fixed cyclone center and the direction to which the storm is moving.
- 4) With respect to the cyclone center and the direction to which the storm is moving with the cyclone motion subtracted out of all the winds.

See our other project reports for more information on this compositing procedure.

The relative positions of the system and the balloon changed due to their respective motions during the balloon's ascent time. These motions were estimated from the data, and the positions of each were corrected at each pressure level. In this study horizontal eddy fluxes were

estimated by compositing individual fluxes of quantities and comparing them to mean fluxes. The radial winds were initially composited and mass balanced from the surface to 100 mb by adding a small constant correction factor (ΔV_r) to each individual radial wind value in a given radial band. Changes in mass of the volume within the radial band were neglected. For each sounding the product of the corrected V_r and the quantity being analyzed was computed at each level. Such products for all of the soundings in an octant were then composited as before, giving a mean transport value for each octant at each level, $\overline{V_r Q}$, where the bar denotes time and space averaging of the $V_r \cdot Q$ products. By subtracting the product of the mean $\overline{V_r}$ and the mean quantity (\overline{Q}) one could achieve a good estimate of horizontal eddy transport:

$$\overline{V_r' Q'} \approx \overline{V_r \cdot Q} - \overline{V_r} \cdot \overline{Q}$$

Summary of Recent and Current Research Projects. Table 1 shows the tropical cyclone research projects which are either now in progress or have been completed since 1972 at CSU. Some of the more useful findings for operational purposes are summarized in the following chapters.

TABLE 1

Recently Completed and Current Tropical Cyclone Research Projects

<u>Completed Studies</u>	<u>Subject</u>	<u>Region</u>	<u>Data Set</u>
(Shea and Gray, 1973)	Inner Core Structure	N. Atlantic	NOAA flight data 1957-67
(Gray and Shea, 1973)	Inner Core Structure	N. Atlantic	" " "
(Gray and Shea, 1976)	Data Summary of NOAA's Hurricane Inner-core Radial Leg Flight Penetrations 1957-1967, 1969	N. Atlantic	" " "
Gray, (1975a, 1975b)	Tropical Cyclone Genesis	Global and N.W. Pacific	Numerous Climatological Sources
Frank, 1976	Tropical Cyclone Structure and Energetics	N.W. Pacific	~18,000 Rawinsonde Soundings (1961-1970)
Arnold, 1977	Cyclone Intensity from Satellite Data	N.W. Pacific	1971-75 DMSP Satellite Data plus Rawinsonde Data
Frank, 1977b, c	Eddy Processes in Tropical Cyclones	N.W. Pacific and W. Atlantic	10 yrs. Pacific and 14 yrs. Atlantic Data
Núñez and Gray, 1977	Tropical Cyclone Structure	N.W. Pacific and W. Atlantic	10 yrs. Pacific and 14 yrs. Atlantic Data
George, 1975	Tropical Cyclone Motion	N.W. Pacific	~18,000 Soundings (1961-1970)
Gray, 1977a 1977b 1977c	Tropical Cyclone Genesis Measurement of Cyclone Intensity Cyclone Motion	Global N.W. Pacific and Atlantic N.W. Pacific and Atlantic	Rawinsonde and Satellite Rawinsonde and Aircraft Data Rawinsonde

TABLE 1 (cont'd)

<u>Completed Studies</u>	<u>Subject</u>	<u>Region</u>	<u>Data Set</u>
Zehr, 1976	Tropical Cyclone Genesis	N.W. Pacific	~ 20,000 Soundings (1961-1970)
Erickson, 1977	Tropical Cyclone Genesis	N.W. Pacific	1971-75 DMSP Satellite Data Plus Rawinsonde Data
McBride, 1979	Tropical Cyclone Genesis	N.W. Pacific and W. Atlantic	N.W. Pacific and W. Atlantic Rawinsonde plus NOAA Satellite Data
Gray, 1979	Global Aspects of Tropical Cyclones	N.W. Pacific and W. Atlantic	
Chan, Gray, and Kidder, 1979	Tropical Cyclone Turning Motion		
<u>Current Tropical Cyclone Research Studies</u>			
<u>Subject</u>			
1) Structure		N. Atlantic	Soundings from 1956-77
2) Motion		N. Atlantic	Soundings from 1956-77
3) Genesis		N. Atlantic	Soundings from 1956-77
4) Intensity Change		N. Atlantic N.W. Pacific	Soundings from 1957-70
5) Satellite Applicability		N.W. Pacific	DMSP (1971-1975)
6) Numerical Modeling of Tropical Cyclone Genesis			

2. STATISTICS ON GLOBAL TROPICAL CYCLONE OCCURRENCE

There are approximately 80 tropical cyclones of maximum sustained winds of 20-25 m/s which occur over the globe per year. Figure 4 shows the location of the initial genesis point of cyclones for a 20-year period. About half to two-thirds of these cyclones reach hurricane strength (maximum sustained winds > 33 m/s). As shown by Table 2, the year to year percentage variation in the global number of tropical cyclones over the last 20 years has ranged from -13% to +23%. The average annual variation is only 8 percent which, considering the individual ocean basin variation of cyclones, is quite small. This table also gives the Northern and Southern Hemisphere occurrences. The ratio of yearly Northern to Southern Hemispheric cyclone frequency varied from 1.5 to 4.0. The numbers of tropical cyclone formations by month and year for the Northern and Southern Hemisphere are given in Tables 3 and 4. Individual monthly variation is large. About 3½ times as many cyclones occur in August and September as in April and May. Individual ocean basins can have wide year to year differences in cyclone occurrences as indicated in Table 5. Basins are defined in Fig. 5.

Figures 6 and 7 show the variation of cyclone initial occurrence by latitude. Note that only about 13% of cyclones form poleward of 20° latitude and nearly all of these occur in the Northern Hemisphere. Large land-sea monsoonal influences do not occur in the Southern Hemisphere and the poleward penetration of the Equatorial Trough is much more restricted than in the Northern Hemisphere. About two-thirds of all cyclones occur in the Northern Hemisphere. Similarly, about two-thirds

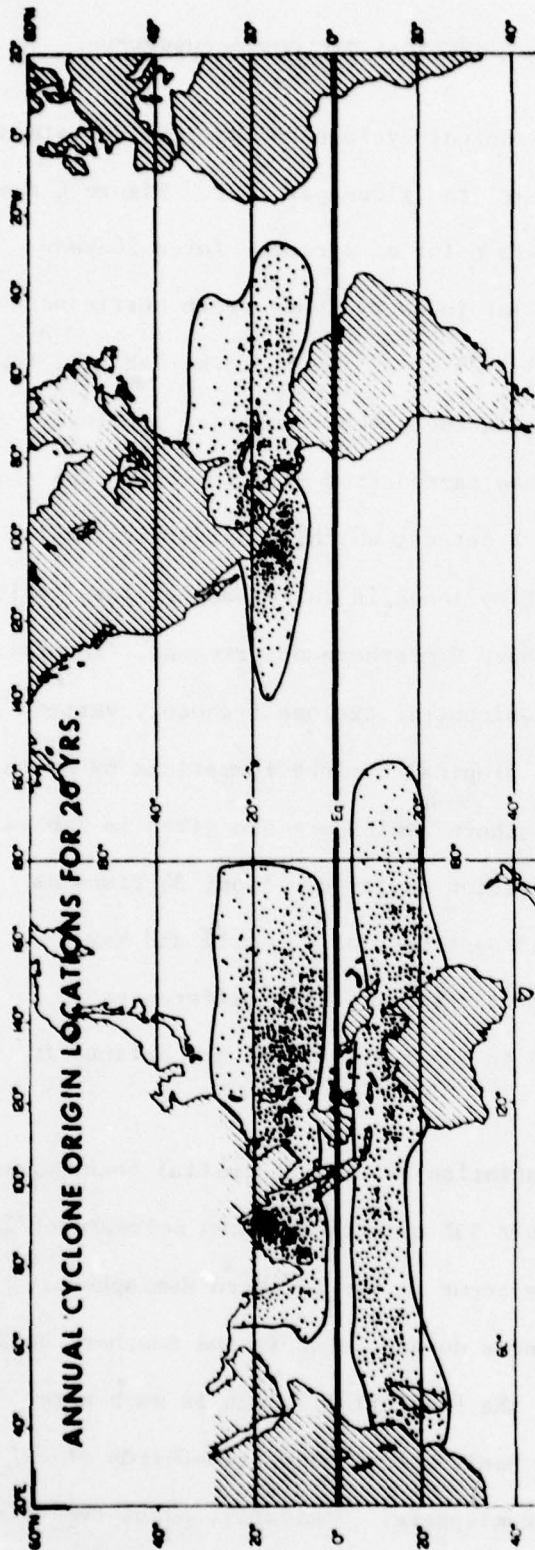


Fig. 4. Annual cyclone origin locations for 20 years.

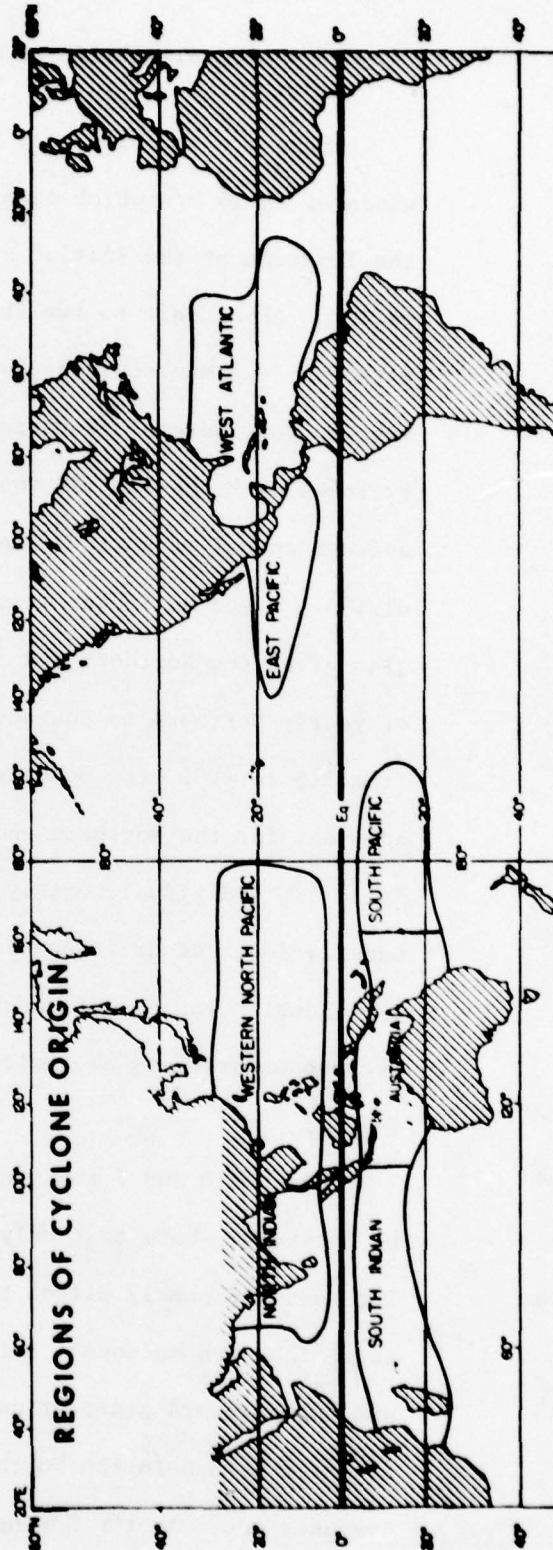


Fig. 5. Regions of cyclone origin.

TABLE 2 LAST 20 YEARS' STATISTICS ON TROPICAL CYCLONE ACTIVITY IN NORTHERN AND SOUTHERN HEMISPHERES

NH.	Year	SH.	No. of cyclones NH.	SH.	Total	% deviation from 20 yr average	Ratio NH. to SH.
1958	1958-59		52	25	77	3	2.1
1959	1959-60		48	21	69	13	2.3
1960	1960-61		48	22	70	12	2.2
1961	1961-62		58	23	81	+2	2.5
1962	1962-63		50	30	80	+1	1.7
1963	1963-64		49	23	72	-9	2.1
1964	1964-65		65	19	84	+6	3.4
1965	1965-66		56	22	78	-1	2.5
1966	1966-67		64	16	78	-1	4.0
1967	1967-68		63	28	91	-15	2.2
1968	1968-69		61	23	84	+6	2.6
1969	1969-70		49	23	72	-9	2.1
1970	1970-71		56	26	82	+4	2.1
1971	1971-72		70	27	97	+23	2.6
1972	1972-73		54	35	91	-15	1.5
1973	1973-74		46	28	74	-6	1.6
1974	1974-75		55	19	75	-5	2.9
1975	1975-76		47	29	76	-4	1.6
1976	1976-77		55	30	85	+7	1.8
1977	1977-78		47	20	67	-15	2.3
Total Average			1093 54.6	489 24.5	1583 79.1	± 8	2.3

TABLE 3 FREQUENCY OF NORTHERN HEMISPHERE TROPICAL CYCLONE GENESIS BY YEAR AND MONTH

Year	Jan.	Feb.	Mar.	Apr.	May	June	July	Aug.	Sep.	Oct.	Nov.	Dec.	Total
1958	1	0	0	0	2	5	10	9	11	9	4	1	52
1959	0	0	0	1	2	6	7	11	9	8	2	2	48
1960	0	0	0	1	3	7	6	14	6	8	2	1	48
1961	1	1	1	1	4	5	10	5	14	9	6	1	58
1962	0	1	0	1	3	2	7	11	11	7	4	3	50
1963	0	0	0	1	3	5	6	5	14	11	0	4	49
1964	0	0	0	0	3	4	11	15	12	8	10	2	65
1965	2	2	1	1	4	8	8	8	12	3	4	3	56
1966	0	0	0	2	2	3	9	13	20	5	7	3	64
1967	2	1	1	1	2	4	10	12	12	13	3	2	63
1968	0	0	0	1	2	5	7	17	11	11	6	1	61
1969	1	0	1	1	1	0	7	13	10	9	4	2	49
1970	0	1	0	0	4	6	11	10	9	8	7	0	56
1971	1	0	1	3	7	3	15	11	15	9	4	1	70
1972	1	0	0	1	4	2	9	12	12	6	4	3	54
1973	0	0	0	0	0	5	12	8	8	7	5	1	46
1974	1	0	0	2	4	6	5	14	13	6	4	0	55
1975	2	0	0	0	2	3	6	11	9	8	6	0	47
1976	1	1	0	3	2	7	9	15	10	4	0	3	55
1977	0	0	1	0	3	4	8	4	13	9	4	1	47
Total Average	13 0.7	7 0.3	6 0.3	20 1.0	57 2.9	90 4.5	173 8.6	218 10.9	231 11.5	158 7.9	86 4.3	34 1.7	1093 54.6

TABLE 4 FREQUENCY OF SOUTHERN HEMISPHERE TROPICAL CYCLONE GENESIS BY YEAR AND MONTH

Year	Oct.	Nov.	Dec.	Jan.	Feb.	Mar.	Apr.	May	Total
1958-59	1	1	3	5	7	6	2	0	25
1959-60	0	1	4	3	2	7	4	0	21
1960-61	0	1	1	9	7	4	0	0	22
1961-62	0	1	4	6	8	2	2	0	23
1962-63	1	0	4	6	9	5	2	3	30
1963-64	0	1	3	7	3	7	1	1	23
1964-65	0	2	5	4	5	3	0	0	19
1965-66	0	0	3	7	6	6	0	0	22
1966-67	0	1	3	5	1	3	2	1	16
1967-68	0	2	4	8	7	3	4	0	28
1968-69	1	1	3	7	8	2	1	0	23
1969-70	0	1	0	5	6	7	3	1	23
1970-71	1	3	6	4	7	4	1	0	26
1971-72	0	1	6	3	10	3	2	2	27
1972-73	1	3	4	10	6	7	3	1	35
1973-74	1	3	5	7	4	6	2	0	28
1974-75	0	0	2	6	2	5	4	0	19
1975-76	0	4	4	8	5	4	3	1	29
1976-77	1	0	4	8	9	5	3	0	30
1977-78	0	3	4	3	4	4	2	0	20
Total	7	29	72	121	117	93	41	10	489
Average	0.4	1.5	3.6	6.1	5.9	4.7	2.1	0.5	24.5

TABLE 5 YEARLY VARIATION OF TROPICAL CYCLONES BY OCEAN BASIN

Year	SH	NW Atl.	NE Pac.	NW Pac.	N Indian	S Indian	Aust.	S Pac.	Total
1958	1958-59	12	13	22	5	11	11	7	81
1959	1959-60	11	13	18	6	6	13	2	69
1960	1960-61	6	10	28	4	6	8	8	70
1961	1961-62	11	12	29	6	12	7	4	81
1962	1962-63	6	9	30	5	8	17	3	78
1963	1963-64	9	9	25	6	9	7	7	72
1964	1964-65	13	6	39	7	6	9	4	84
1965	1965-66	5	11	34	6	12	7	4	79
1966	1966-67	11	13	31	9	5	5	6	80
1967	1967-68	8	14	35	6	11	9	8	91
1968	1968-69	7	20	27	7	8	7	8	84
1969	1969-70	14	10	19	6	10	7	6	72
1970	1970-71	8	18	23	7	11	12	3	82
1971	1971-72	14	16	34	6	7	14	6	97
1972	1972-73	4	14	28	6	13	12	10	88
1973	1973-74	7	12	21	6	4	16	8	74
1974	1974-75	8	17	23	7	6	10	3	74
1975	1975-76	8	16	17	6	8	16	5	76
1976	1976-77	8	18	24	5	9	12	9	85
1977	1977-78	6	17	19	5	6	7	7	67
Total		176	268	526	121	168	206	118	1583
Average		8.8	13.4	26.3	6.4	8.4	10.3	5.9	79.1

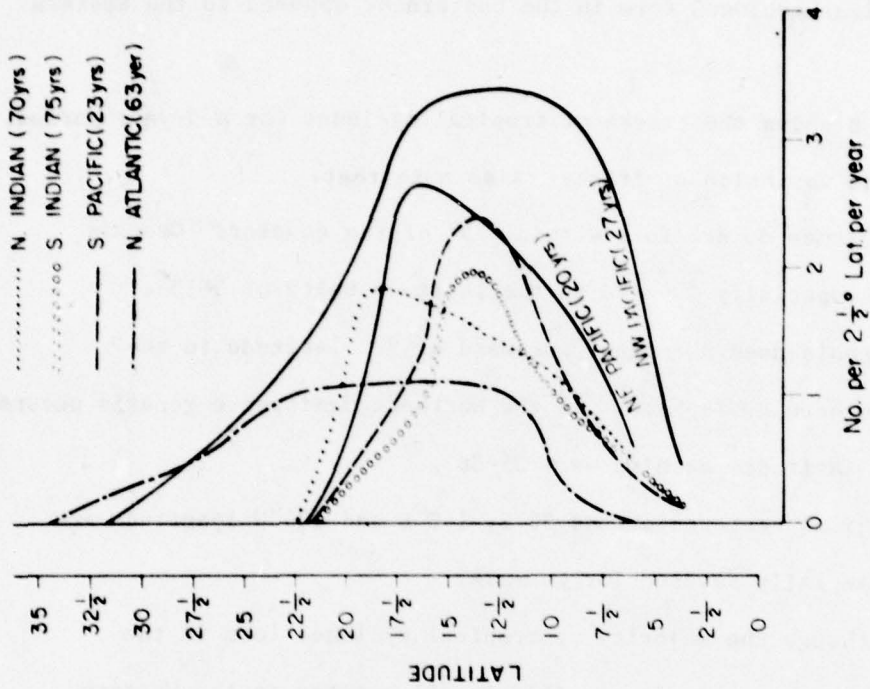


Fig. 7. Latitude at which initial disturbances which later became tropical storms were first detected for the various development regions. Number of years in data average in parenthesis.

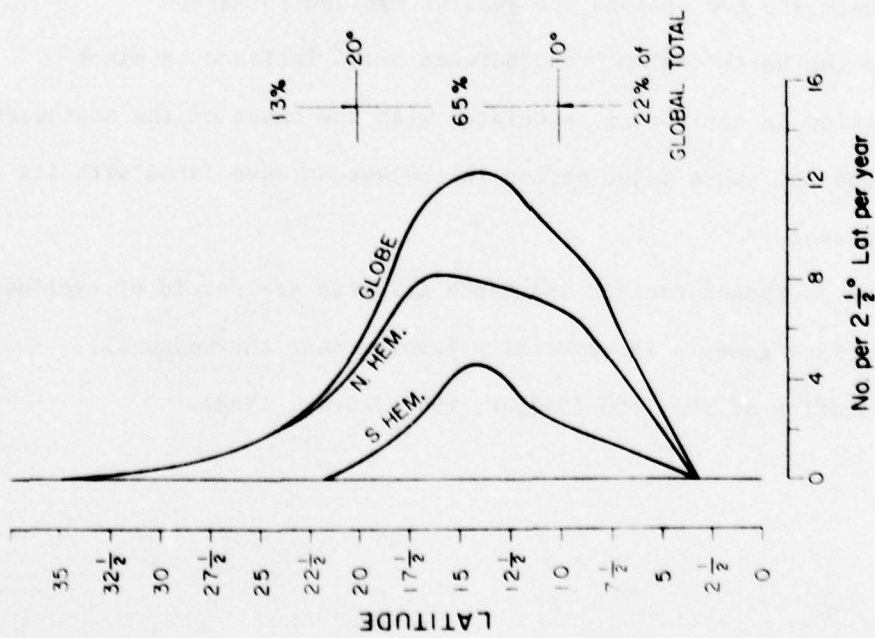


Fig. 6. Latitude at which initial disturbances which later became tropical storms were first detected.

of all tropical cyclones form in the Eastern as opposed to the Western Hemisphere.

Figure 8 shows the tracks of tropical cyclones for a 3-year period. Note the wide variation of tracks. Also note that:

- 1) Cyclones do not form within $4-5^{\circ}$ of the equator. Genesis is especially favored in the latitude belts of $5-15^{\circ}$. Genesis does not occur poleward of 22° latitude in the Southern Hemisphere. In the Northern Hemisphere genesis occurs at latitudes as high as $\sim 35-36^{\circ}$.
- 2) Regions centered around 90°E , 140°E and 105°W longitude are especially favored for genesis.
- 3) Although the majority of tropical cyclones form in the summer, genesis is possible in all seasons in the Western North Pacific. This region has nearly one-third of all the globe's tropical cyclones.
- 4) There are two seasons per year of cyclone formation in the North Indian Ocean between $5-15^{\circ}$ latitude, a minor period in the spring associated with the onset of the southwest monsoon, and a major period in the autumn associated with its retreat.
- 5) The Southeast Pacific and South Atlantic are devoid of cyclones.
- 6) Cyclone genesis is especially favored near the seasonal location of the ITCZ (Sadler, 1967a; Gray, 1968).

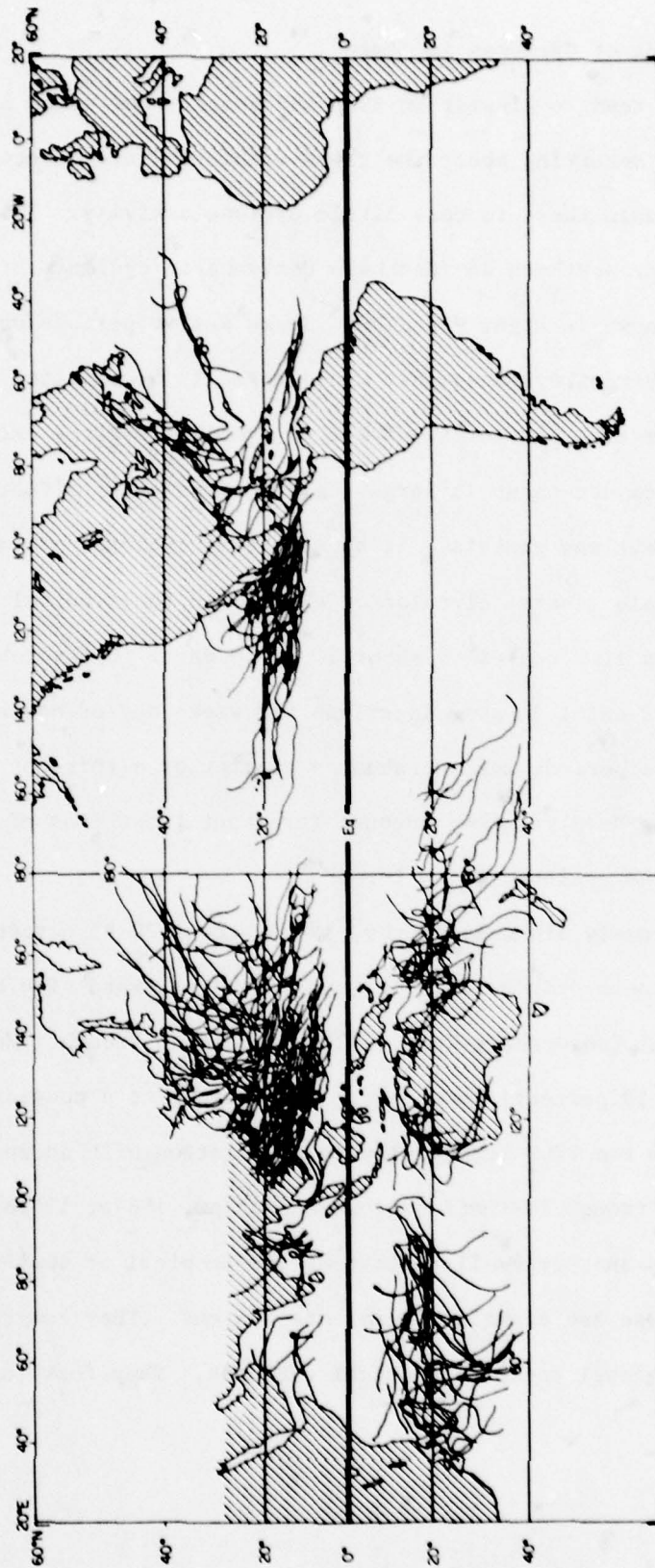


Fig. 8. The tracks of tropical cyclones for a 3-year period.

2.1 Clustering of Cyclones in Time

Cyclones tend to cluster in time and space. One often observes 5-15 cyclones occurring about the globe within 1-2 weeks between 2-3 week periods when there is very little cyclone activity. This clustering in time for Northern and Southern Hemispheric cyclones of the last 20 years is shown in Figs. 9 and 10. These active periods produce 2-6 times the number of cyclones that would normally be expected for that date. Similar time clustering of weaker tropical systems exist most of the time and can occur in large-scale environmental situations not conducive to cyclone genesis. It appears that cyclones are a result of the larger scale general circulation changes in the tropical atmosphere which occur on time scales of about 10 to 20 days. Unfavorable genesis situations can exist in some locations for weeks and/or months. These active genesis periods make up about a quarter or a third of the hurricane-typhoon season days yet they account for about two-thirds of three-quarters of the cyclones which form.

As previously discussed (Gray, 1968), about 80-85 percent of the tropical cyclones originate in or just on the poleward side of the Inter-Tropical Convergence Zone (ITCZ) or doldrum trough. Most of the remainder (~ 15 percent) form in the trade winds at a considerable distance from the ITCZ but usually in association with an upper tropospheric trough to their northwest (Sadler, 1967a, 1967b, 1974).

There is another smaller class of sub-tropical or semi-tropical cyclone. These are anomalous warm core systems. They comprise about 3-5% of the global total of tropical cyclones. They form in sub-

YEAR	APR	MAY	JUN	JUL	AUG	SEP	OCT	NOV	DEC	YEARLY TOTAL
1958	4									6
1959	6									5
1960	3									7
1961	9									58
1962	9									50
1963	7									49
1964	7									4
1965	8									10
1966	8									56
1967	11									64
1968	4									63
1969	7									61
1970	8									49
1971	5									56
1972	2									70
1973	3									54
1974	5									46
1975	5									55
1976	7									47
1977	4									55
										47

Fig. 9. Time and space clustering of Northern Hemisphere cyclone genesis. Numbers in shaded areas give the number of tropical cyclone formations during active genesis periods. Number of formations during inactive periods are also shown in areas without shading. Numbers between arrows indicate the number of cyclone formations before and after the active genesis periods.

	OCT	NOV	DEC	JAN	FEB	MAR	APR	MAY	YEARLY TOTAL
1958-59	3	3	4	0	4	1	5	3	25
1959-60	1	1	4	4	4	0	0	2	21
1960-61	2	2	3	3	3	4	0	0	22
1961-62	1	1	3	2	2	2	6	6	23
1962-63	6	6	4	4	0	0	6	6	30
1963-64	8	8	3	0	0	6	6	6	23
1964-65	12	12	4	4	4	4	3	3	19
1965-66	0	0	4	0	0	0	6	6	22
1966-67									16
1967-68	2	2	3	7	1	7	3	0	28
1968-69	8	8	4	0	0	0	4	4	23
1969-70	7	7	7	5	5	1	4	4	23
1970-71	5	5	5	0	2	0	0	2	26
1971-72	1	1	4	4	0	0	7	7	27
1972-73	6	6	7	0	2	0	6	6	35
1973-74	10	10	8	8	2	2	6	2	28
1974-75	2	2	5	5	4	4	4	4	19
1975-76	4	4	4	0	3	4	6	6	29
1976-77	1	1	4	0	0	0	5	5	30
1977-78	10	10	3	3	3	3	0	0	20

Fig. 10. Same as Fig. 9 except for the Southern Hemisphere.

tropical latitudes in baroclinic regions within stagnant frontal zones or to the east of a westerly upper trough. Typically, they produce weak intensity storms.

3. CYCLONE GENESIS

This subject is being extensively studied. Recent papers relating to this subject can be found in the reports of Zehr (1976), S. Erickson (1977), Arnold (1977), Gray (1977b) and a more extensive survey report on this subject by McBride (1979). Older Colorado State University Project studies on cyclone genesis are contained in the bibliography.

The main findings from our analysis of the composite fields regarding cyclone genesis are:

- 1) Pre-typhoon and pre-hurricane systems are located in large areas of high values of low level relative vorticity. The low level vorticity within 6° radius of the center of a developing cloud cluster is approximately two to three times larger than that observed with non-developing cloud clusters.
- 2) Mean divergence and vertical motion for the typical Western Atlantic weather system are well below the magnitudes found in pre-tropical storm systems.
- 3) Once a system has sufficient divergence to maintain 100 mb or more per day upward vertical motion over a 4° radius area, there appears to be little relationship between the amount of upward vertical velocity and the potential of the system for development.
- 4) Cyclone genesis takes place under conditions of zero vertical wind shear near the system center.
- 5) There is a requirement for large positive zonal shear to the north and negative zonal shear close to the south of a developing system. There is also a requirement for southerly shear to the west and northerly shear to the east. The scale of this shear pattern is over a 10° latitude radius circle with maximum amplitude at approximately 6° radius.
- 6) The large scale flow, therefore, rather than the properties of the system itself, appears to be the main differentiating factor for cyclone genesis.

These six findings can be synthesized into one parameter for the potential of a system for development into a hurricane or typhoon:

$$\text{Genesis Potential (GP)} = \tau_{900\text{mb}} - \tau_{200\text{mb}},$$

when applied over $0-6^\circ$ radius. GP is three times greater for developing tropical weather systems than for non-developing systems.

All of the above factors relate to dynamic parameters or the wind fields around the disturbances. There are no consistent differences between developing and non-developing systems in thermodynamic parameters such as moisture content or vertical stability.

The analysis of the composite fields does show some temperature differences between the developing and non-developing systems. The whole tropical region in which the developing disturbance is embedded is slightly warmer than the region surrounding the typical non-developing disturbance. This temperature difference is of a much smaller magnitude, however, than the difference in the wind fields.

Many past authors have emphasized warm-core versus cold-core differences between developing and non-developing disturbances. All composite tropical weather systems have an upper level warm core. In the lower atmosphere there are some differences. The Pacific non-developing cloud cluster has a low level cold core. In the Atlantic the N1 non-developing cloud cluster has a cold core, but the N2 non-developing cluster has a low level warm core. All developing data sets have low level warm cores. The low-level warm core is on the cluster scale, but the vorticity is on a very much greater scale extending out to 10° latitude in all directions. The vorticity difference therefore must be a dominant effect, since its large scale implies that its source is external to the system.

3.1 Individual Day Cyclone Genesis

During the hurricane season the National Hurricane Center in Miami routinely performs computer analyses over the North Atlantic Ocean of the wind fields at the 200 mb level and at the ATOLL level (Analysis of the Tropical Oceanic Lower Layer). Grid point values of these fields (at 1.5° grid resolution) were subtracted to provide fields of vertical shear by Mr. Mark Zimmer of the National Hurricane Center (NHC). This is representative of the vertical wind shear between 200 and 900 mb. Maps were also provided of zonal and meridional shear for the Atlantic Ocean covering the region from the equator to 45° North, and from 36° West to 95° West. Data were provided twice daily for the hurricane seasons of 1975, 1976 and 1977. The data were taken from the operational data tapes of the NHC, so there were some retrieval problems and some periods of missing data. The Atlantic Ocean is a relatively data void area, so there are, of course, many deficiencies in the analyses. The data sources and the analysis techniques used by the NHC have been described by Wise and Simpson (1971). The 200 mb analysis includes both aircraft and satellite winds and is considered to be the most reliable upper air analysis. The ATOLL (~ 900 mb) is augmented by surface ship observations. These two levels are considered to be the best levels available in the tropics.

There were 22 named tropical cyclones in the Atlantic in the period 1975-1977, 16 of which were classified as distinct tropical systems and had sufficient data coverage around them so that a reasonable accurate analysis could be made.

For these 16 tropical cyclones, maps of the vertical shear of the zonal wind and the meridional wind were examined for every 12 hours,

beginning 60 hours before the point at which the system first reached a maximum sustained wind of 35 knots. The former time is labelled -60, the latter 00.

Seven parameters were examined for each system. They are:

- (i) ΔU : the value of the vertical shear of the zonal wind at a point 6° latitude north of the position of the system minus the value of the shear at a point 6° south of the system;
 ΔU is proportional to $\partial/\partial y(-\partial U/\partial p)_{900-200mb}$;
- (ii) ΔV : the vertical shear of the meridional wind 6° west of the system minus the shear 6° east of the system;
 ΔV is proportional to $\partial/\partial x(\partial V/\partial p)_{900-200mb}$;
- (iii) $\Delta U + \Delta V$: this is proportional to $\bar{\epsilon}_{900mb} - \bar{\epsilon}_{200mb}$, averaged over the $0-6^{\circ}$ area;
- (iv) existence of a zonal zero line: the value of this parameter is YES if the vertical U shear is positive 6° to the north and negative 6° to the south; otherwise the value is NO;
- (v) existence of a meridional zero line: the value is YES if the vertical V shear is positive 6° to the west and negative 6° to the east;
- (vi) subjective existence of zonal zero line: the zero line often exists but does not meet the strict criteria of item (iv) above; for example the zonal zero line exists at position -60 for storm Amy shown in Fig. 11, but the shear 6° to the south of the storm position is positive;
- (vii) subjective existence of meridional zero line.

Typical maps of zonal and meridional shear at representative times for the thirteen systems showing a positive response are displayed in Figs. 11 and 12. Point X on the figure is the position of the prestorm disturbance. Point T is the position at which it eventually becomes a named tropical storm. The important features of the figure are that every pre-storm disturbance has a large region of positive zonal shear to the north and negative zonal shear to the south. In the meridional shear it has a positive area immediately to the west and a negative area to the east. The shears close to but not over the position of the

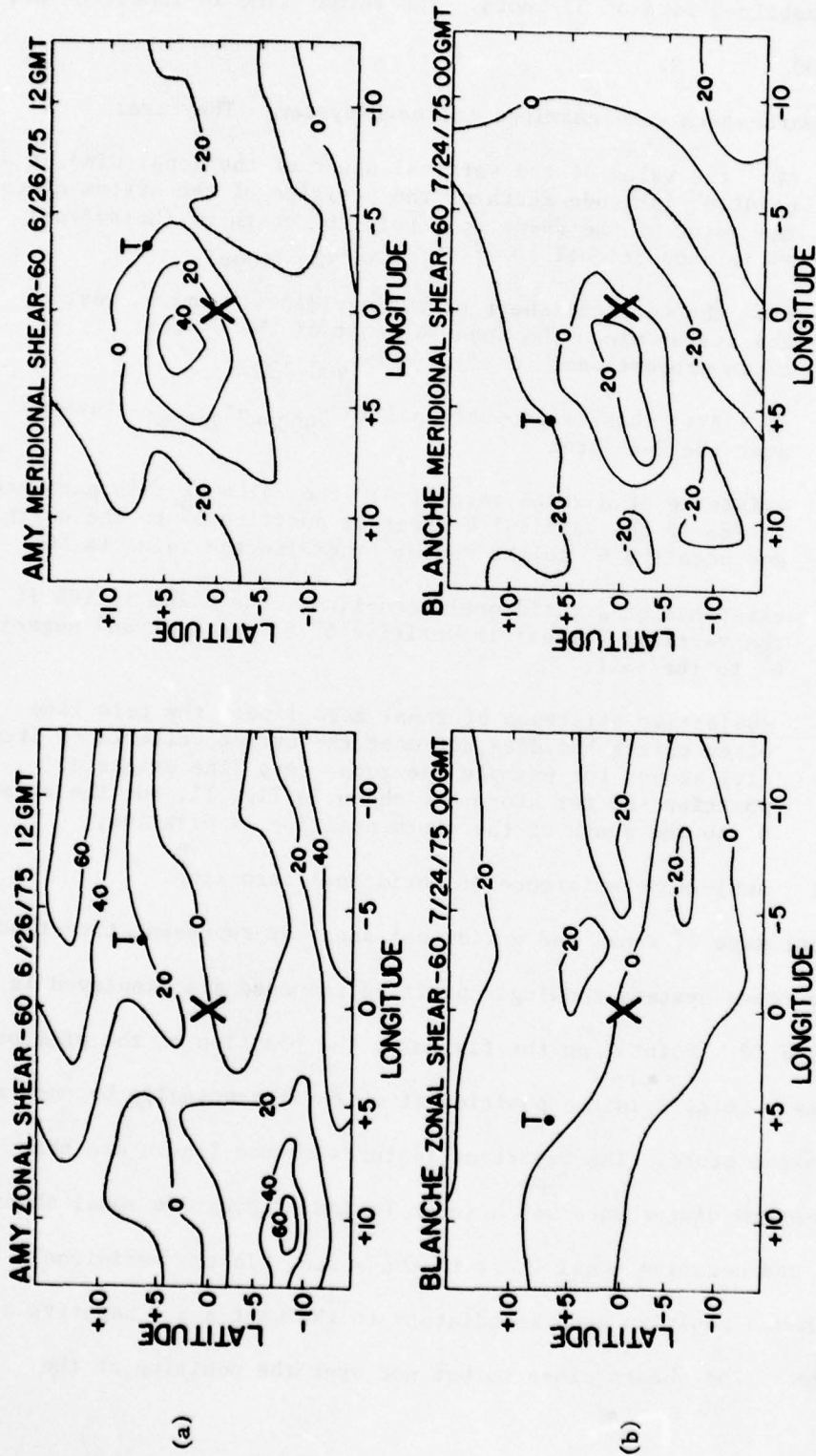


Fig. 11. Maps of vertical shear (knots) of the zonal wind ($U_{200\text{mb}} - U_{\text{ATOLL}}$) and the meridional wind ($V_{200\text{mb}} - V_{\text{ATOLL}}$) surrounding pre-tropical storm disturbances. T marks the position it will be in when it attains tropical storm status. The abscissa is degrees longitude; the ordinate is degrees latitude relative to the position of the disturbance. (a) is for 60 hours prior to the development of Tropical Storm Amy. (b) is for 60 hours prior to the development of Hurricane Blanche.

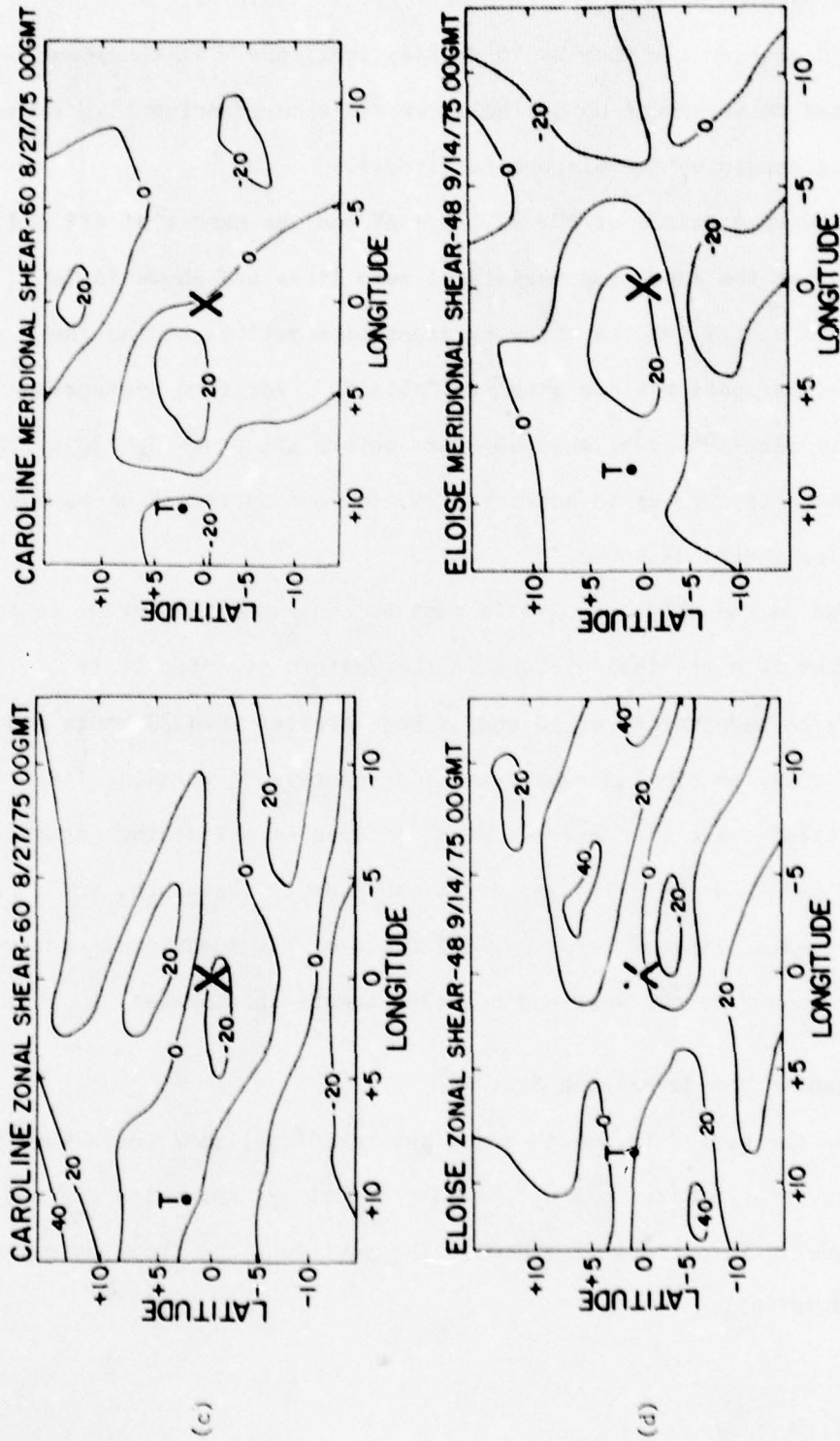


Fig. 12. (c) 60 hours prior to the development of Hurricane Caroline. (d) 48 hours prior to the development of Hurricane Eloise.

disturbance are typically very large. It can be seen from the figure that this particular configuration of vertical shear extends over an area of 20 degrees latitude by 20 degrees longitude. It thus must be interpreted as being set up by the large scale surrounding flow rather than being caused by the disturbance itself.

The average values of ΔU , ΔV , $\Delta U + \Delta V$ and the number of YES and NO values for the zonal and meridional zero lines are shown in Table 6. The average values for the three earliest time periods having the required shear patterns are given in Table 7. For five systems the pattern is already established 60 hours before the storm develops. For four systems it sets up 48 hours before, for one system 36 hours before and for one system 24 hours.

Based on the above results it must be concluded that prior to the development of a tropical cyclone in the Western Atlantic it is necessary to have values of ΔU and ΔV both greater than 20 knots and also for there to simultaneously exist an east-west extending line of zero vertical shear of the zonal wind centered on the disturbance with positive shear to the north and negative shear to the south, and a north-south extending line of zero vertical shear of the meridional wind with positive shears to the west and negative shears to the east.

3.2 Atlantic Non-developing Systems

From the period for which zonal and meridional shear data were available, tracks were made up for 63 tropical systems which did not later develop into tropical storms. The positions for these systems were obtained as follows:

TABLE 6

Mean characteristics of the patterns of vertical shear for the sixteen pre-tropical storm disturbances. Values are in knots. ΔU is proportional to $\partial/\partial y(-\partial U/\partial p)_{900-200\text{mb}}$; ΔV is proportional to $\partial/\partial x(\partial V/\partial p)_{900-200\text{mb}}$; $\Delta U + \Delta V$ is proportional to $\zeta_{900\text{mb}-\zeta_{200\text{mb}}}$, averaged over the $0-6^\circ$ radius area centered on the system.

Position	ΔU	ΔV	$\Delta U + \Delta V$	Zonal Zero Line	Meridional Zero Line
-60	11	7	18	3 YES 10 NO	5 YES 8 NO
-48	17	10	24	6 YES 7 NO	7 YES 5 NO
-36	28	18	46	9 YES 5 NO	6 YES 7 NO
-24	35	27	64	8 YES 5 NO	9 YES 4 NO
-12	50	34	82	12 YES 4 NO	11 YES 4 NO
00	54	33	86	12 YES 4 NO	9 YES 6 NO
Mean	33	22	53	50 YES 35 NO (59%, 41%)	47 YES 34 NO (58%, 42%)

TABLE 7

Mean characteristics of the patterns of vertical shear for the three optimum time periods prior to the development of each tropical storm (values are in knots). These are not the three time periods with the highest values, but rather the earliest three time periods showing the required shear pattern. ΔU is proportional to $\partial/\partial y(-\partial U/\partial p)_{900-200\text{mb}}$; ΔV is proportional to $\partial/\partial x(\partial V/\partial p)_{900-200\text{mb}}$; $\Delta U + \Delta V$ is proportional to $\zeta_{900\text{mb}-\zeta_{200\text{mb}}}$, averaged over the $0-6^\circ$ radius area centered on the system.

ΔU	ΔV	$\Delta U + \Delta V$	Zonal Zero Line	Meridional Zero Line
37	28	65	28 YES 7 NO (80%, 20%)	25 YES 4 NO (86%, 14%)

Non-developing tropical depressions (16 systems): The official tracks of Atlantic depressions were used as obtained from the National Hurricane Center. Only systems were used that died over the ocean. (Systems are from the 1975, 1976 and 1977 seasons).

Dvorak systems (8 systems): These systems are from the same source as the systems making up the Atlantic cloud cluster data set of Chapter 7 (Systems from 1975).

Frank systems (11 systems): These systems are from the same source as the systems making up the Atlantic wave trough cluster data set of Chapter 7. (Systems from 1975.)

Shapiro systems (11 systems): Shapiro (1977a, b) of the National Hurricane and Experimental Meteorology Laboratory, NOAA, has also studied the differences between developing and non-developing tropical disturbances. The tracks of the systems which he used as non-developing cases were provided by him for this study. (Systems from 1976, 1977.)

McBride systems (17 systems): The author picked positions of prominent conservative (lifetime greater than 24 hours) cloud clusters in the Western Atlantic from geosynchronous satellite imagery. (Systems from 1976, 1977.)

Shear patterns for these systems were analyzed at only 12 GMT, though at least 2 satellite pictures per day were used in the actual positioning of the systems. For the 63 disturbances vertical shear data were available at 178 different 12 GMT time periods, an average of 2.8 per system. Four randomly chosen examples of the zonal and meridional vertical shear patterns surrounding the positions (marked X) of non-developing disturbances are shown in Figs. 13 and 14. The mean values of the shear parameters for the non-developing systems are shown in Table 8.

All the non-developing systems have very low values of ΔV . A zonal zero line exists for 25 percent of the positions and a meridional zero line for 19 percent. This compares with 46 percent and 58 percent for prehurricane systems 48 hours before development.

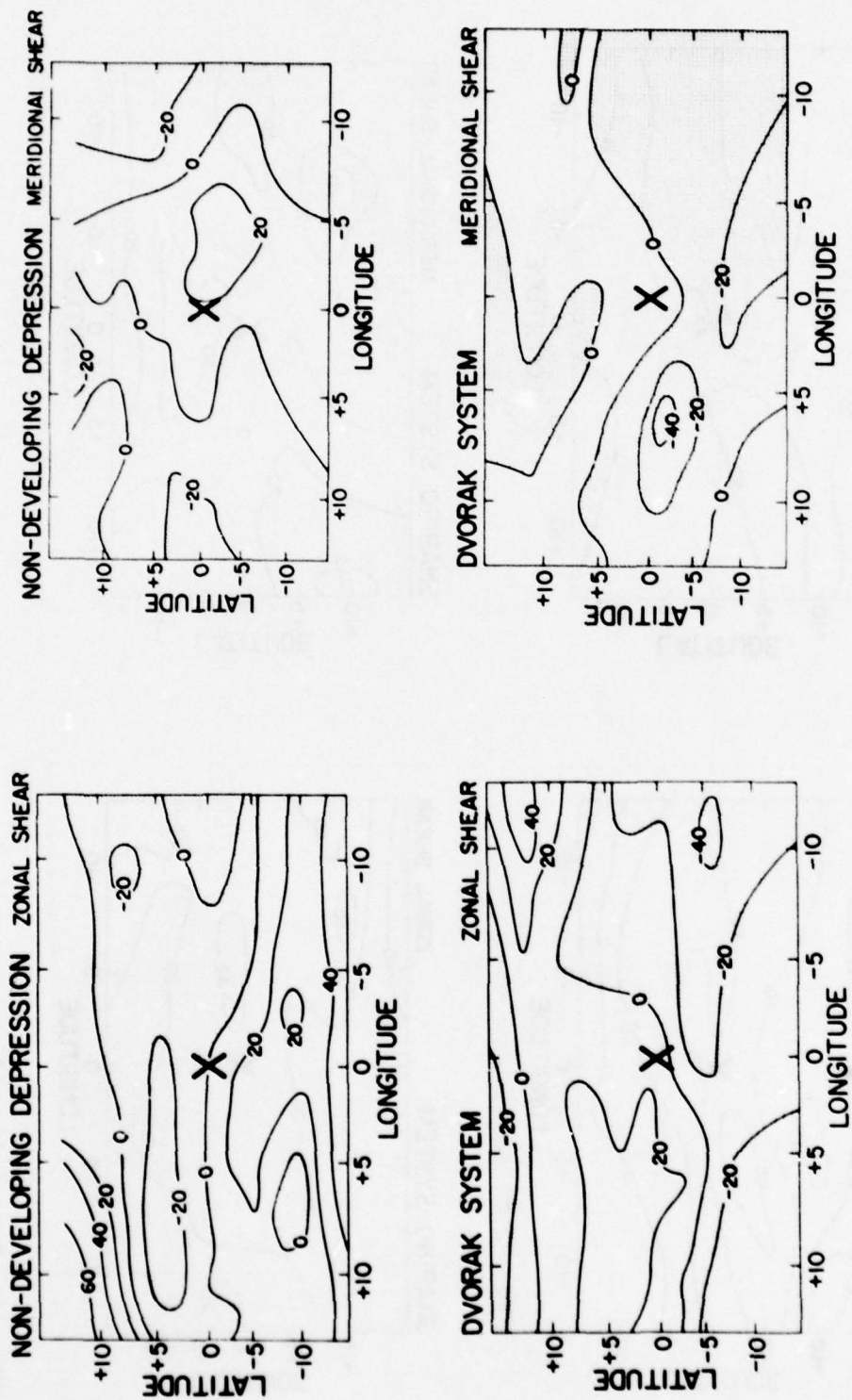


Fig. 13. Maps of vertical shear of the zonal and meridional wind surrounding four non-developing tropical disturbances.

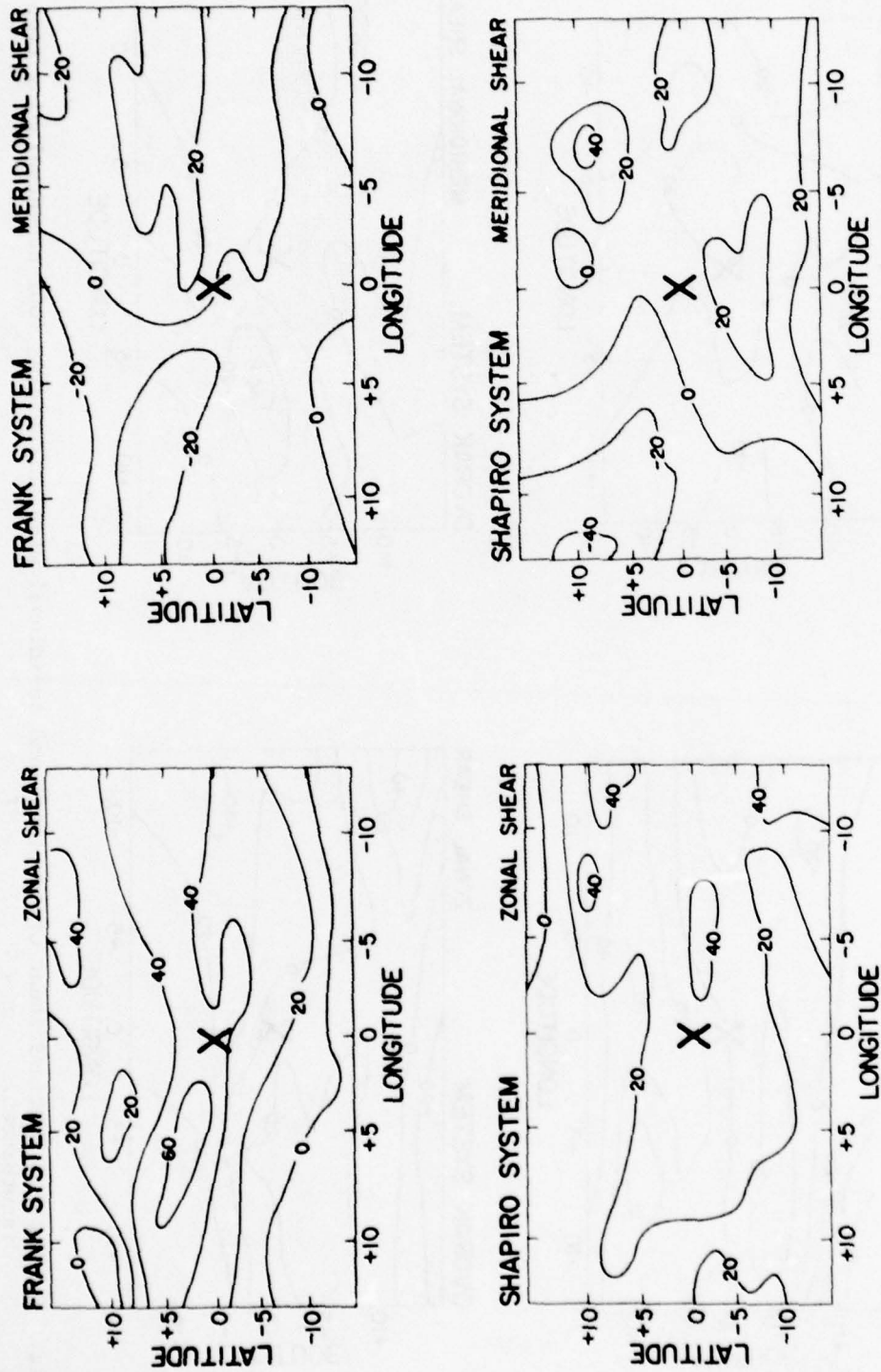


Fig. 14. Same as Fig. 13.

TABLE 8

Mean properties of the vertical shear for the 63 non-developing disturbances (values in knots). AU is proportional to $\partial/\partial y(-\partial u/\partial p)$, 00-200mb; AV is proportional to $\partial/\partial x(\partial v/\partial p)$, 900-200mb; AU + AV is proportional to $\zeta_{900mb}-\zeta_{200mb}$, averaged over the $0-6^\circ$ radius area centered on the system.

	No. of Systems	No. of Positions	AU	AV	AU + AV	Zonal Zero Line	Meridional Zero Line
Non-developing depressions	16	35	-1	-1	-2	3 YES 32 NO	11 YES 24 NO
Dvorak systems	8	25	23	-4	19	17 YES 8 NO	3 YES 22 NO
Frank systems	11	25	8	-13	-5	10 YES 15 NO	2 YES 23 NO
Shapiro systems	11	56	15	1	16	11 YES 45 NO	13 YES 43 NO
McBride systems	17	37	2	-7	-5	4 YES 33 NO	4 YES 33 NO
	63	178	9	-4	5	45 YES 133 NO (25%, 75%)	33 YES 145 NO (19%, 81%)

It does seem, however, from Table 8 that large values of ΔU or ΔV shear or the existence of a zero line are fairly frequent events in the Western Atlantic. The important factor for tropical cyclone genesis is whether large values of shear exist concurrently and whether these shears persist for more than one day.

The 178 non-developing positions were examined for the concurrent appearance of (i) ΔU greater than 20 knots, (ii) ΔV greater than 20 knots, (iii) the existence of a zonal zero line, and (iv) the existence of a meridional zero line.

There were only 14 positions out of 178 (or 8%) such that three of the four criteria were met. By contrast, for the 16 developing systems considered 13 (or 82%) of them had a period of at least 36 hours, such that 3 of the 4 criteria were met, sometime in the 60 hours prior to cyclone development.

Of the 63 non-developing systems only 2 (or 3%) had more than one time period satisfying 3 or the 4 criteria. If the vertical shear criteria were being used to predict cyclone genesis, these two systems (one Shapiro system and one Dvorak system) would have been predicted to develop. The shear criteria therefore appear to slightly overpredict genesis.

In summary, for the hurricane season of 1975-1977 in the Western Atlantic, the use of the vertical shear data would have correctly predicted the development of 13 out of 16 tropical storms. It would have correctly predicted non-development for 61 out of 63 non-developing weather systems. The general skill of operational forecasting of tropical cyclone genesis is much below this success rate.

3.3 Pacific Pretyphoon Versus Non-developing Cloud Clusters

In the Western Pacific no grid point data on vertical shear were available. Nevertheless, a limited test on the use of vertical shear as a predictor of tropical storms in this area was performed by subjectively picking wind values around clusters off weather maps. Positions were tabulated for non-developing and pretyphoon cloud clusters from the years 1972 and 1974. Values of the U and V component of the wind at 200 mb and the surface were estimated from the weather maps at points 6° to the north, 6° to the south, 6° to the east and 6° to the west of each cluster. The positions of the clusters were those obtained in the DMSP satellite study of S. Erickson (1977). Weather maps were available at 182 time periods for 18 pretyphoon clusters and 31 non-developing cloud clusters. The wind values were picked off the weather maps without the knowledge of whether the position was for a developing or a non-developing system.

This method is crude, since there is no consistent and detailed wind information around most systems and best estimates had to be made. The values are also biased greatly by whether or not the operational analyst drew either an upper level anticyclone or a low level cyclone over the system. Despite these drawbacks the method shows some predictive skill.

Wind values at all different time periods for a particular system were averaged together to yield one value per system. From the resultant numbers three parameters were extracted: (i) a value of $\Delta U + \Delta V$, following the same convention as used in the Atlantic, (ii) the existence of a zero line in the vertical shear of the zonal wind, and (iii) the existence of a zero line in the vertical shear of the meridional wind. The actual values of each parameter for each system are listed in the Appendix A, Tables A1 and A2.

The results are summarized in Table 9. Both the values of $\Delta U + \Delta V$ and the percentage of systems with zero lines are significantly greater for the developing systems.

The systems which had high values of $\Delta U + \Delta V$ were usually the same systems that had zero lines. Using the criteria that to develop into a typhoon a system must have zero lines in both zonal and meridional shear, the data give 10 out of 18 (56%) correct answers for the developing systems and 25 correct out of 31 (81%) for the non-developing.

Using the criteria that a system must have a mean value of $\Delta U + \Delta V$ greater than 40 knots gives 11 correct developing systems (61%) versus 22 correct (71%) non-developers.

Using the criteria that 2 out of the 3 conditions, zero line in zonal shear, zero line in meridional shear and $\Delta U + \Delta V$ greater than 40 knots, be met yields 11 correct developing systems (61%) and 21 correct non-developing predictions (68%).

These results are not as good as were obtained in the previous sections for the Atlantic, but they are very encouraging when the crudity of the approach and the poor quality of the Pacific wind data are taken into account.

In the Atlantic only vertical shear data were available, but in the Pacific separate wind values were used from each level. This allows

TABLE 9

Mean properties of the vertical shear (knots) for the Pacific pretyphoon and non-developing cloud clusters. $\Delta U + \Delta V$ is proportional to $\bar{u}_{900mb} - \bar{u}_{200mb}$, averaged over the $0-6^\circ$ radius area centered on the system.

	$\Delta U + \Delta V$	<u>Zonal Zero Line</u>		<u>Meridional Zero Line</u>	
Non-developing systems (31 systems)	25	21 YES	10 NO (68%, 32%)	8 YES	23 NO (26%, 74%)
Developing systems (18 systems)	45	15 YES	3 NO (83%, 17%)	12 YES	6 NO (67%, 33%)

the opportunity to evaluate the magnitude of the separate contribution from each level, upper and lower, to $\Delta U + \Delta V$. U and V values of the wind added together with the appropriate signs give a contribution to $\Delta U + \Delta V$ at the surface of 16 knots (developing) versus 10 knots (non-developing). At 200 mb the contribution is 29 knots (developing) versus 15 knots (non-developing). This is tabulated in Table 10. The table shows that both the upper level and the lower level make important contributions to the observed differences in vertical shear between developing and non-developing weather system.

TABLE 10

$\Delta U + \Delta V$ (knots) for the Pacific cloud clusters. $\Delta U + \Delta V$ is proportional to $\zeta_{900\text{mb}} - \zeta_{200\text{mb}}$, averaged over the $0-6^\circ$ radius area centered on the system.

	Contribution from the Surface	Contribution from 200 mb Level	Total
Non-developing systems	10	15	25
Developing systems	16	29	45
Ratio of Developing/Non-developing	1.6/1	1.9/1	1.8/1

Discussion. There can be no doubt that large scale upper level anticyclonic flow and low level cyclonic flow exist over the area of the disturbance well before the time at which it becomes a tropical cyclone. This has particular significance in the upper levels because much previous research on tropical cyclone structure and development have made either the explicit or implicit assumption that the large upper level negative tangential winds around the system are the result of the Coriolis force acting on the outflowing air. This is typically not the case. In the early stages of cyclone development the surrounding

region 200 mb anticyclonic flow is the result of already existing mid-latitude westerlies to the north, equatorial easterlies to the south and/or large scale upper level troughs to the northwest. The source of the anticyclonic flow is thus external rather than internal to the developing system.

The main distinguishing feature of cyclone genesis is a favorable upper and lower level environmental relative vorticity or tangential wind fields, all other parameters indicate much less differences. This has not received the previous emphasis that it should have. Most authors in the past have emphasized the divergence or vertical motion field. Ramage (1974) and Sadler (1976, 1978) have stressed the importance of upper level outflow channels for cyclone development to occur. The current study interprets those anticyclonic outflow channels as indicators of strong surrounding region anticyclonic flow and not necessarily that of an enhanced in and out radial circulation.

A picture is emerging from both the composite data and the individual case data that tropical storm development is a result of large scale influences. It appears that the unique feature to specifying time and location of tropical cyclone genesis is not so much the characteristic of the individual meso-scale system itself. These systems are common and occur in all seasons and at most locations. Once the climatological conditions of genesis are met, it appears that favorable large scale changes in the tropical general circulation are the primary factors determining whether the often present individual organized meso-scale systems will intensify or not. It appears that genesis occurs when an organized tropical cloud cluster forms or moves into a favorable large-scale environment. In particular, both low level positive relative

vorticity and upper level negative relative vorticity over a very large surrounding area must be present.

These results indicate that a realistic theory of tropical cyclone genesis and development must give primary consideration to the influence of the tropical system's surrounding flow patterns and much less consideration to the characteristics of the disturbance itself. This may explain the large time clustering of tropical cyclones.

These large scale general circulation changes of the tropics are likely related to the strengthening and weakening of the ITCZ in association with the equatorial penetration of middle-latitude baroclinic patterns from both hemispheres. The association of these large tropical general circulation changes with tropical cyclone activity needs more documentation.

4. TROPICAL CYCLONE INTENSITY CHANGE

Most current theoretical and numerical models of tropical cyclones show the rate of the cyclone's intensity change being dependent on the strength of the vertical motion field and therefore on the strength of the low level mass inflow and upper level mass outflow.

There are now, however, several sets of observations available that indicate that the strength of the disturbance or cyclone's vertical motion fields is not related to its genesis or intensification potential.

Figure 15 shows vertical profiles of vertical velocity averaged over the $0-4^{\circ}$ area for Pacific composite data sets D1 to D4. D1 is for the cloud cluster, D2 for depression stage, D3 for tropical storm stage and D4 for typhoon stage. Figure 16 shows the same data for the Atlantic systems. In both oceans, the upward vertical velocity actually decreases prior to the intensification to tropical cyclone stage. Thus, in both oceans, the maximum vertical velocity in stage D2 is less than that in stage D1. This phenomenon was observed by Arnold (1977) in a study of the amount of convection around individual developing tropical weather systems using Defense Military Satellite Program (DMSP) data. Arnold had four stages of development for Pacific typhoons, stage I being the cloud cluster and stage IV the typhoon. He considered three quantitative measures of the amount of cloudiness or upward vertical motion: the percentage area of visible deep convective cells, the percentage area of cirrus at an infrared temperature of less than -50°C , and the percentage area of cirrus with temperature less than -63°C . For all three fields he found a decrease in the amount of cloudiness from stage I to stage II. His results are shown in Table 11.

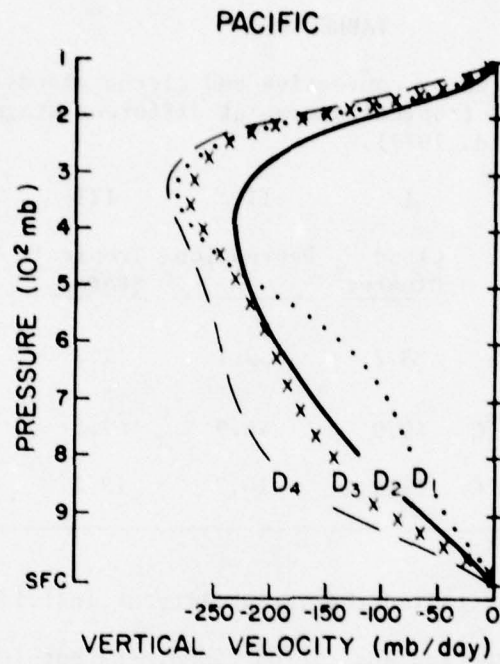


Fig. 15. Vertical velocity averaged over the $0-4^{\circ}$ area for Pacific composite data sets D1 to D4.

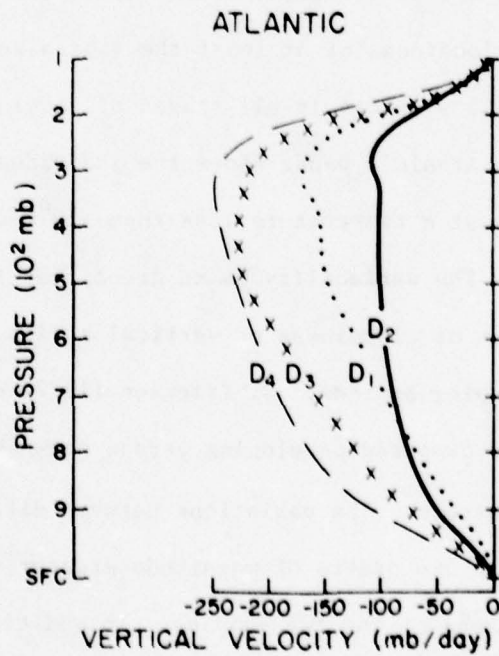


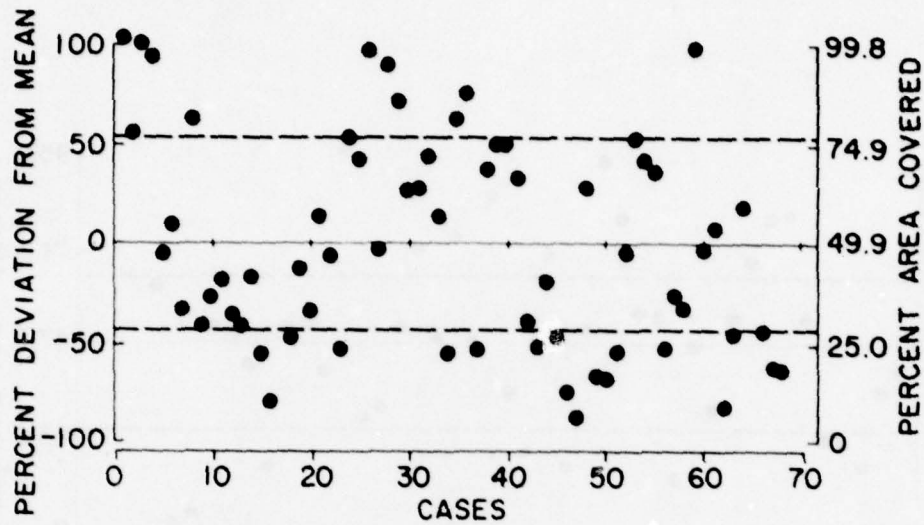
Fig. 16. Vertical velocity averaged over the $0-4^{\circ}$ area for Atlantic composite data sets D1 to D4.

TABLE 11

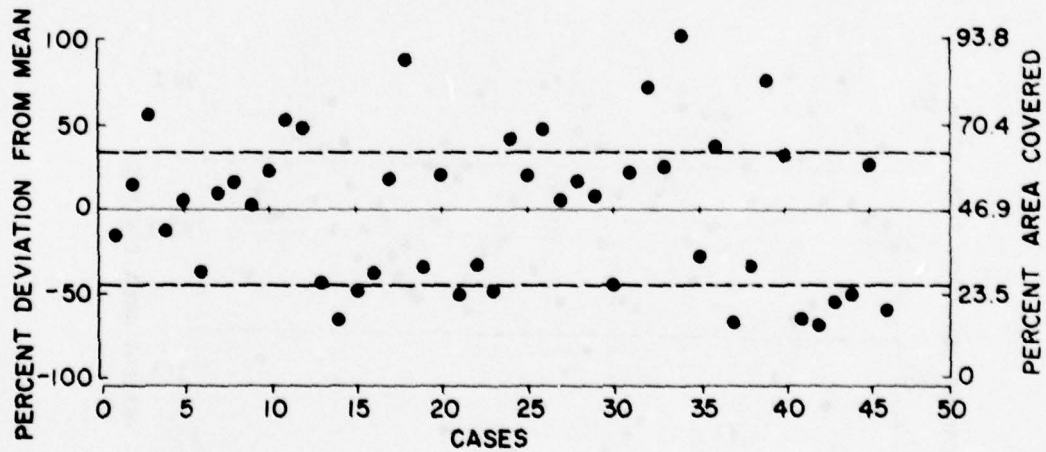
Percentage of area covered by convective and cirrus clouds within the $R = 0-4.2^\circ$ region around tropical storms at different stages of development (adapted from Arnold, 1977).

	I	II	III	IV
	<u>Cloud Cluster</u>	<u>Depression</u>	<u>Tropical Storm</u>	<u>Typhoon</u>
Area of visible deep convective cells	3.2	2.1	2.2	4.5
Area of cirrus, $T < -50^\circ\text{C}$	49.9	46.9	47.5	62.8
Area of cirrus, $T < -63^\circ\text{C}$	16.1	10.7	13.2	32.8

Arnold (1977) also studied the variability of individual time period penetrative convection and cirrus cloudiness both of which are closely related to upper level vertical motion. He found that between different weather systems and at different times within the same system there is a variation in cloudiness of at least the same size as the mean cloudiness. This variability exists in all stages of development. Figure 17 reproduced from Arnold's paper shows the individual values of percentage area of cirrus at a temperature less than -50°C for all the separate storms studied. The variability is so great that it renders meaningless any comparison of cloudiness or vertical motion between developing and non-developing systems. S. Erickson (1977) using the same techniques as Arnold compared developing versus non-developing Western Pacific cloud clusters. The variations between different systems within each sample are orders of magnitude greater than the difference between the means of the two samples. In addition it is observed that Atlantic prehurricane depressions have less vertical motion

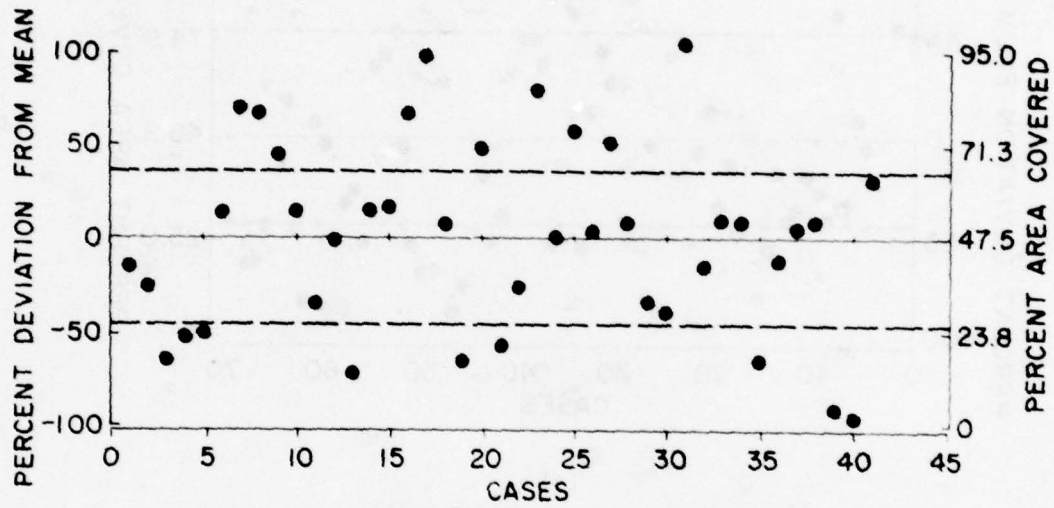


(a)

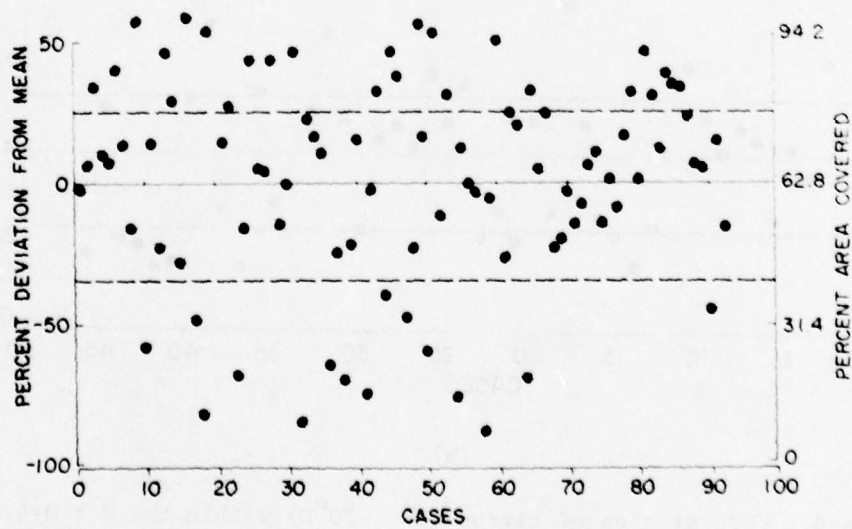


(b)

Fig. 17 a-d. Percent area of cirrus ($T < -50^{\circ}\text{C}$) within the $R = 0-4.2^{\circ}$ region of different storms. The order of the cases is random (from Arnold, 1977). (a) Developing cluster (stage I); (b) Tropical depression (stage II); (c) Tropical storm (stage III); (d) Typhoon (stage IV). Dashed lines above and below the mean show the mean positive and negative deviations respectively.



(c)



(d)

Fig. 17. Continued.

than non-developing depressions. These observations make a forceful case for the argument that the potential of a disturbance for development is not directly related to the magnitude of the vertical motion field.

Within 4° radius of these various cyclone classes, it is observed that the mean vorticity increases about five times from stage D1 to D4, but the mean vertical motion increases only by $1\frac{1}{2}$ times or less. A comparison of the radial wind (V_r) flowing into filling and deepening Pacific storms shows that at lower levels, the filling systems have greater inflow.

Eighteen of our tropical cyclone data sets have been divided into two groups: a) deepening cyclones and b) filling or steady cyclones. Table 12 compares the average inflow angle, integrated from the surface to 850 mb, of the deepening vs. the filling or steady systems. Little difference is found. What difference there is indicates that the filling systems have slightly larger inflow.

Budgets of Moist Static Energy. All tropical disturbances import total moist static energy (h)¹ at lower levels and export it at the upper levels. There is a loss of energy due to radiation and a substantial energy gain due to a flux from the surface. When integrated through the whole troposphere it is found that the net result is an export of h as illustrated in Table 13. This means that, other conditions remaining the same, if the radial circulation through the system is reduced, then the system will accumulate energy and intensify.

$$l_h = gz + C_p T + Lq .$$

TABLE 12

Inflow angle integrated from the surface to 850 mb for different radii of deepening vs. filling or steady systems.

	Radius		Area Weighted
	2°	4°	0-6°
<u>Data Sets</u>			
Deepening	5.8°	11.3°	10.7°
Filling or Steady	10.3°	12.3°	11.4°

We may thus better understand the findings of the previous section. Genesis (D1 → D2) takes place when the radial circulation is decreased and the system accumulates energy. Since the time scale for a spin-down of these systems is of the order of a couple of days, surface energy fluxes are not much affected by a decrease in the radial wind. Once the system has started to intensify, a larger radial circulation can be maintained for a storm at equilibrium. However, if the new radial circulation is smaller than what is demanded by equilibrium, the system can keep accumulating energy and intensifying.

Wind-pressure Balance. The ratio of the wind to pressure gradient acceleration has been calculated using the gradient wind equation.

$$\frac{dV}{dt} \frac{r}{r} = fV_{\theta} + \frac{V_{\theta}^2}{2} - g \frac{\partial Z}{\partial r} \quad (4.1)$$

accelerations due to wind	acceleration due to pressure gradient
---------------------------	---------------------------------------

where the normal symbols are used.

TABLE 13

The export of moist static energy (h) due to horizontal divergence ($-\bar{W} \cdot \bar{W}h$) within various radial intervals. A negative sign denotes a loss of energy from the system. Values are expressed in equivalent mean surface to 100 mb temperature increase ($^{\circ}\text{C/d}$) - from McBride (1979).

	<u>0-4^o</u>	<u>0-6^o</u>	<u>0-8^o</u>
<u>PACIFIC NON-DEVELOPING</u>			
N1 Cloud cluster	-0.5	-0.5	-0.5
<u>PACIFIC DEVELOPING</u>			
D2 Pretyphoon cloud cluster	-1.3	-0.7	-0.6
D3 Intensifying cyclone	-1.3	-1.0	-0.6
D4 Typhoon	-2.6	-1.6	-1.0
<u>ATLANTIC NON-DEVELOPING</u>			
N1 Cloud cluster	-0.3	-0.5	-0.3
N2 Wave trough cluster	-0.1	-0.2	0
N3 Non-developing depression	-1.7	-1.3	-0.6
<u>ATLANTIC DEVELOPING</u>			
D1 Prehurricane cloud cluster	-1.0	-0.5	-0.5
D2 Prehurricane depression	-0.8	-0.5	-0.3
D3 Intensifying cyclone	-1.2	-0.7	-0.9
D4 Hurricane	-1.4	-1.2	-0.7

Eighteen data sets were divided into deepening vs. filling or steady systems. The terms of Eq. (4.1) were area weighted and averaged from 3° to 11° radius. The ratio of wind to pressure acceleration was calculated in the upper and lower troposphere and then averaged. The results are shown in Table 14. In the lower level the deepening systems show super-gradient wind while the filling or steady systems indicate sub-gradient winds. At the upper level, both systems have subgradient winds. The deepening systems however indicate less subgradient winds. Similar results are obtained for calculations between $5-9^{\circ}$ radius and $7-11^{\circ}$ radius.

Supergradient or less subgradient winds would result in a decrease in the radial circulation through the system as Fig. 18 illustrates for the lower troposphere. Given a gradient balance wind V_0 , if it becomes supergradient by an amount s , then an outward acceleration a would result.

TABLE 14

Ratio of the wind to pressure gradient accelerations for the deepening and filling or steady data sets area weighted from 3° to 11° .

	<u>Deepening</u>	<u>Filling or Steady</u>	<u>Difference</u>
200 mb	0.74	0.64	16%
900 mb	1.14	0.86	33%

Mechanism for Supergradient Winds. An obvious question is: what type of mechanism would produce an increase in the winds to make them supergradient or less subgradient? It is hypothesized that they could be brought about by Cb up-and-downdrafts existing in a sheared environment. Downdrafts spread out in the boundary layer and act to produce wind

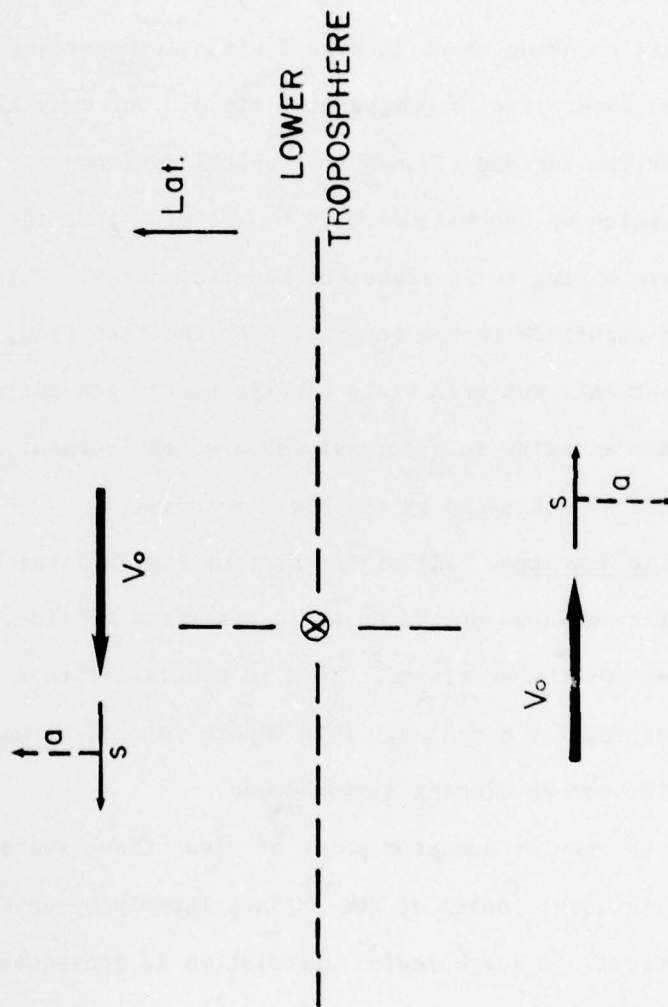


Fig. 18. Schematic view of the unbalanced acceleration (a) produced in the lower troposphere of an intensifying disturbance when an initial wind V_0 in gradient balance, becomes supergradient by an amount s .

increases not related to the cyclone's large-scale convergence. Moncrieff and Miller (1976) and Moncrieff and Green (1972) have shown that Cb clouds existing in a sheared environment can produce wind accelerations in the upper and lower troposphere. The active convection existing in the strong squall-lines of spiral bands would certainly fulfill the requirements to bring about increased winds at upper and lower levels and cause lower level supergradient winds. Our many kinetic energy budgets for the various classes of tropical cyclones are showing large residuals which we can balance only by assuming that the deep convective elements are acting to increase the kinetic energy. This residual is of comparable magnitude to the generation by the mean flow, $-V \cdot \nabla \phi$. It is thought that this sub-grid scale kinetic energy generation is accomplished by Cb clouds existing in a strongly sheared environment in a fashion akin to that hypothesized by the above authors.

Angular Momentum. All of our systems show a large export of negative angular momentum at the upper levels (from McBride, 1979) as Fig. 19 illustrates for the hurricane. This is equivalent to a large import of positive angular momentum. This import is much stronger for developing than for non-developing disturbances.

From an angular momentum point of view, these systems are maintained against frictional losses at the surface largely by upper level inward eddy transport. A large radial circulation is consequently not needed to maintain them.

Figures 20 and 21 show how inward angular momentum transport at large radii can be accomplished through horizontal standing eddy processes due to large asymmetries in the outflow layer indicated (from Núñez and Gray, 1977).

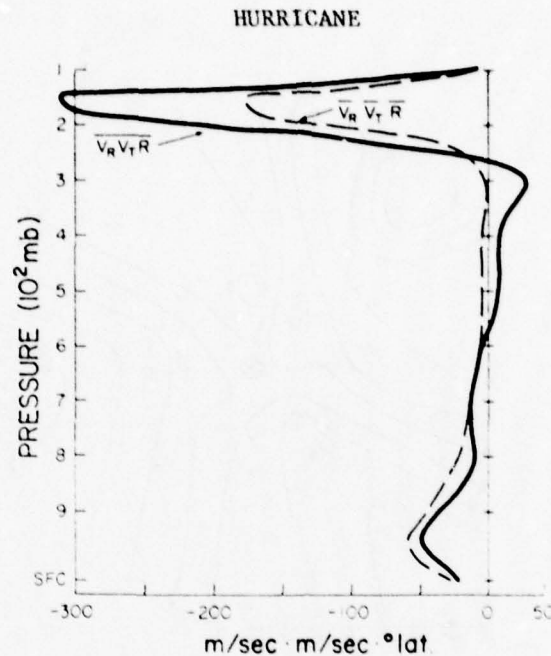


Fig. 19. Total horizontal flux of relative angular momentum ($\overline{V_r V_T r}$) and flux by the mean circulation ($\overline{V_r V_T r}$) at 6° radius for the hurricane.

Discussion. Tropical cyclone forecasters generally agree that skill at operational forecasting of tropical cyclone intensity change is nearly zero. Our results are showing that kinetic energy export in the upper troposphere out of the cyclones on their poleward side is a major characteristic of their filling-intensifying process. Outward kinetic energy transport at 200 mb is 4-6 times greater for filling cyclones than for growing ones. It is from 2-3 times larger when comparison is made of the filling and steady-state cyclones. We believe there is a skill to be derived in intensity forecasting change if the upper tropospheric (~ 200 mb) flow patterns to the poleward side of the cyclone can be continuously monitored with the geo-stationary satellite. Before quantitative forecasting rules for intensity change

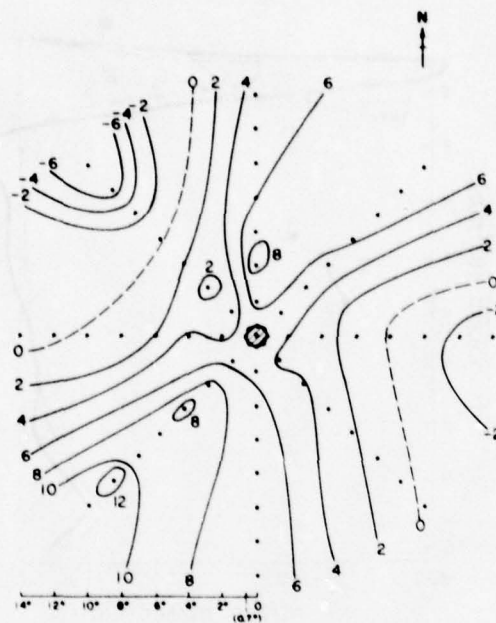


Fig. 20. 150 mb plan view of radial wind for the mean steady state typhoon

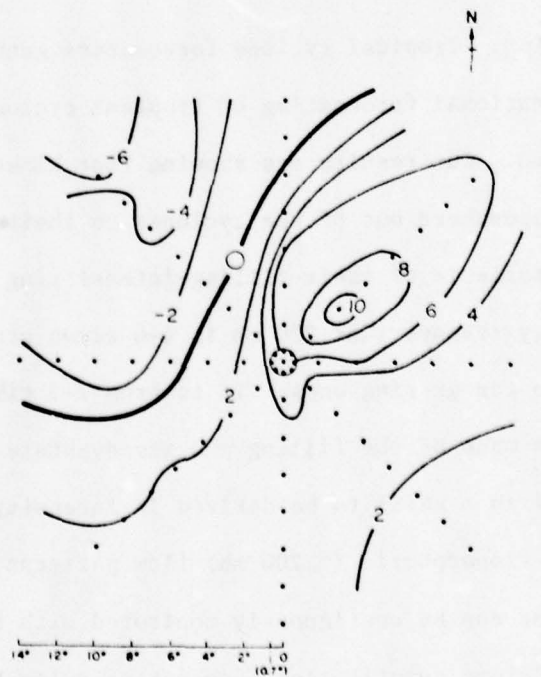


Fig. 21. 150 mb plan view of radial wind for the mean steady state hurricane.

can be confidently established, much statistical background work and study has to be accomplished. Not only for the average cases of growing, steady, and filling storms must such relationships be found, but also for the individual case situations. We propose that the 900 mb and 200 mb weather maps at individual times can be used to better forecast tropical cyclone intensity change. It appears that there exists meaningful relationships between the large-scale upper tropospheric outflow of the tropical cyclone and its inner region tangential winds.

5. FORECASTING TROPICAL CYCLONE TURNING MOTION

The largest track forecast errors for tropical cyclones are usually associated with cyclones undergoing a turn. To examine this forecast problem more closely we have made a special study of tropical cyclones occurring in the West Indies during the period 1961-1977 that underwent a left or right turn or moved relatively straight for a period of at least 48 hours. The forecast errors made around the time when the storm began to turn (hereafter referred to as the turn time T) were analyzed. Table 15 gives the average 24-hour official forecast errors issued by the National Hurricane Center (NHC) for these storms at three time periods: 24 hours before turn time (T-24), the turn time (T), and 24 hours after turn time (T+24). It can be seen that for either a left- or right-turning storm, there is a large jump in the forecast errors made at the turn time compared with those made before and after the turn or for straight-moving cyclones. The forecast errors are even larger for 16 of the 22 right turn cases. For these cases the average 24 hour forecast error nearly tripled, jumping from 80 n mi before the turn to 225 n mi at turn time.

Figure 22 shows the scatter of 24-hour forecast positions made at turn time and the corresponding verifying positions for each turn class. The forecast positions for right-turning storms are nearly always to the left of the actual storm track while the reverse is true for left-turning storms. Forecast positions tend to cluster around the extrapolated position of the storm on its current path. The strong bias based on persistence is evident. For straight-moving storms, there is a tendency to forecast the future position slightly to the right of the actual track, a likely indication of a slight climatological bias. It appears

TABLE 15

Average 24-hour official tropical cyclone track forecast errors (n mi) issued by the National Hurricane Center, Miami. T is the time when the storm starts to turn. See Section 5.1 for description of T for a straight-moving storm. Special right turn cases have forecast errors at T greater than 100 n mi.

<u>Turn Classification</u>	<u>24 hour forecast error (n mi) for forecasts issued at the following times</u>		
	<u>T-24</u>	<u>T</u>	<u>T+24</u>
Left Turn (10 Cases)	127	156	111
Straight (23 Cases)	80	91	106
Right Turn (22 Cases)	96	175	129
<u>Special Right Turn (16 Cases)</u>	80	225	132

that there is a deficiency in the skill of forecasting turning motion. This is probably a result of insufficient observational knowledge of the characteristics of the cyclone's surrounding environmental flow pattern, and/or a reluctance of the forecaster to commit himself to a forecast very different from the climatology-persistence techniques which usually verify well.

This paper presents information on the environmental flow patterns around turning and straight-moving tropical cyclones prior to and at turn time. It will be shown that there are significant differences in the large-scale surrounding wind fields at 500 mb, and also at upper (200 mb) and lower tropospheric (900 mb) levels for these turn classes. Temperature sounding data from the Nimbus-6 Scanning Microwave Spectrometer provide further evidence of these differences. It is anticipated that knowledge of surrounding flow patterns may improve the skill in turning motion forecasting.

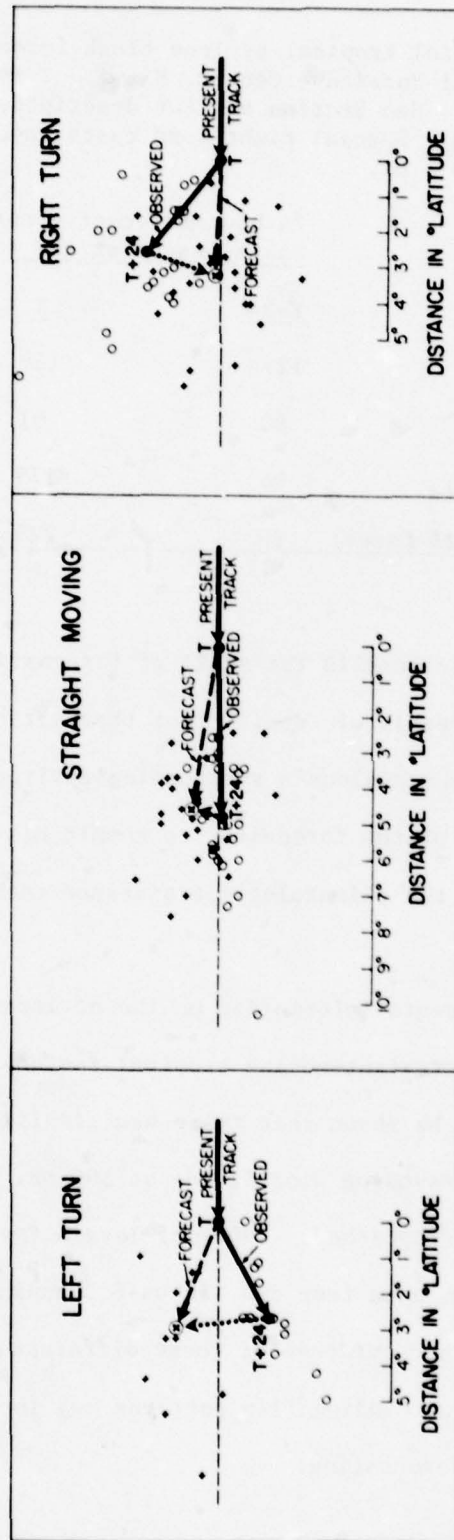


Fig. 22. 24-hour forecast positions (denoted by +) made at the turn time for individual storms in each class and their actual positions (denoted by 0) at the time T+24. The \bar{X} is the mean forecast position. The dashed arrow is the 24 hour mean forecast track. The solid arrow from T to T+24 is the mean distance (and direction) the storm has traversed during the 24 hours. The dotted arrow indicates the average displacement of the forecast position from the actual position.

5.1 Composite Data

Because of the scarcity of oceanic rawinsonde data, representative information on the characteristics of tropical systems is usually not available for individual situations. To overcome this problem a rawinsonde compositing approach has been used in which data from storm systems having similar characteristics are averaged together. The rationale behind this type of data compositing has been discussed in a number of recent papers (Williams and Gray, 1973; Frank, 1977a; and others). This study composites tropical cyclones according to the different turning classifications.

Composited data samples enable reliable quantitative analyses to be made, and allow meaningful conclusions to be drawn about the "average" differences in the surrounding environment between different data sets. Compositing tends to suppress random data noise and isolate the mean characteristics common to each composite class. Differences between turning classes (if present) will give hints to forecasters as to which surrounding cyclone parameters to monitor in individual cases. One can usually find meaningful relationships in data deficient individual case situations much easier if one knows what to look for.

This study investigates tropical cyclone turning motion which occurred within the West Indies rawinsonde network (see Fig. 23) during 1961-1977. Cyclones which underwent a left or right turn or moved relatively straight for a period of at least 48 hours were selected, giving a total of 16 left-turn, 36 straight-moving and 29 right-turn cases. The tracks for these cyclone turn classes are shown in Figs. 24, 25 and 26. For each turn classification, the following time periods were

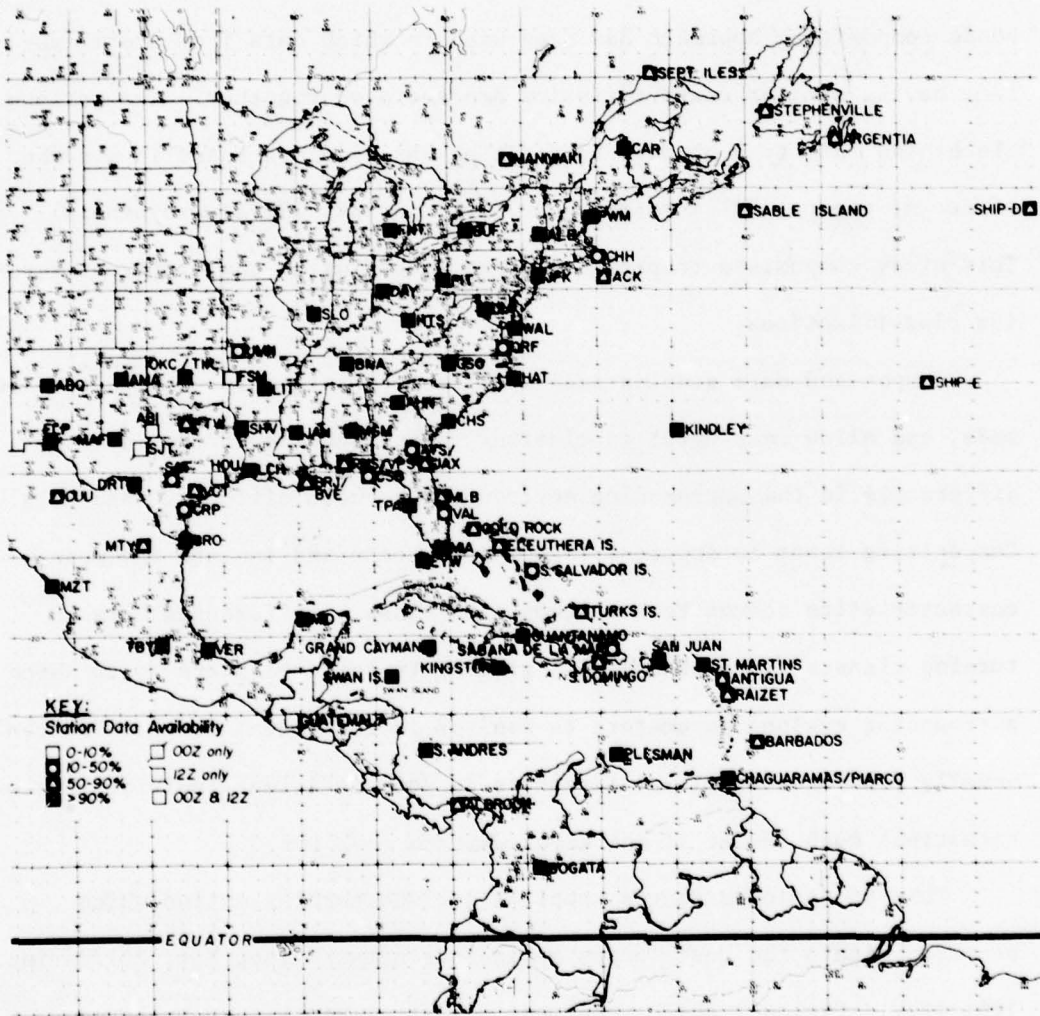


Fig. 23. Northwest Atlantic rawinsonde data network.

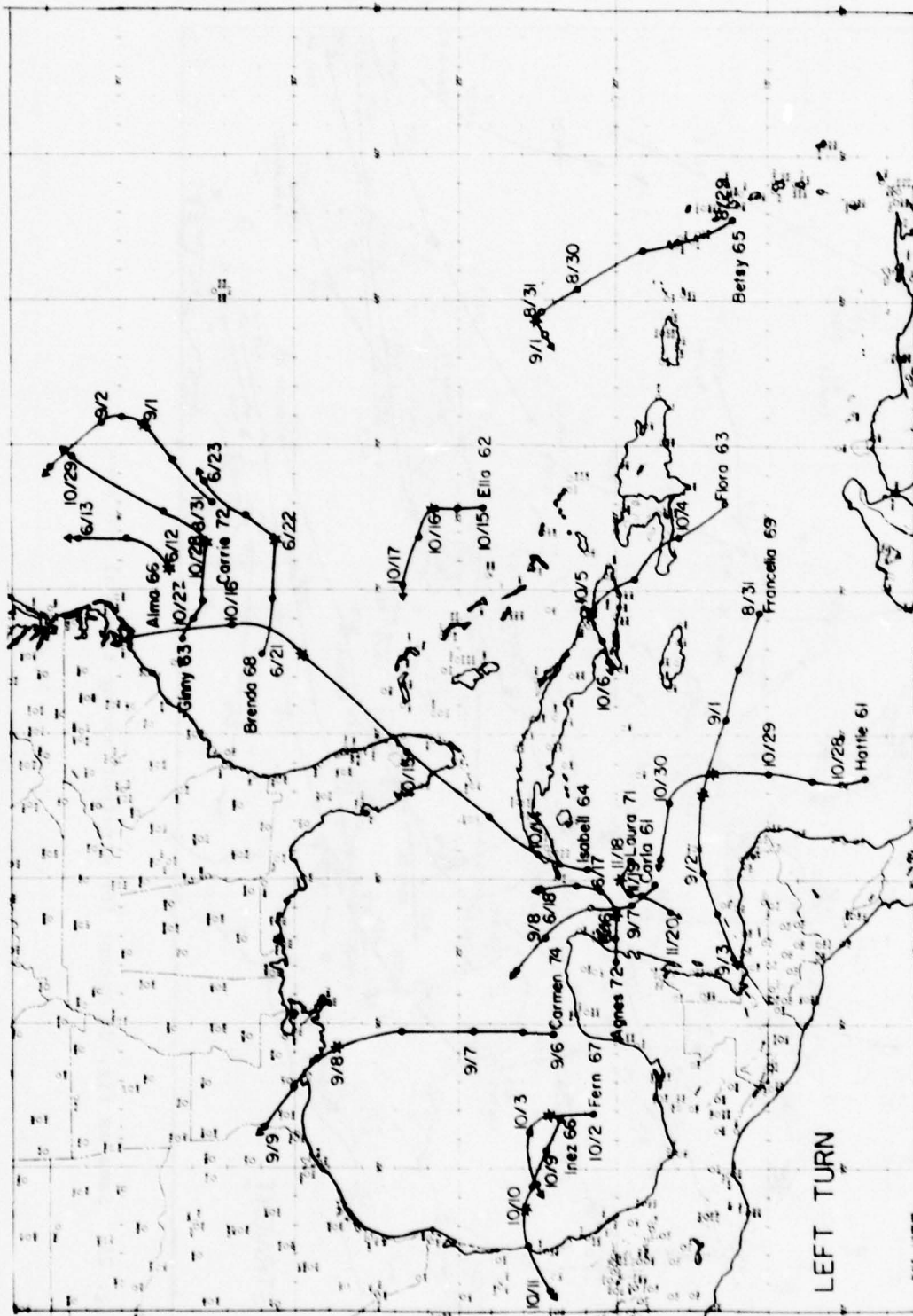


Fig. 24. Tracks of tropical cyclones used in this study which made a left turn. The asterisk on each track indicates the turn time T. • is the 00Z position (with the date next to it) and 0 is the 12Z position.

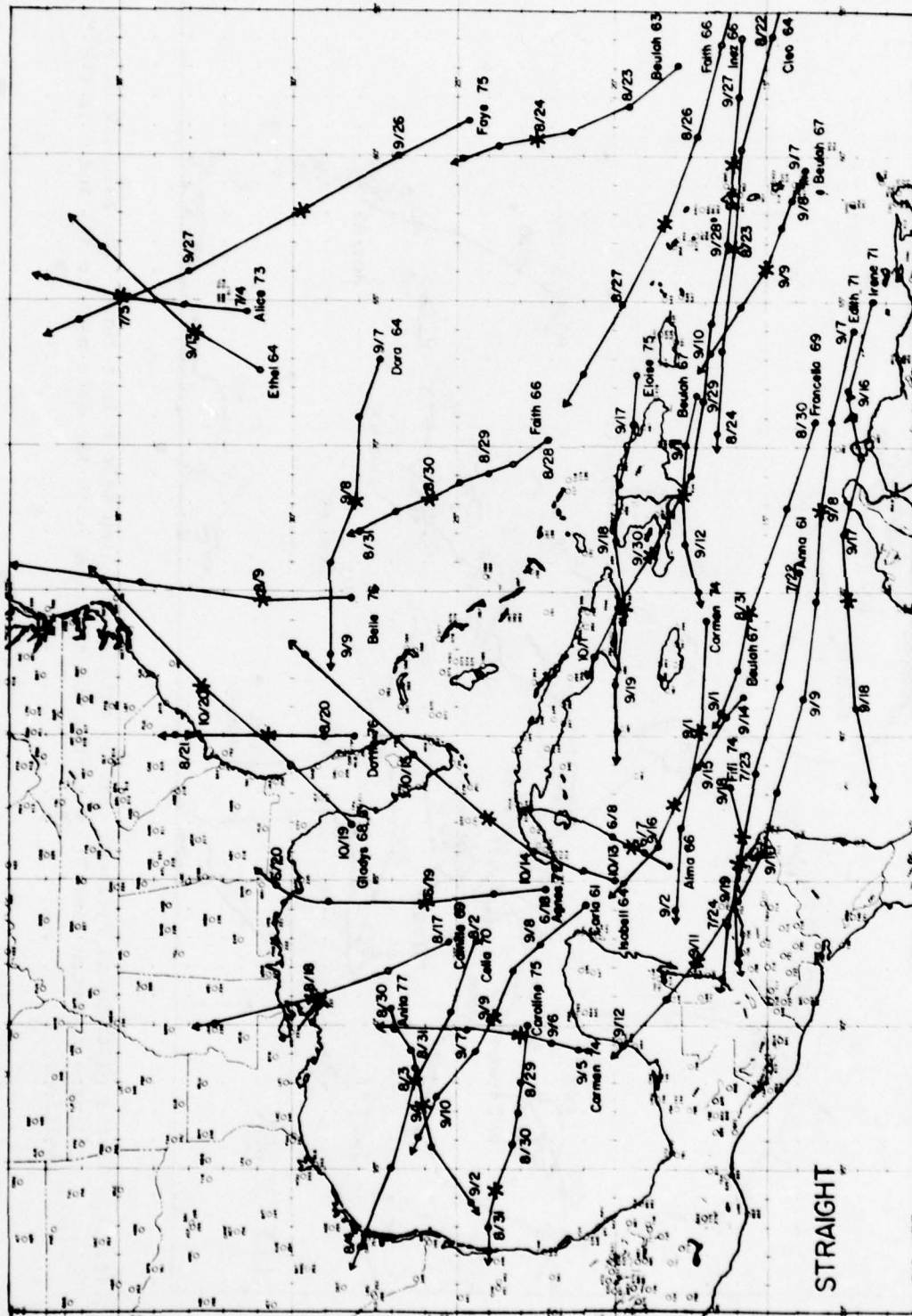


Fig. 25. Same as Fig. 24 except for straight-moving tropical cyclones.

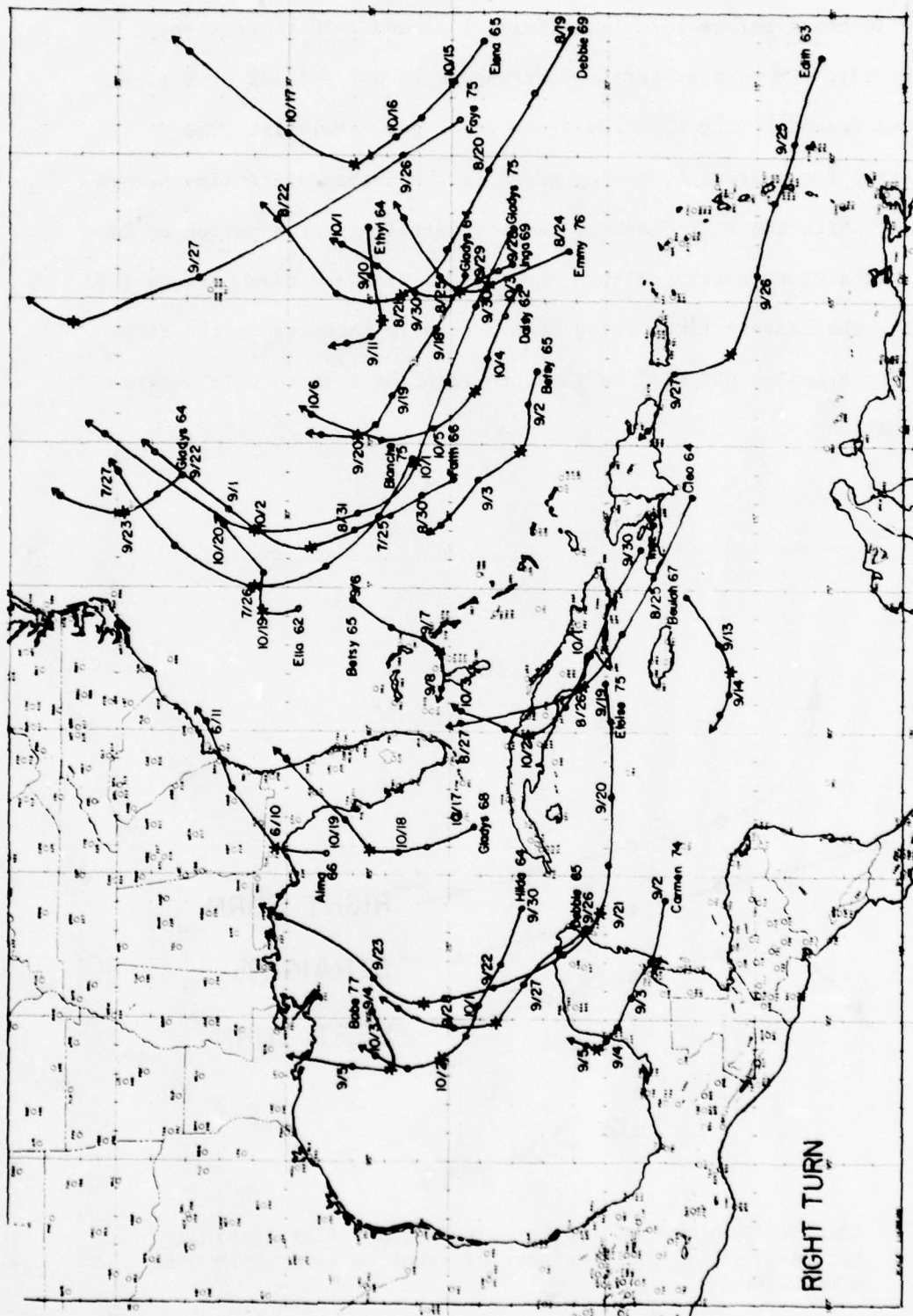


Fig. 26. Same as Fig. 24 except for right-turn tropical cyclones.

composited: time when the storm starts to turn (turn time, T), and 12, 24, and 36 hours before turn time (T-12, T-24 and T-36 respectively, see Fig. 27). These time periods correspond to 00Z and 12Z best track positions issued by the NHC from storm track post-analysis. The T designation for a straight-moving storm is the intermediate time before and after which the storm moved relatively straight for a period of 24 hours. If a storm starts to turn between two standard time periods (00Z and 12Z), the nearest time period before turn is taken to be the turn time. For example, 00Z will be the turn time for a storm which starts to turn at 06Z.

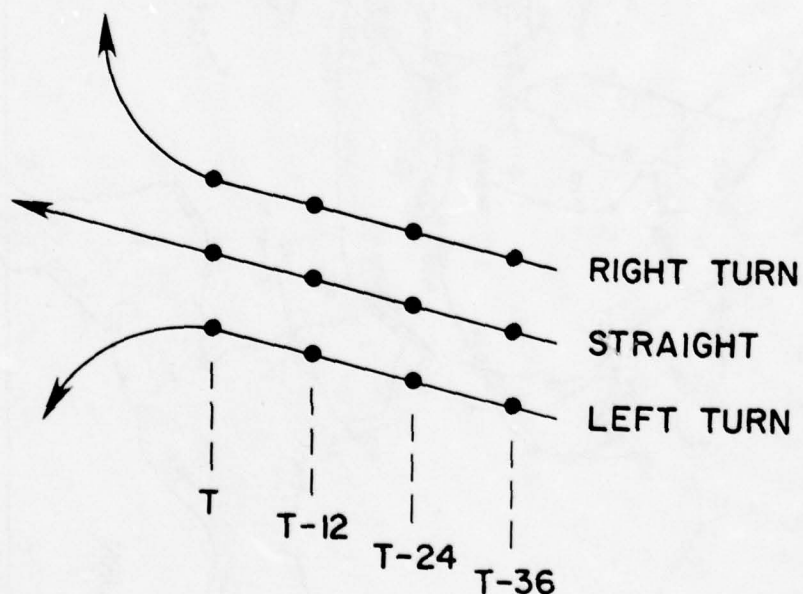


Fig. 27. Idealized picture of the three turn classes of tropical cyclones and of the time periods prior to turn which were composited.

Compositing is performed on a 15° latitude radius¹ cylindrical grid consisting of eight octants and eight radial bands, as shown in Fig. 28. The center of the grid corresponds to the storm center. The grid is rotated so that Octant 1 is aligned along the direction of storm motion (see Fig. 28). See George and Gray (1976) for a more detailed description of this coordinate system.

Each wind vector is resolved into two components, one parallel to the direction of storm motion (V_p) and one normal to it (V_N), as shown in Fig. 29. All wind observations falling within a particular octant and radial band are averaged to give the composite V_p and V_N within that sector. The averaging processes are described in greater detail by Frank (1977a).

5.2 Surrounding Flow at Turn Time

The motion of tropical cyclones seems to be best related to mid-tropospheric flow patterns. George and Gray (1976) in a composite study of tropical cyclones stratified according to direction of storm motion, intensity, etc. found that 500 mb is the best steering level for direction and 700 mb is the best for cyclone speed. To better refine our knowledge of the steering flow associated with cyclones undergoing turning motion, we have studied the composite flow fields at 900 mb, 700 mb, 500 mb, and 200 mb at turn time for the three turn classes. Although 500 mb is found to be the best steering level, flow fields at the upper (200 mb) and lower (900 mb) tropospheric levels also appear quite useful. The component of the wind normal to the direction of storm motion (or V_N) appears to correlate best with turning motion at turn time.

¹ Hereafter, all distances are referred to in degrees latitude.

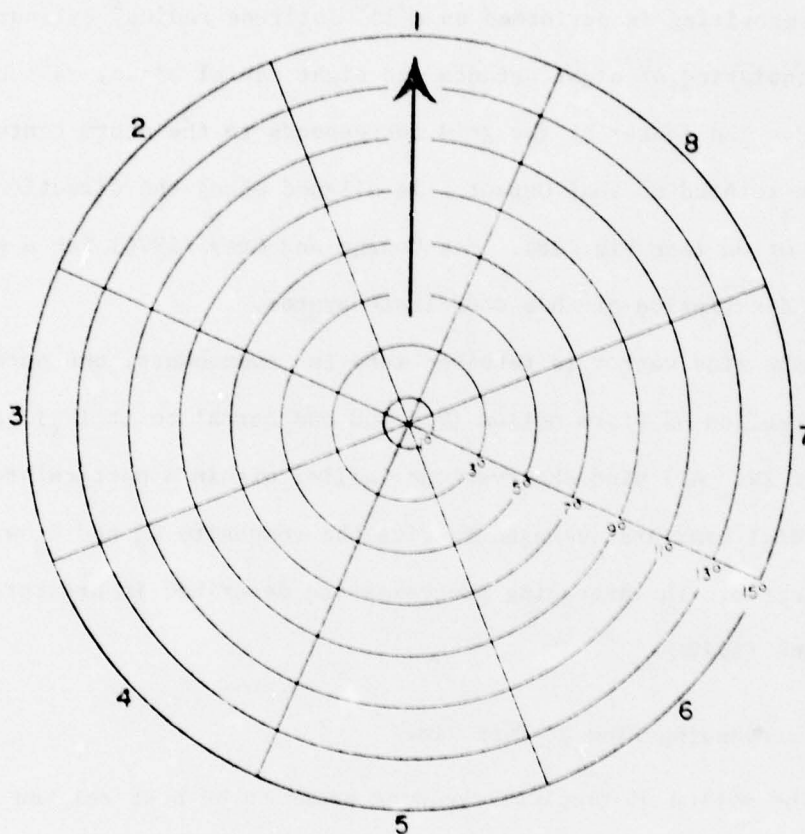


Fig. 28. Grid used for compositing rawinsonde data. The arrow points in the direction of storm motion. Outer numbers denote octants. Numbers inside grid indicate distances from the center in degrees latitude.

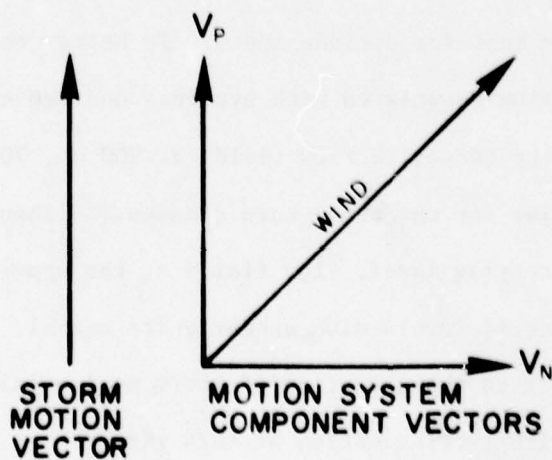


Fig. 29. Parallel (V_P) and perpendicular (V_N) components of a wind vector showing their relation to the storm motion vector.

Flow field at 500 mb. Figure 30 shows the composited 500 mb flow fields at turn time for the three turning classes. These streamline patterns clearly verify the middle level steering flow concept.

To describe this in more quantitative terms, the V_N components of the wind at 500 mb in the front and back octants are shown in Fig. 31. The number next to each arrow indicates the magnitude of the V_N component in m s^{-1} within radii 5° to 11° . Taking a weighted average of V_N in the front three and back three octants (V_N in octants 1 (front) and 5 (back) are given a weight of one and those in the right and left octants a weight of 0.5), and subtracting the back octant average from the front octant average, we obtain the V_N shear values shown at the bottom of the figure. These front to back V_N shear differences correlate well with turning motion at turn time.

With the present and increasingly limited oceanic middle level observation network, such 500 mb level information would be regularly available only if special reconnaissance flights are made around storms at these outer radii. Since upper and lower tropospheric wind data are becoming more available with time from satellite and jet aircraft observations it would be more useful to establish (if possible) steering flow relationships at these levels.

Upper and Lower Tropospheric Flow. The $5-11^\circ$ radius average of the front and back octants V_N (200 mb) and V_N (900 mb) for the three turn classes at turn time is shown in Fig. 32. About the same magnitude front minus back V_N shear differences are found for the turn classes as those found for 500 mb. It should thus be possible to use the average 200 mb and 900 mb winds to infer turning motion of tropical cyclones at turn time.

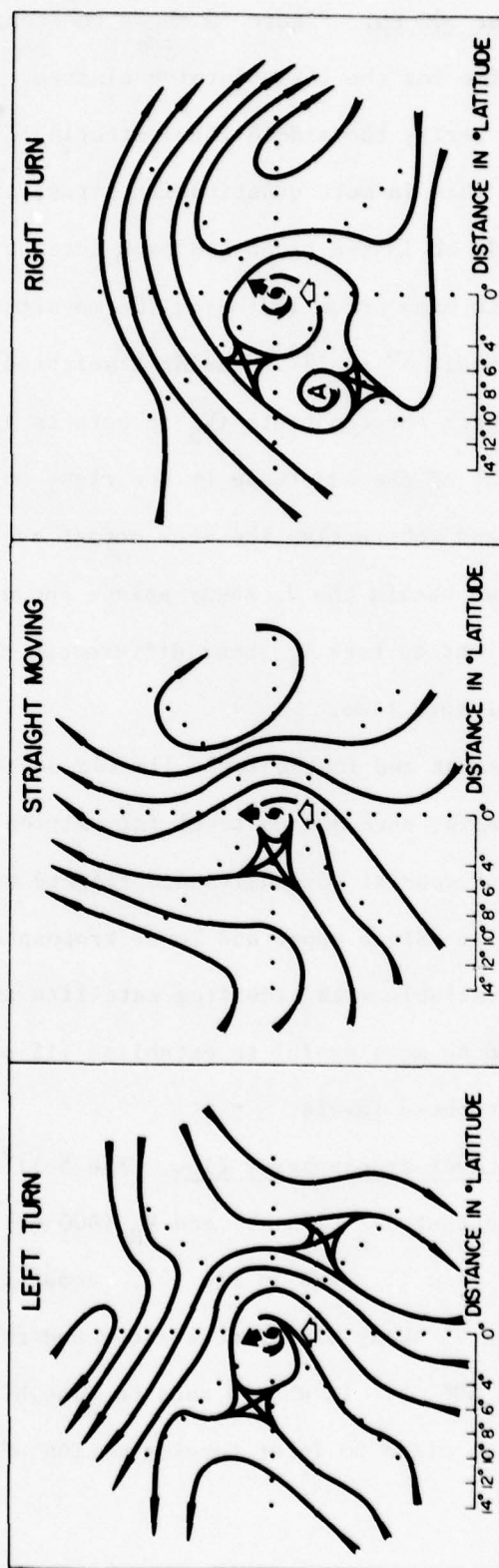


Fig. 30. 500 mb streamlines for the three turn classes at turn time. Open arrows indicate the instantaneous direction of storm motion. Solid arrows indicate the movement of the storm during the next 12 hours.

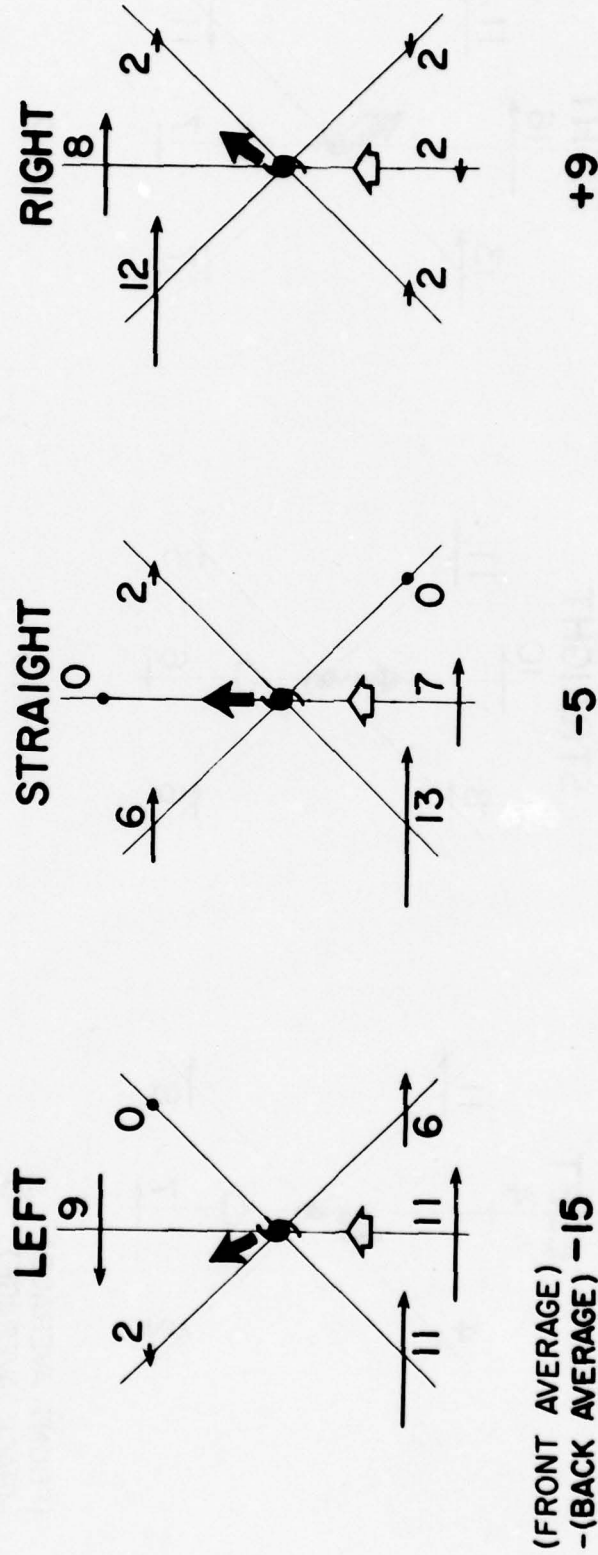


Fig. 31. Sum of V_N in m s^{-1} at 500 mb within 5° to 11° radii from the storm center in various octants at the turn time T . The length of the arrow is proportional to the magnitude of the wind. See text for description of averaging process. Open arrows indicate the instantaneous direction of storm motion and solid arrows the movement of the storm during the next 12 hours.

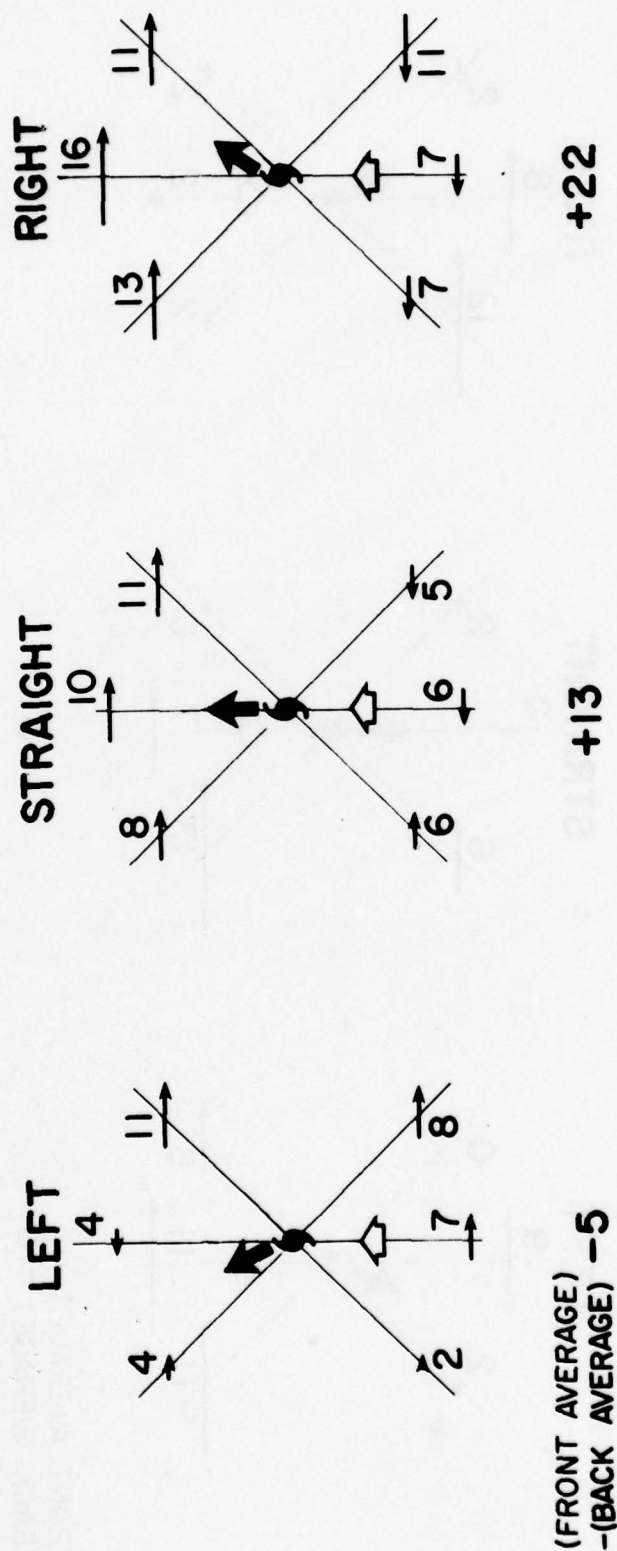


Fig. 32. Same as Fig. 31 except V_N is the sum of the average winds between 200 mb and 900 mb at the turn time (T).

5.3 Surrounding Flow Before Turn Time

A study of the composite V_N flow fields 24 or 36 hours before turn time at various levels reveals no significant differences between the turn classes. This is to be expected since, by definition, storms will still be moving straight. The V_p component of the wind at 500 mb and the upper (200 mb) and lower (900 mb) troposphere, however, shows important relationships with cyclone turning motion 24-36 hours before it takes place.

500 mb Flow. The V_p component of the winds (parallel to the direction of storm motion) at 500 mb in the front left (2), back left (4), back right (6), and front right (8) octants are found to best correlate with turning motion 24 to 36 hours before turn time. These components are shown in Fig. 33. At 24 hours before turn time (T-24), there exists at the front of the storm a strong cyclonic shear of V_p ($V_p(\text{right}) - V_p(\text{left})$) for the left-turning storms. This shear is denoted by $\Delta V_p / \Delta n$, where Δn represents the distance between octants 2 and 8 or 4 and 6. This front V_p shear is about zero for the other two turn classes. Behind the cyclone, the right minus left V_p shear is cyclonic for all three classes. The magnitude of this V_p shear is largest for right-turning storms. Subtracting the V_p right minus left shear behind the storm from that in front of the storm, $[(V_{p_8} - V_{p_2}) / \Delta n] - [(V_{p_6} - V_{p_4}) / \Delta n]$ where the subscripts denote octant numbers, we obtain a front minus back V_p shear which might be used to identify the type of motion a storm is going to take in 24 hours: a positive value for left-turning, small negative value for straight-moving and large negative value for right-turning.

At 36 hours before turn time (T-36) a similar difference in the

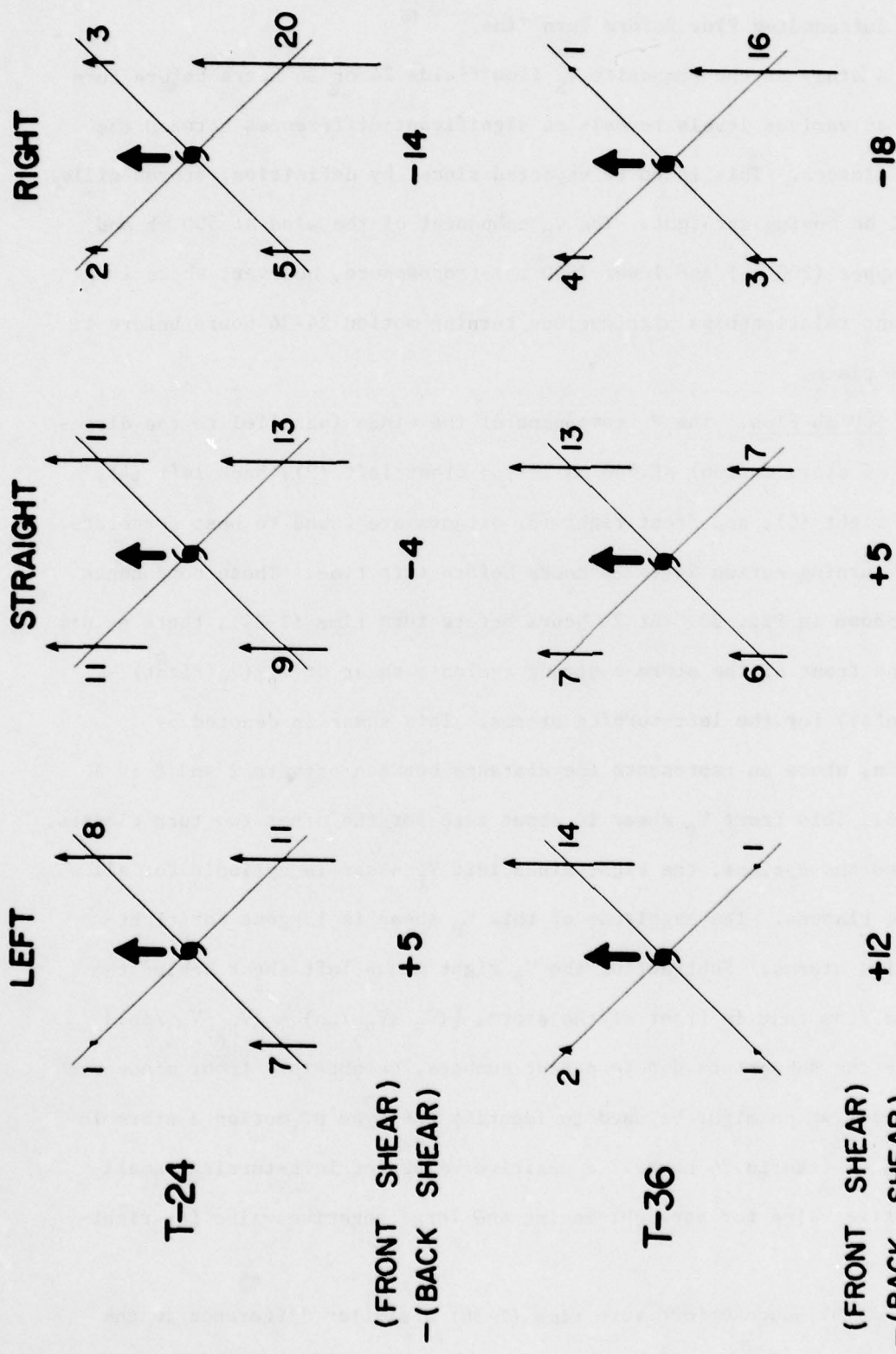


Fig. 33. Sum of 500 mb V_p component of the winds within 5-11° from the storm center in octants 2, 4, 6, 8 for the three turn classes at 24 (T-24) and 36 (T-36) hours before turn time. The heavy arrow indicates the direction of storm motion. See text for description of calculating the front and back shear.

front minus back V_p shear exists between the three turn classes, as indicated in the lower half of Fig. 33. Notice that the front minus back V_p shear for straight-moving storms at T-36 is the same as that for left-turning storms at T-24. This appears to reduce the distinguishing power of this shear to forecast turning. However, given the current low skill of forecasting turning motion, this 500 mb shear information may still be useful.

If aircraft reconnaissance flights were available to better measure these middle level outer radius shear patterns, then an improvement in forecasting turning motion might result. Such aircraft reconnaissance requires special prop aircraft capability and will likely be unavailable in many or most cyclone forecast situations. By contrast, satellite-derived winds in the upper and lower troposphere should be available in most forecast situations.

Upper and Lower Tropospheric Flow. The components of the 200 mb and 900 mb vertical wind shear parallel to the direction of storm motion 24 to 36 hours before turn time are significantly different between the three turn categories.

Figure 34 shows the average V_p wind within 7° to 11° radius from the storm center in octants 1 (front) and 5 (back) at 200 mb and 900 mb 24 hours before the turn time (T-24). In front of the storm, right-turning cyclones show a large negative wind shear between these two levels ($V_p(200 \text{ mb}) - V_p(900 \text{ mb})$) while both left-turning and straight-moving storms have positive wind shear values. Behind the storm, the vertical wind shear is negative for straight-moving storms and slightly positive for the other two turn classes. If we add the front and back wind shear values, we obtain net vertical wind shears in the direction

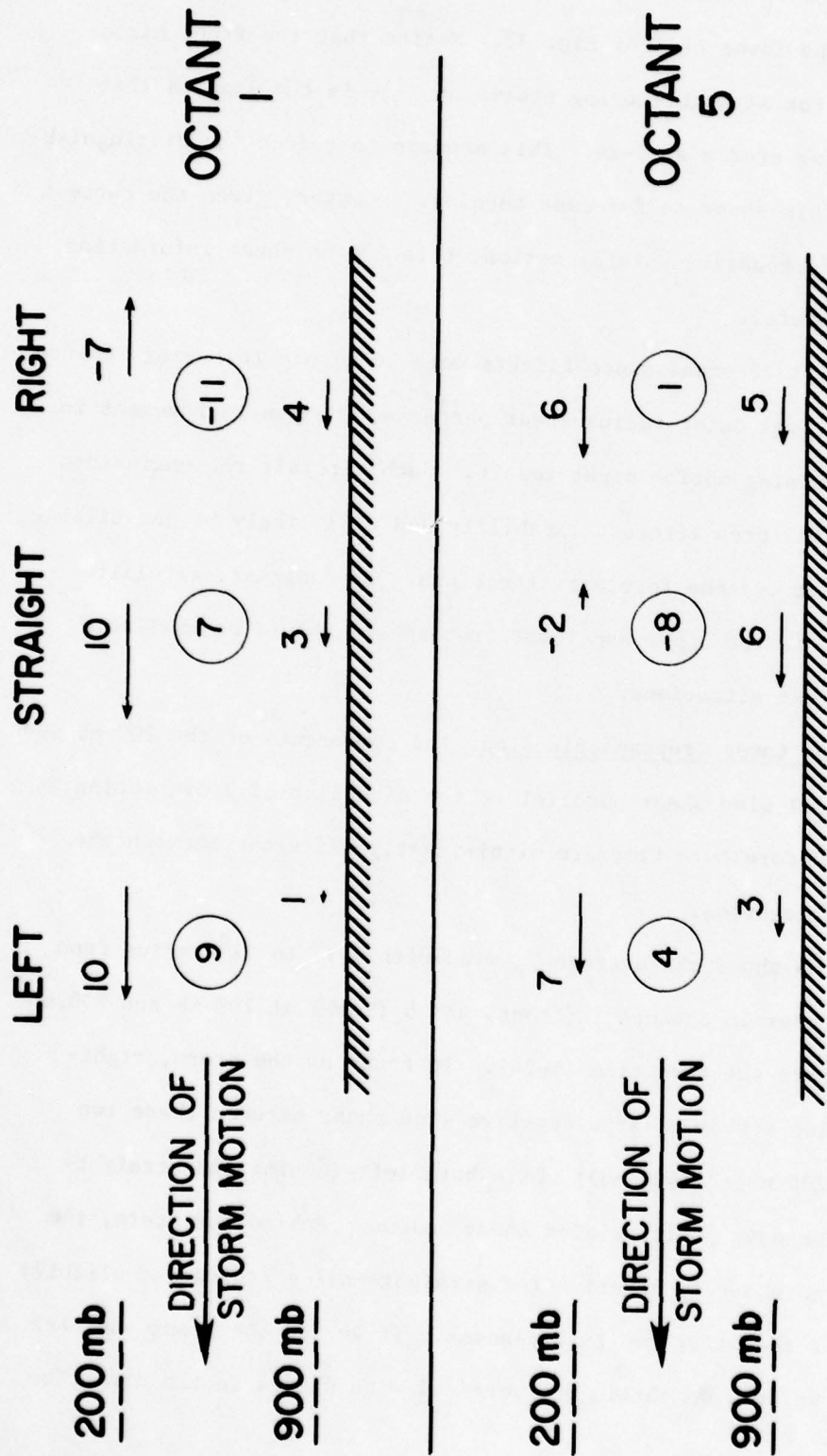


Fig. 34. Cross-sectional view of the average V_p wind components at 200 mb and 900 mb in m s^{-1} within $7^\circ-11^\circ$ radius from the storm center in octants 1 and 5 24 hours before turn time $(T-24)_{-1}$. The circled numbers are the values of the vertical wind shear ($V_p(200 \text{ mb}) - V_p(900 \text{ mb})$) in m s^{-1} .

of storm motion of 13, -1, and -10 m s^{-1} for left, straight, and right-moving cyclones, respectively. The same shear values at T-36 are 7, -1, and -20 m s^{-1} (see Fig. 35). Thus, for left-turning storms the net vertical wind shear in the direction of storm motion in octants 1 (front) and 5 (back) is positive. The shear is about zero for a straight-moving storm and negative for a right-turning storm.

Such differences in tropospheric vertical wind shear between the turn classes only exist 24 and 36 hours prior to turn time (see Fig. 36). Shear differences disappear as the storm approaches its turn time.

If one is able to obtain winds in the upper and lower troposphere around a storm (for example, from satellite observations), it may be possible to better anticipate cyclone turning motion 24-36 hours before it takes place.

Individual Case Analysis. To see how valid the composite results are for individual turning storms, we also investigated the V_p vertical shear for individual cases in the sample. Individual case analysis is severely handicapped by data availability. Wind and height data must be interpolated from analyzed weather maps. Nevertheless, an attempt was made to evaluate this vertical shear parameter ($V_p(200 \text{ mb}) - V_p(900 \text{ mb})$) for individual turning situations. The 200 mb winds were estimated from the height contours, using the geostrophic wind relationship. If there were no contour maps an estimate was made from the 200 mb streamline analysis. If neither was available, the case was not analyzed. The 900 mb winds were estimated from either the 3000' PIBAL maps or from the National Hurricane Center ATOLL (top of the Ekman Layer) maps. If neither was available, an estimate was made from surface pressure maps, again using the geostrophic wind relationship. These methods

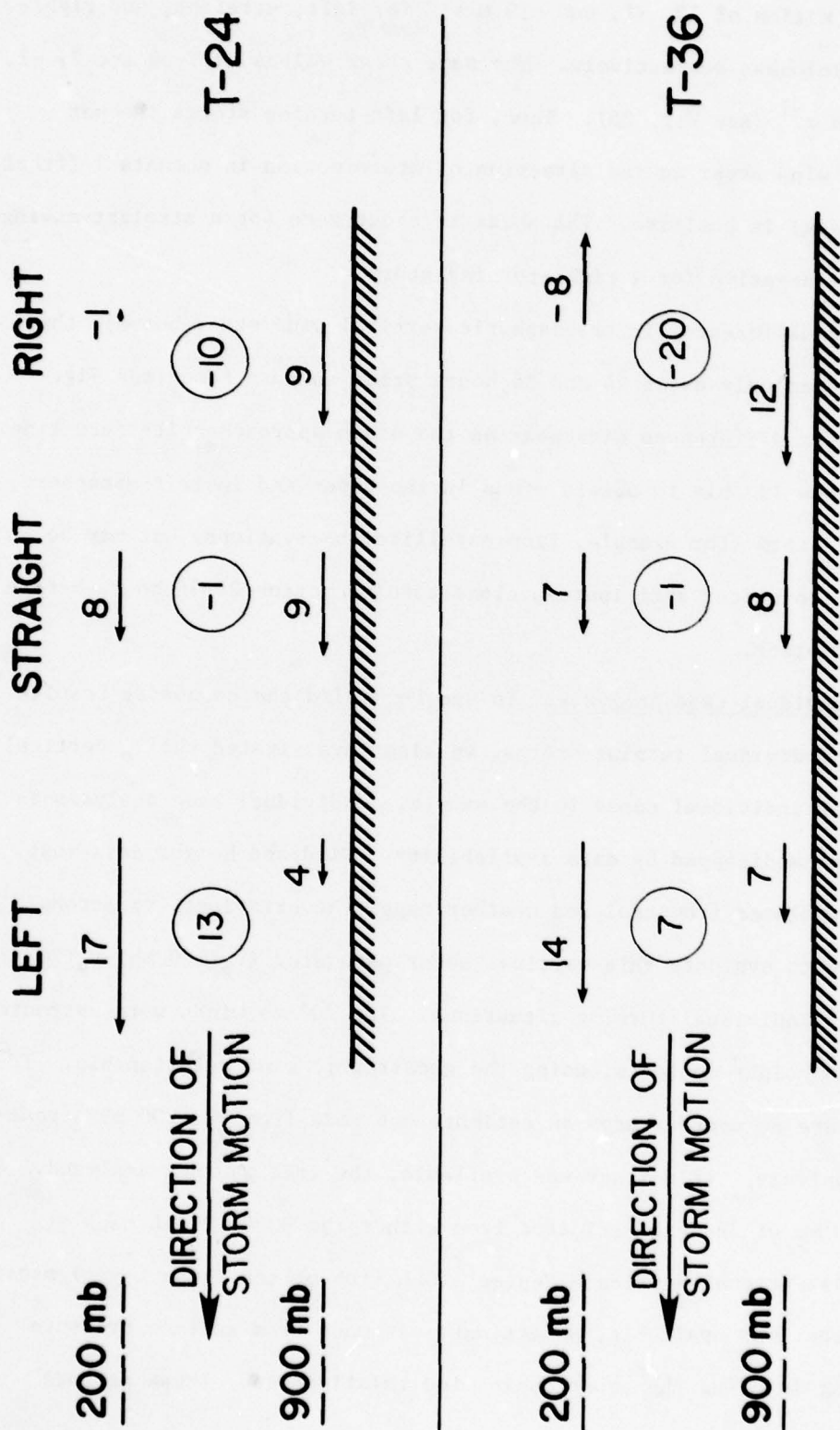


Fig. 35. Cross-sectional view of the sum of average V_p wind components within $7^\circ-11^\circ$ from the storm center in octants 1 and 5 at 200 mb and 900 mb at 24 (T-24) and 36 (T-36) hours before turn time for the three turn classes.

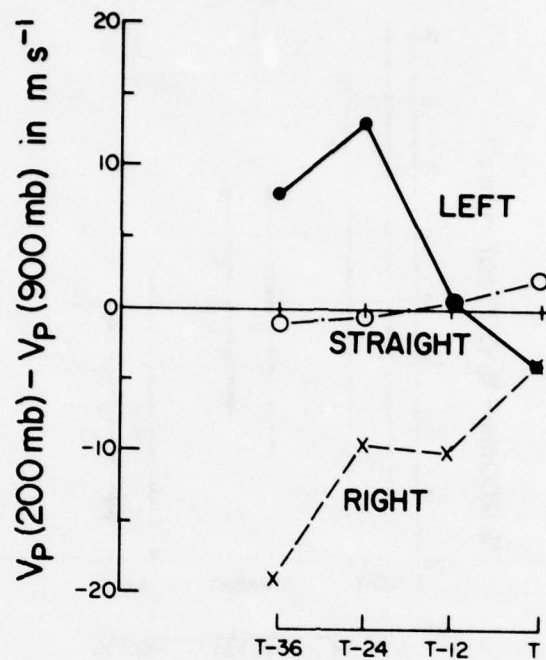


Fig. 36. Vertical wind shear for different time periods. The ordinate is the value of the average vertical wind shear in m s^{-1} within 7° - 11° radius from the storm center.

restricted the analysis of the V_p vertical wind shear to only about two-thirds of the individual cases in the sample. Figure 37 shows the spread of shear values obtained. Although there is a large spread in the vertical wind shear for each classification (which is to be expected because of the inherent data uncertainties) a satisfactory relationship between the vertical wind shear and the turning motion exists for most cases. If we set threshold values for the 200-900 mb V_p vertical wind shear as:

- > 5 LEFT TURN
- 5 to 5 STRAIGHT
- < -5 RIGHT TURN

it is found that 64% of the left turning storms have vertical wind shears greater than 5 for both T-24 and T-36 time periods. For the straight-moving storms, 77% occurred within the range at T-36 and 75%

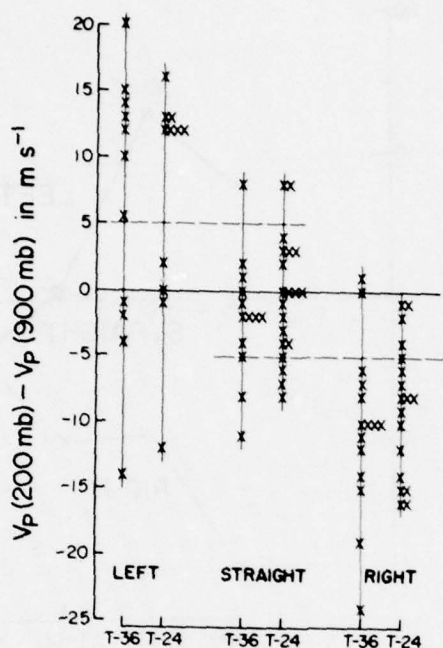


Fig. 37. Vertical wind shear at T-24 and T-36 time periods for individual storms. The ordinate is the same as in Fig. 36. Each cross represents the wind shear value from one storm. Equal values of the wind shear are plotted next to each other. The dashed lines indicate the threshold values described in the text.

at T-24. 87% of the right-turning storms have vertical wind shears less than -5 at T-36 and 72% at T-24. The present skill in forecasting turning motion is considered to be significantly less than this, as evident from the scatter of forecast points shown in Fig. 22.

Since the skill in deriving lower and upper tropospheric winds from (geostationary) satellite observations is increasing, the information on such vertical wind shear should become more available as time goes on. One might then expect an improvement in future turning motion forecasts.

5.4 Study of Satellite Temperature Sounding Data

The vertical wind shear structure described in the last section should be related through the thermal wind relationship to the mean

tropospheric temperature gradients across these storms. An estimate of the magnitude of the temperature gradient can be obtained from the thermal wind equation:

$$\frac{\Delta T}{\Delta n} \approx \frac{f}{R} \left[\ln \left(\frac{p_1}{p_2} \right) \right]^{-1} V_T \quad (5.1)$$

where Δn = horizontal distance across which a temperature difference ΔT is measured, V_T is the thermal wind, or in this case, $V_p(200\text{mb}) - V_p(900\text{mb})$, $p_1 = 900$ mb, $p_2 = 200$ mb, f the Coriolis parameter and R the gas constant. If we assume f to be $5 \times 10^{-5} \text{ s}^{-1}$ (corresponding to 20°N) and $\Delta n = 18^\circ$ latitude, then for a vertical wind shear of 10 m s^{-1} , $\Delta T \approx 2.2^\circ\text{C}$.

To investigate the existence of such a gradient, temperature sounding data from the Nimbus 6 Scanning Microwave Spectrometer (SCAMS) were examined. Since the wind shear obtained from the composite study is of this order of magnitude, we should expect the sounder data to specify turning motion.

The Scanning Microwave Spectrometer. The Scanning Microwave Spectrometer (SCAMS) on board the Nimbus 6 polar-orbiting satellite is a five channel instrument sensing radiation nominally at 22.235, 31.65, 52.85, 53.85, and 55.45 GHz (Staelin et al., 1975a). The upper three channels are used for sounding the atmosphere, while the lower two are used to infer vertically integrated atmospheric water vapor and liquid water content. The Nimbus 6 spacecraft is in a sunsynchronous (1130 and 2230 Local Time) near-polar orbit at an altitude of approximately 1100 km. The SCAMS instrument scans across the spacecraft track in 13 steps at 7.2° intervals each 16 s which results in a spatial resolution of

145 km near nadir, degrading to 200 km downtrack by 360 km crosstrack at the maximum scan angle. Approximately 400 individual soundings can be obtained within 15° of the center of a tropical cyclone for each 12 hour period.

Tropical Cyclones Analyzed. A total of 13 cases (11 individual storms) in both the Pacific (NE and NW) and Atlantic Oceans during 1975 were examined. This is all the SCAMS information available to us at this time. The tracks for these storms are shown in Fig. 38. The distribution of storms in each turn class is given in Table 16. Satellite data were categorized by time (T, T-12, T-24, T-36) as described in section 5.1. The mean 1000-250 mb temperatures around each storm for each time period were derived from the brightness temperatures (the raw data obtained from the sounder) as described in Waters *et al.* (1975). The same method used in the rawinsonde composite was employed to obtain average layer mean temperature at each of the grid points in Fig. 38 for each storm. To minimize contamination by precipitation, data points with integrated liquid water contents $\geq 0.5 \text{ kg m}^{-2}$ (precipitable mm) were not used in the averaging process. This, according to Staelin *et al.* (1975b), should eliminate most of the contaminated data.

The accuracy of atmospheric temperatures derived from satellite sounders is a pertinent point. Data from a microwave sounder were used because microwave soundings are unaffected by non-raining clouds (Staelin *et al.*, 1975b). The extensive cloudiness near tropical cyclones precludes the exclusive use of infrared sounding data. When the 1000-250 mb layer mean temperature at a single spot is compared with the nearest grid point layer analyzed by the National Meteorological Center (NMC) the root-mean-square difference is approximately 2 K (Landsat/

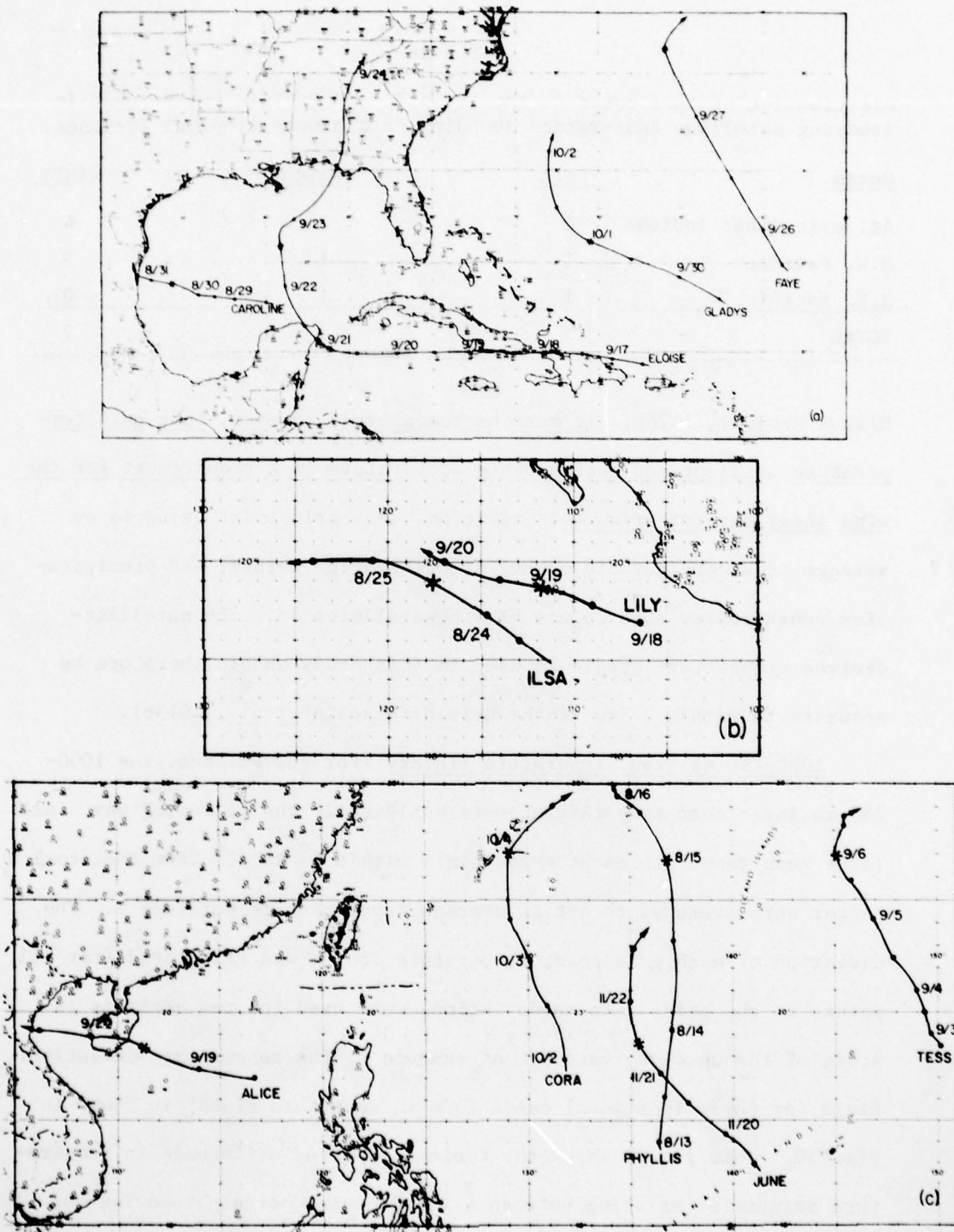


Fig. 38. Tracks of 1975 tropical cyclones in various oceans used in the Nimbus 6 SCAMS temperature sounding study. (a) NW Atlantic Ocean (West Indies); (b) NE Pacific Ocean; (c) NW Pacific Ocean. Track symbols are the same as in Fig. 24.

TABLE 16

Distribution of turn cases in the Atlantic and Pacific Oceans used in studying satellite temperature sounding data around tropical cyclones.

<u>Ocean</u>	<u>Left</u>	<u>Straight</u>	<u>Right</u>
Atlantic (West Indies)	0	2	4
N.W. Pacific	1	1	3
N.E. Pacific	1	1	0
TOTAL	2	4	7

Nimbus Project, 1976). It must be remembered, however, that only temperature gradient and not absolute temperature is a requirement for the wind shear determination. In addition, each grid point value is an average of a considerable number of observation points, and precipitation-contaminated data points have been eliminated. The satellite-derived temperature gradients used in this study should therefore be accurate to within a few tenths kelvin (Staelin et al., 1975b).

1000-250 mb Mean Temperature Fields. For convenience, the 1000-250 mb layer mean temperatures were analyzed in the following way. All layer mean temperatures at grid points within 5° to 15° from the storm center were averaged to get an average layer mean temperature \bar{T} . The deviation of each grid point temperature from \bar{T} was calculated (for all points in the grid). These deviations were used for the analysis instead of the absolute values. An example of the temperature deviation field for three individual cases (one in each turn class) is shown in Fig. 39. This figure shows the typical expected difference in temperature structure existing between a left-turning, straight-moving and right-turning storm as implied by the difference in vertical wind shear structure discussed in the last section. The left-turning storm shows

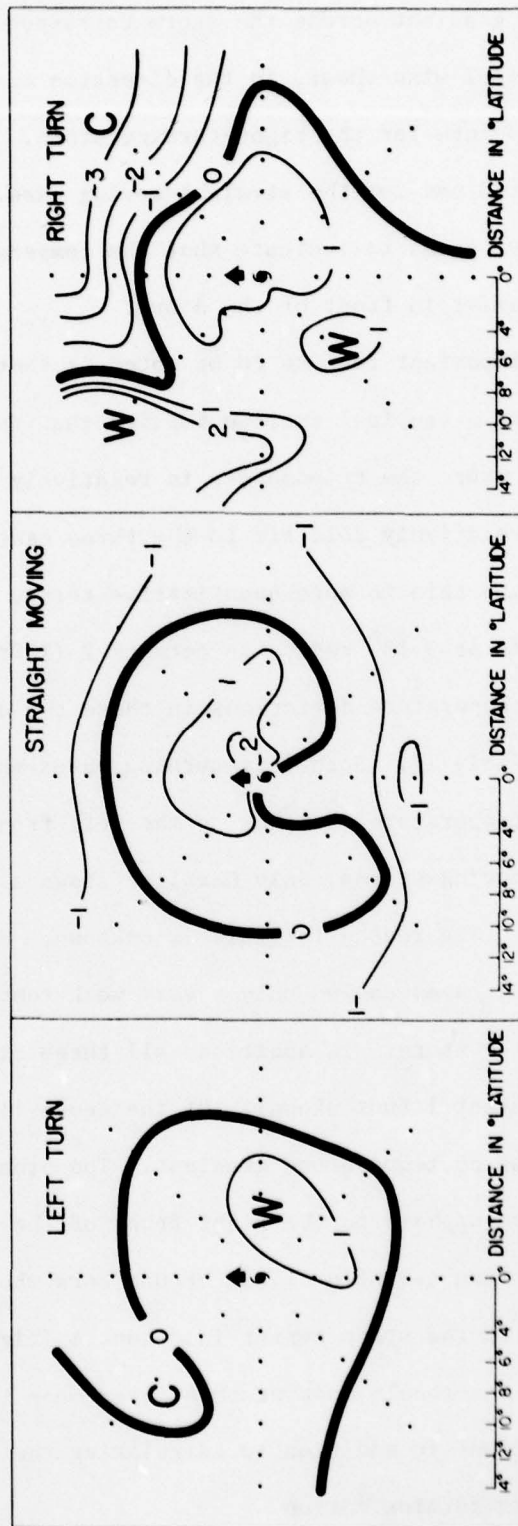


Fig. 39. 1000 mb to 250 mb layer mean temperature deviation from the 5° to 15° average mean temperature derived from the Nimbus 6 SCAMS temperature sounding data 24 hours before turn time. The arrow from the storm center indicates the direction of storm motion.

a temperature gradient across the storm corresponding to a thermal wind, or vertical wind shear, in the direction of storm motion while the opposite occurs for the right-turning storm. There is very little temperature gradient for the straight-moving case. An examination of all other cases seems to indicate that the temperature gradients of most significance exist in front of the storm.

Another important feature to be noted is that such a temperature gradient across a tropical cyclone implies that the storm tends to move into a region where the troposphere is relatively cold - as indicated by the areas of relatively cold air in the three cases shown in Fig. 39.

To describe this in more quantitative terms, we studied the temperature deviations at $9-13^{\circ}$ radius in octants 2 (left front) and 8 (right front). The temperature deviations in these two octants for all cases are shown in Table 17. Both left-turning cases show that the mean tropospheric temperature is lower to the left front of the storm. For the straight-moving storms, only Caroline shows a large negative tropospheric shear. The reason for this is unknown. However, all other straight-moving cases showed only a very weak temperature gradient across the front of the storm. In addition, all three cases show a region of cold air in octant 1 (not shown). Of the seven right-turning storms, only Cora shows no temperature gradient. The others indicate a relatively cold troposphere to the right front of the storm. An examination of the temperature deviation field around Cora shows that the coldest spot is 15° from the storm center in octant 8 (right front). This suggests that one should look at this layer mean temperature field around a tropical cyclone in addition to calculating the temperature gradients to forecast its turning motion.

TABLE 17

1000-250 mb layer mean temperature deviations from 5° - 15° average in octants 2 (left front) and 8 (right front) within 9° to 13° radius from the storm center for various storms in the Northern Pacific and Atlantic Oceans 24 hours before turn time. Vertical wind shear in the direction in which the storm is going is calculated from the thermal wind relationship using a horizontal gradient of 18° . f is taken to be $5 \times 10^{-5} \text{ s}^{-1}$.

Storm	Region	Octant 2	Octant 8	(Octant 2)-(Octant 8)	Corresponding Vertical Wind Shear (m s^{-1})	Turn
Phyllis	W. Pacific	-0.8	0.2	-1.0	4.5	Left
Ilisa	E. Pacific	-0.9	1.5	-2.4	10.9	Left
Alice	W. Pacific	-0.7	0.0	-0.7	3.2	Straight
Lily	E. Pacific	-0.6	-0.1	-0.5	2.3	Straight
Eloise	W. Atlantic	0.2	0.2	0.0	0.0	Straight
Caroline	W. Atlantic	-1.1	2.9	-4.0	18.2	Straight
Eloise	W. Atlantic	1.5	-0.2	1.7	-7.7	Right
Eloise	W. Atlantic	1.6	-2.0	3.6	-16.4	Right
Gladys	W. Atlantic	0.1	-1.4	1.5	-6.8	Right
Faye	W. Atlantic	0.3	-0.4	0.7	-3.2	Right
June	W. Pacific	0.7	-1.6	2.3	-10.5	Right
Tess	W. Pacific	-0.7	-1.9	1.2	-5.5	Right
Cora	W. Pacific	1.0	1.0	0.0	0.0	Right

These results were obtained, as described earlier, after elimination of data points with integrated liquid water content ≥ 0.5 precipitable mm. To see if this process is of any great significance, we also analyzed the temperature deviation fields without eliminating any data. A comparison between the two sets of results shows very little difference in the temperature structure and temperature gradients at large radii from the storm center. It would seem therefore that it is not necessary to eliminate those data points with appreciable liquid water content provided temperatures at large distances from the storm center are used.

This satellite sounder data indicates that very pertinent information on forecasting tropical cyclone turning motion 24 to 36 hours in advance may be obtained in regions devoid of rawinsonde, aircraft and clouds for wind vector determination.

5.5 Discussion

The results of this study indicate that there are parameters in the large-scale environment around tropical cyclones at upper and lower tropospheric levels (in addition to the previously-considered crucial middle level) which can provide information about their turning motion 24-36 hours before it occurs. An estimate of the V_N component of the winds at 200 mb and 900 mb for $5-11^\circ$ radius around the storm from satellite observations may be used to make a more reliable short range (0-12 hour) forecast of turning motion. Of greater significance is the possibility of obtaining the V_p vertical wind shear to specify the probability of turning motion 24-36 hours in advance. The fact that 'favorable' environmental conditions are evident 24-36 hours prior to turn time indicates that there may be a time lag between a change in the surrounding flow parameters and the response of storm to such changes.

Sometimes, it may be difficult to derive winds at these two levels from satellite observations because of an extensive cirrus canopy or because upper-level cloud motions are lacking. In these cases satellite sounder data, with its tropospheric temperature measurement capability, may be useful to augment missing wind data. Since contamination of the sounding data by precipitation is negligible at large radii, the Microwave Sounding Unit (which does not have any water vapor channel) on board the TIROS-N satellite now in orbit might be used to monitor tropospheric temperature gradients across a storm to determine the upper to lower tropospheric vertical wind shear. We suggest that temperature data obtained from such a sounder be used on an operational basis to test the applicability of these results.

Another important result of this study is the time difference between the presence of a temperature gradient (at 24-36 hours before turn time) and the appearance of a suitable steering flow at middle-level (at turn time). This may suggest that winds in the middle level are responding to the large-scale temperature gradients. One of the problems in cyclone track forecasting is the fact that we still do not know the physical mechanism which causes the movement of tropical cyclones. A study on the dynamics of this process may lead to a better understanding of the underlying physics of storm motion.

With the large increase in computer technology and the development of more sophisticated cyclone forecast schemes, one would expect a continuous increase in tropical cyclone forecast skill. While this has been true on the average in the 1960's and early 1970's, cyclone track 24 hour forecast errors have been showing a slight increase in the last

90

three to four years². These forecast error increases are likely a result of an over-reliance by the various forecast techniques on middle level flow patterns, and a subsequent gradual reduction of oceanic rawinsonde and aircraft data to measure such flow patterns. Atlantic weather ships Echo and Delta were decommissioned in 1973. Very few oceanic prop aircraft flights are now made. These changes have significantly reduced the already-scanty mid-tropospheric Atlantic wind-height data. Accurate analysis of middle-level flow fields has always been difficult. At some locations and time periods it is now nearly impossible to obtain a meaningful analysis. Neumann³ has discussed how NMC tropical analysis schemes can produce a quite unrepresentative oceanic analysis which then gives an incorrect (but strong) bias to middle-level steering current determination. He has documented cases in which an erroneous wind observation drastically changes middle-level computer-analyzed flow fields to make them quite unrepresentative of actual conditions. This seriously affects the performance of tropical cyclone forecast models based on middle-level steering flow concepts (Neumann, 1979; Lawrence, 1979). New forecasting schemes (regardless of how sophisticated) which utilize middle level flow patterns will encounter similar unsurmountable observational problems.

Because of the increasing availability of satellite-derived information at upper and lower tropospheric levels, it is suggested that research on storm motion be concentrated on studying the relationships between upper and lower tropospheric parameters and storm movement. The next step to carry this research further will be to try to relate these parameters with cyclone speed changes, stalling and looping motions, and other special cyclone motion characteristics.

^{2,3}Panel discussion, 12th Tech. Conf. on Hurricanes and Tropical Meteorology, April 24-27, 1979, New Orleans, LA, AMS.

6. TROPICAL CYCLONE INTENSITY DETERMINATION FROM UPPER TROPOSPHERIC AIRCRAFT RECONNAISSANCE

It is proposed that attention be given to the possibility of tropical cyclone intensity determination through upper tropospheric jet aircraft reconnaissance. The cyclone's upper level temperature anomaly and its gradient can be related to surface pressure and wind. This is particularly relevant to foreign countries affected by these cyclones who do not have a dedicated low altitude aircraft reconnaissance capability, but have available jet aircraft. No special aircraft instrumentation would be required. Jet flights are faster, longer ranged, and less turbulent (if echoes are avoided), than prop flights. Many more aircraft are available for such missions.

Although very significant strides have been made in the utilization of satellite picture data for cyclone intensity determination (as demonstrated by V. Dvorak, 1975) operational forecasters usually also desire verifying aircraft intensity information when cyclones are nearing populated coastal regions and they must make major forecasting decisions.

Despite the fact that cyclone intensity estimates from satellite picture configurations by Dvorak (1975) have been found to be generally satisfactory in the majority of cases (especially when applied by experts such as V. Dvorak) the relationship between cloudiness configuration and intensity is quite complex and significant difficulties in intensity determination can occur in individual situations. Arnold (1977) has documented some of these cases for West Pacific cyclones. In addition, the satellite reception and interpretation experience in many foreign countries is not adequate for cyclone intensity determination.

Even when maximum wind and central pressure are known there is a question about the reliability of these parameters for estimation of the outer cyclone strength and damage potential. Cyclone damage will vary greatly with the horizontal size of the high wind-low pressure region and the concentrated nature of the inner-core circulation. A specified value of maximum wind or central pressure, as currently available from the satellite intensity estimations, even if accurate, may not allow a forecaster to always make a very reliable evaluation of potential cyclone damage from storm surge, wind, and rainfall.

It is important that the outward horizontal extent of the cyclone's circulation and asymmetry are known. Such information is often not readily available from satellite picture images. Storm cirrus canopies often obscure the measurement of low level wind vectors. Until satellite measurements can provide this information there is likely to be a continued requirement for aircraft reconnaissance in important forecast situations. This is especially true with the improvements in storm warning and evacuation procedures which allow for more wise and orderly civilian response to cyclone alerts.

There are, nevertheless, growing financial and technical difficulties to the continuation of traditional (since mid 1940's) low and middle level aircraft reconnaissance by the United States. The financial and technical requirements of maintaining prop aircraft are becoming more difficult as aviation interests focus more on jet operations. Low level reconnaissance as currently used requires specially equipped and maintained prop aircraft with high instrument and maintenance costs. Also, specially trained crews have to be committed for extended periods of a tropical cyclone season. This is not cost effective.

Those regions affected by these storms typically require only a few crucial cyclone strength determination measurements per year and sometimes none. It is only when cyclones are within 24-48 hours of populated coastal areas that such measurements become so important and redundancy of intensity determination with the satellite becomes critically important. The growing expense of maintaining a traditional prop aircraft reconnaissance capability along with the major developments in satellite technology have led to decisions causing significant reductions in United States reconnaissance flights.

Flights at low levels by prop aircraft are slow (by jet standards) and are usually quite turbulent. Center penetration occasionally cannot be made when cyclones are very intense and extreme turbulence occurs such as with Hurricane Camille (1969). This situation can occur during critical forecast periods just prior to landfall. By contrast, jet aircraft reconnaissance accomplished in the upper troposphere encounters significantly weaker winds, generally less intensity of turbulence (if echoes are avoided), and flight missions can be conducted in half to a third of the time required for conventional prop missions. Nearly all countries have jet aircraft that could be made available on short notice for such upper tropospheric reconnaissance. No special crew training would be required if the flights are conducted with a few trained meteorologists who are temporarily deployed for such flights.

This paper is written to suggest the examination of a new tropical cyclone reconnaissance technique. For emergency situations caused by the approach of a tropical cyclone it is suggested that a jet aircraft could be obtained on an emergency basis for 6-8 hours to make a flight at 250 mb through the center of a threatening cyclone. A determination

of the magnitude and areal extent of the approaching cyclone's upper tropospheric temperature structure could be readily made. Previously prepared monographs and information could be available to translate this upper level temperature information into estimates of low level pressure and wind and horizontal extent of the strong winds. Only the measurement of temperature on a constant pressure surface would be made. Such measurements are routine on jet aircraft. Most oceanic jet airliners have weather radar for echo avoidance. Satellite information would likely be available at the take-off point (major national airports) for flight planning. No extra aircraft crew personnel would be required. Only one or possibly two passes through the upper cyclone would be required. The aircraft would fly a constant pressure level and record temperature at specified intervals of 5-10 n mi. The execution of this flight track might be approximately as indicated in Fig. 40.

Determination of Cyclone Intensity. Tropical cyclones are warm-core systems. Their intensity is proportional to the magnitude of upper-tropospheric temperature anomaly at the cyclone's center. A cyclone's intensity might be directly determined by measurement of this temperature anomaly. Aircraft flights between 200-300 mb - optimum level for jet aircraft flying - may likely give a very accurate measurement of the cyclone's overall intensity and damage potential.

Figures 41 and 42 portray rawinsonde composited temperature anomaly in typhoons and hurricanes as obtained from composited rawinsonde data in the Western Pacific and Western Atlantic. Note that the maximum temperature anomaly occurs in the upper troposphere and that significant temperature anomaly extends 2-4° radius outward from the cyclone's center. Large positive temperature anomaly is not present in the lower layers. At inner radii these upper tropospheric temperature anomalies

AD-A078 624

COLORADO STATE UNIV FORT COLLINS

F/6 4/2

TROPICAL CYCLONE ORIGIN, MOVEMENT, AND INTENSITY CHARACTERISTIC--ETC(U)

AUG 79 W M GRAY

N00228-76-C-2129

UNCLASSIFIED

NEPRF-CR-79-06

NL

2 OF 2

AD
A078624



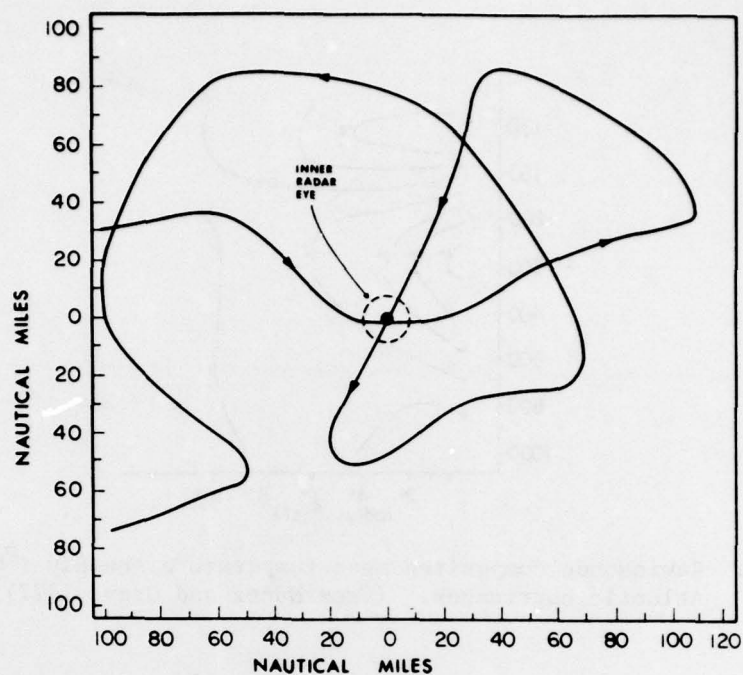


Fig. 40. Flight track flown at 250 mb into Helene on 26 Sept. 1958 by a National Hurricane Research Laboratory B-47 aircraft.

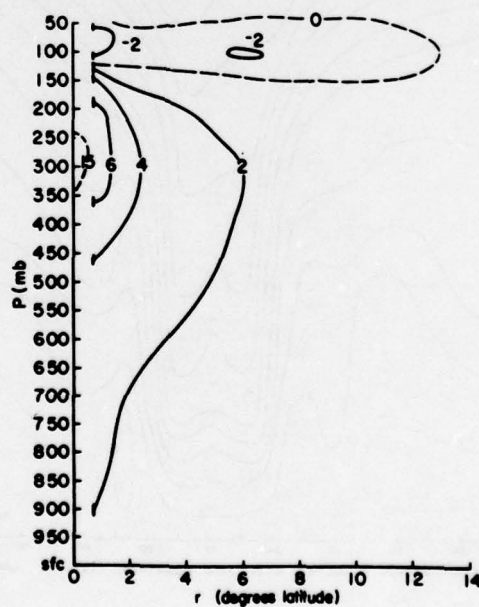


Fig. 41. Rawinsonde composited mean temperature anomaly ($^{\circ}\text{C}$) for West Pacific (from Frank, 1977a). The dashed inner isotherms have been inferred from NHRL aircraft data.

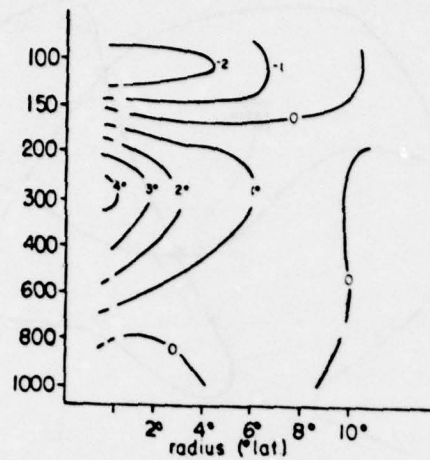


Fig. 42. Rawinsonde composited mean temperature anomaly ($^{\circ}\text{C}$) for West Atlantic hurricanes. (From Núñez and Gray, 1977).

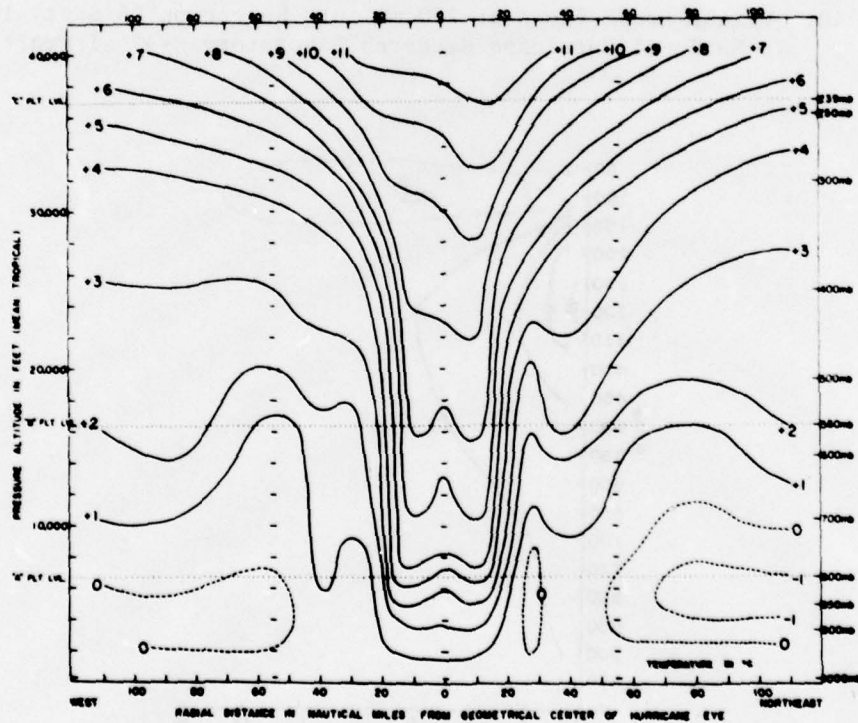


Fig. 43. Vertical cross section of temperature anomaly from mean tropical atmosphere along radial traverse of Hurricane Cleo, 1958. (From LaSeur and Hawkins, 1963).

can be as large as $10-15^{\circ}$ (Figs. 43-44). Figure 45 portrays the inner core (5-50 n mi) radial distribution of upper tropospheric temperature anomaly from the mean summertime tropical atmosphere which has been measured by the National Hurricane Research Laboratory upper tropospheric research flight missions during the late 1950's and 1960's. Note the large inner core gradient of upper tropospheric temperature anomaly which are portrayed. Figure 46 portrays mean inner cyclone region ($0-3^{\circ}$ radius) temperature excess over temperature at $3-7^{\circ}$ radius for five progressively more intense classes of West Pacific cyclones as determined by C. Arnold (1977) from composited West Pacific rawinsonde data. Table 18 describes these intensity classes. Note the direct correlation of average upper level temperature anomaly with intensity class.

TABLE 18

Five West Pacific Tropical Cyclone Intensity Classes (from Arnold, 1977).

Stage	Name	Estimated Mean Central Pressure	Estimated Ave. Max- imum Sustained Surface Winds
		(mb)	(kts)
I	Developing Cluster	1005	15
II	Tropical Depression	1002	25
III	Tropical Storm	990	50
IV	Typhoon	965	80
STY	Super-Typhoon	935	115

Hydrostatic considerations dictate that the surface pressure anomaly (P'_{sfc}) be very closely related to upper tropospheric temperature anomaly (T'). Thus,

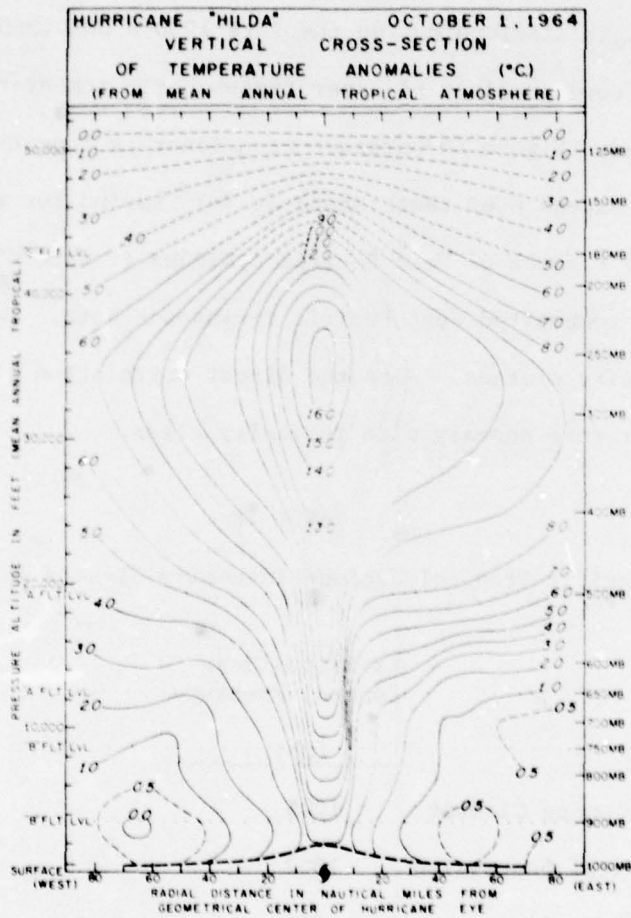


Fig. 44. Vertical cross section of temperature anomaly for Hurricane Hilda on 1 Oct. 1964. (From Hawkins and Rubsam, 1968).

Fig. 46. Mean $0-3^{\circ}$ radius temperature anomaly (ΔT) profiles for five progressively more intense tropical storm stages I, II, III, IV and STY. $\Delta T = \bar{T}(0-3^{\circ}) - (3-7^{\circ})$ for stages I, II and III. $\Delta T = (0-3^{\circ}) - 8^{\circ}$ for stages IV and STY. See Table 18 for a description of these classes of cyclone intensity (from Arnold, 1977).

$$P'_{sfc} = K_1 T' \quad (6.1)$$

where K_1 is a correction coefficient which will vary with T' , pressure level, and radius. K_1 can be empirically specified from aircraft and composited rawinsonde data.

The cyclone's lower tropospheric wind velocity (V) will be related to the radial gradient of T' , radius (r), and some correction coefficient K_2 related to T' , r , pressure level, cyclone azimuth, and also latitude. It can also be empirically determined. Thus,

$$V = K_2 \frac{1}{r} \frac{\partial T'}{\partial r} \quad (6.2)$$

Through a combination of rawinsonde and National Hurricane Research Laboratory research flight information a reliable determination of the K_1 and K_2 correction factors should be obtainable.

Figures 47 and 48 illustrate how (in a statistical sense) upper tropospheric temperature anomaly for different West Pacific cyclone intensity groups is related to lower tropospheric height and wind speed for the different intensity cyclones defined in Table 18. These are only statistical relationships and, for application in individual situations, more specific knowledge of the T' and wind relationship must be obtained. If research were focused on this subject, very useful individual case relationships could likely be obtained.

More refined evaluation of the cyclones' temperature and resulting low-level pressure-wind could be obtained if a downward pointing microwave spectrometer similar to that flown on the Nimbus VI satellite was also made a part of the jet aircraft instrument package. As discussed by Rosenkranz and Staelin (1977) and Kidder *et al.* (1978) such

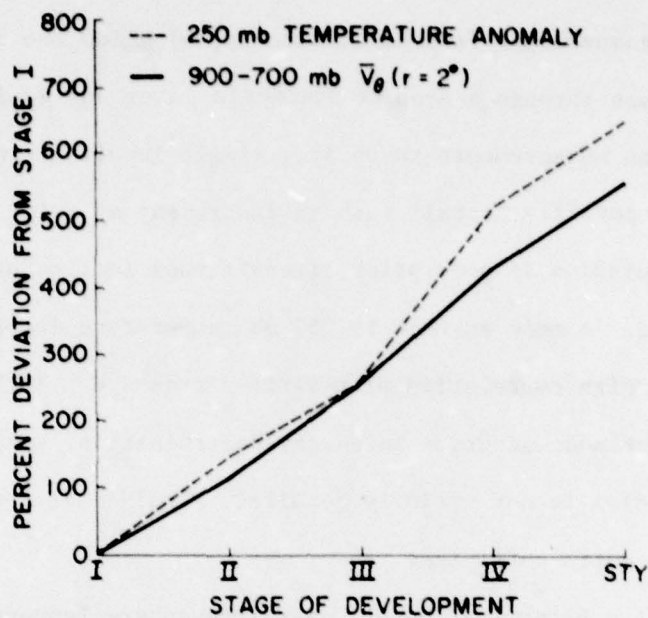


Fig. 47. The 250 mb temperature anomaly and 900-700 mb tangential wind at $r = 2^\circ$, each expressed as a percent deviation from the corresponding developing cluster (Stage I) values (from Arnold, 1977).

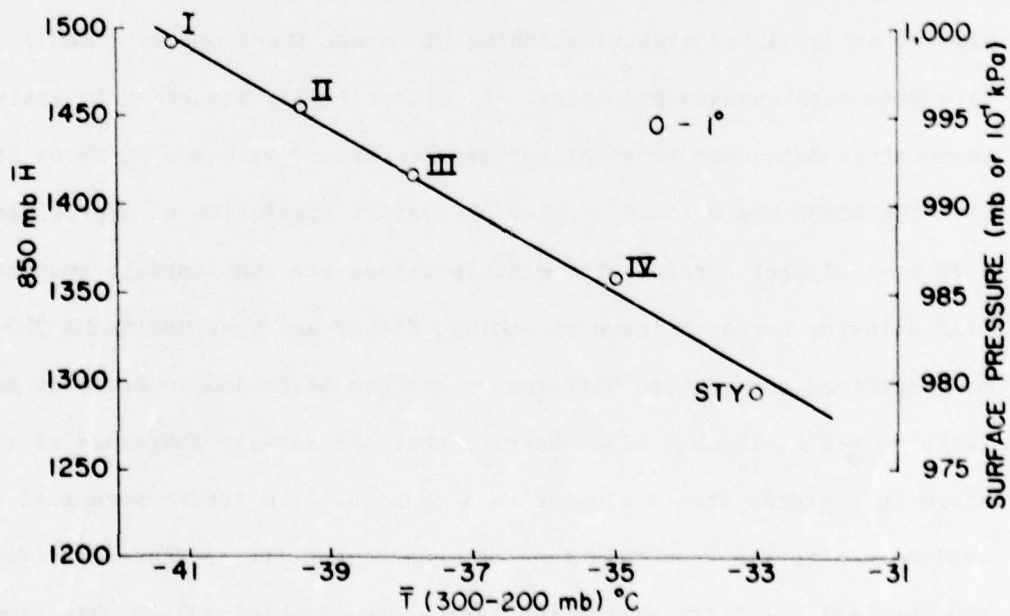


Fig. 48. The mean 300-200 mb temperature from $0-1^\circ$ vs. mean 850 mb height from $0-1^\circ$ (from Arnold, 1977).

microwave measurements (see discussion below) allow the determination of temperature through a deep tropospheric layer and would be more reliable than measurements taken at a single level. It might be possible to temporarily install such an instrument on a jet aircraft just prior to a mission if some prior aircraft modification has been accomplished. A mean surface to 250 mb temperature determination would have a very high correlation with surface pressure. Although highly desirable for most accurate intensity determination, such additional instrumentation is not strictly required. Individual level values may prove to be quite sufficient.

Satellite Determination of Upper Troposphere Temperature. A similar approach to tropical cyclone intensity determination has been proposed by Rosenkranz and Staelin (1977) and S. Kidder *et al.* (1978). They suggest using satellite measurements of the cyclone's upper tropospheric temperature to infer its strength. Research so far accomplished using Nimbus channel Scanning Microwave Spectrometer (SCAMS) satellite data appears promising. S. Kidder (1979) has recently analyzed temperature data over tropical cyclones retrieved with the SCAMS on Nimbus VI. The SCAMS has a field of view or spatial resolution of approximately a 78 n mi diameter circle. Temperature values are considerably smoothed. Even allowing for such large smoothing, Kidder has observed SCAMS 250-100 mb determined temperature differences between storm and environment as large as $4-5^{\circ}\text{C}$. He has also observed that the anomaly increases as the storm intensifies from a cluster to a typhoon. The future potential for cyclone monitoring from this type of measurement (if increased horizontal and vertical satellite sensor resolution can be obtained) appears promising.

This is an encouraging avenue to gain increased knowledge of tropical cyclone intensity. It is especially relevant because there appears to be a limit to cyclone intensity knowledge which may be obtained from further and more refined analysis of satellite cloud configurations.

Summary. It is suggested that consideration be given by foreign governments and the United States to tropical cyclone intensity determinations from jet aircraft. Measurements of the cyclone's upper tropospheric temperature anomaly and horizontal configuration may prove as reliable a measure of the cyclone's intensity as low level prop aircraft reconnaissance. Such measurements would likely be a more reliable source of cyclone intensity than that of satellite observed cloud configuration and quite desirable to have when cyclones approach populated areas.

7. DIURNAL VARIATIONS OF VERTICAL MOTION IN TROPICAL WEATHER SYSTEMS

The diurnal variation of mass divergence and vertical velocity is documented for tropical summertime oceanic weather systems in the Western Pacific, Western Atlantic and the GATE region. It is shown that this diurnal variation is very large and has the same basic character in all regions.

The existence of a single diurnal cycle in the mass divergence of oceanic tropical weather systems was first demonstrated by Ruprecht and Gray (1976a, b) and Gray and Jacobson (1977) for the western Pacific. Corroborating evidence on the diurnal variation of heavy precipitation has been presented by Gray and Jacobson (*loc. cit.*), Dewart (1978) and by McGarry and Reed (1978).

Use is made of data from the 1974 GATE experiment and from the many tropical data sets composited over the past decade by the tropical storm research project of William M. Gray (Williams and Gray, 1973; Ruprecht and Gray, 1976a, b; Zehr, 1976; W. Frank, 1977a, b, c; S. Erickson, 1977; McBride, 1977; Frank, 1978a, b; Dewart, 1978 and Grube, 1978).

From these sources, eleven totally independent composite data sets are put together for three different tropical oceanic regions. Each data set represents one type of tropical summertime convective weather system. The diurnal variation of each data set is investigated and intercomparisons are made between the different data sets to determine consistencies in their diurnal behavior.

Western Pacific Convective Systems. Following the technique of Williams and Gray (1973), twice daily rawinsonde observations from the

standard observational network in the Northwest Pacific Ocean have been composited relative to the central positions of tropical convective systems. 00Z and 12Z rawinsonde data were used from the summer months of the years 1961-1970.

Five different types of Western Pacific convective systems have been composited. They are numbered one to five:

1. CLOUD CLUSTER. Summertime cloud clusters were composited for the years 1967 and 1968. Only clusters which did not later develop into tropical cyclones were used. This data set is the "STAGE 00" data set of Zehr (1976).
2. PRETYPHOON CLOUD CLUSTER. This data set consists of cloud clusters which later develop into typhoons. Data for this and the following three data sets are from the full ten year period 1961-1970. This data set is "STAGE 2" of Zehr. It consists of that portion of each storm's track prior to one day before the first reconnaissance aircraft observation. Positions were obtained from satellite pictures and by extrapolation from Joint Typhoon Warning Center, Guam (JTWC) best tracks.
3. TROPICAL STORMS. $P_c > 1000$ mb. This and the following two data sets consist of a stratification of the official best tracks of the JTWC according to the central Pressure (P_c) of each storm.
4. TROPICAL STORMS. $980 \text{ mb} \leq P_c \leq 1000 \text{ mb}$.
5. TROPICAL STORMS. $P_c \leq 980 \text{ mb}$.

Positioning for the cloud cluster data sets (data sets 1, 2 and 6, 7 of the following section) was obtained from visual daytime satellite imagery. Interpolation had to be used, therefore, to obtain nighttime positions for these systems. This procedure did not yield any significant day vs. night variation in the composited thermodynamic fields associated with the clusters.

To insure that the vertically integrated net radial mass flux between the surface and 100 mb is zero, small mass balance corrections had to be added to the radial component of the wind at each level.

Every feature of the divergence profile described in this study is insensitive to the mass balance correction, however. The correction had to be made so that vertical velocities would simultaneously be zero at the surface and 100 mb.

Data were composited at 19 vertical levels extending from sea level to 100 mb. The horizontal grid was an annulus, 2° to 4° latitude distance from the center of the convective system. The radial component of the wind was composited in eight octants of 45° azimuthal extent. These eight values of the radial wind, V_R , were considered to be true at 3° latitude distance from the system center. The average horizontal divergence (\overline{DIV}) inside the 3° radius area of each weather system was calculated by an application of the divergence theorem. Vertical profiles of divergence averaged over the $0-3^{\circ}$ area for the five Pacific data sets are shown in Fig. 49. Profiles are shown for the two standard observation times, 00 and 12 GMT (10 AM and 10 PM Local Time). The corresponding kinematically derived vertical velocities are shown in Fig. 50. The general character of these profiles is convergence or inflow in the lower troposphere compensated for by divergence or outflow near the 200 mb level. The features of interest for the present study are as follows:

- a) The low level convergence in the layer from the surface to 850 mb is greater at 10 AM than at 10 PM.
- b) There is convergence at 10PM in the middle troposphere near 450 mb.
- c) In the morning the upper level outflow extends through a deeper layer of the atmosphere than it does in the evening.

The corresponding properties of the vertical motion profile are:

- d) The mean tropospheric upward vertical motion is greater in the morning than in the evening.

- e) The level at which the maximum upward vertical velocity occurs is higher in the atmosphere in the evening than in the morning.
- f) The low level upward vertical velocity (at 800 mb) is greater in the morning than in the evening.

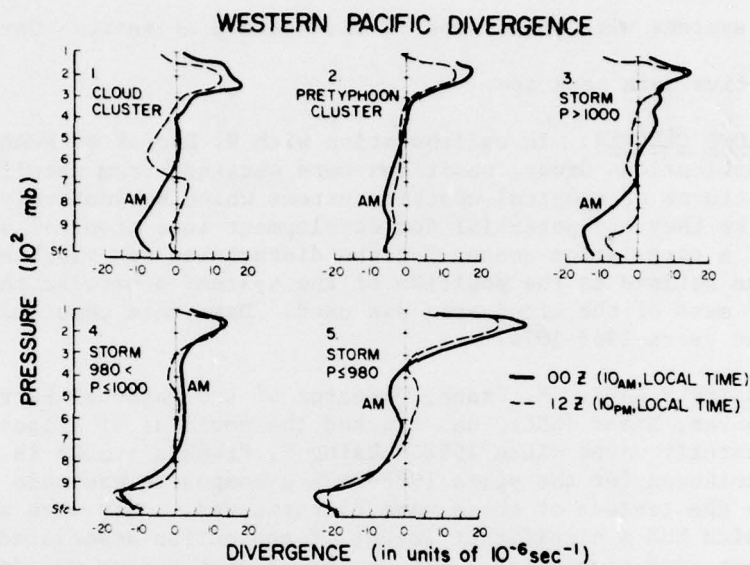


Fig. 49. Mean divergence within the $r = 0-3^\circ$ latitude area for the five Western Pacific composite weather systems.

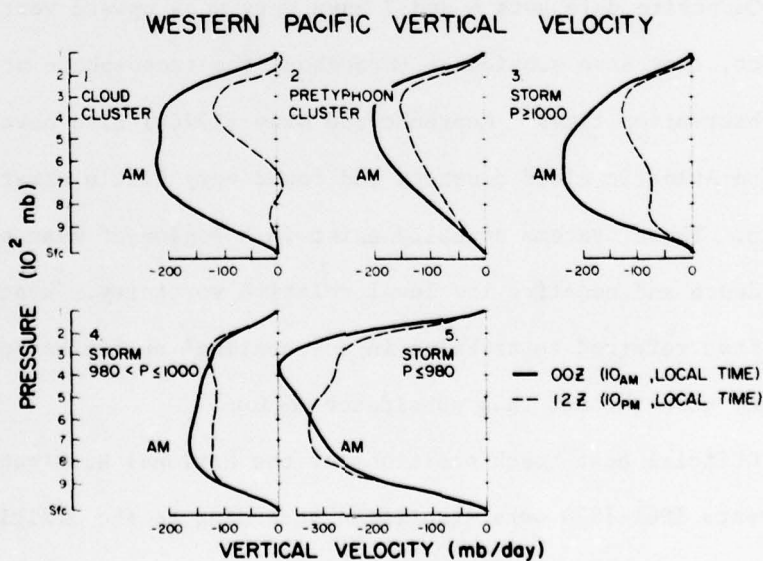


Fig. 50. Mean vertical velocity within the $r = 0-3^\circ$ area for the five Western Pacific composite weather systems.

Data sets 1 to 4 exhibit all six of these features. The typhoon data set (data set 5, $P_c \geq 980$ mb) exhibits only properties c) and d).

Western Atlantic Convective Systems. Using the same technique as described above for the Pacific, five different types of summertime convective systems were composited in the Western Atlantic - Caribbean area. The five data sets are:

6. CLOUD CLUSTER. In collaboration with V. Dvorak of NOAA/NESS Applications Group, positions were obtained from satellite pictures of tropical weather systems which subjectively looked like they had potential for development into tropical storms. If a circulation center for the disturbance was visible, it was defined as the position of the system; otherwise the center of mass of the cloud area was used. Data were compiled from the years 1968-1974.
7. EASTERLY WAVE. N. Frank, Director of the National Hurricane Center, Miami (NHC), has tracked the movement of Atlantic easterly waves since 1968. Using N. Frank's tracks in the Caribbean for the years 1968-1974 a composite was made relative to the centers of these wave disturbances. Only wave systems which had a significant amount of convection associated with them were composited. The center of each system was defined such that the longitude was that of N. Frank's trough axis, and the latitude was the central latitude of convective activity as determined from satellite images.

Composite data sets 6 and 7 have very weak upward vertical velocity. In fact, they have subsidence throughout the troposphere at one of the two observation times. Ruprecht and Gray (1976a) also have composited Western Atlantic cloud clusters and found very little upward vertical motion. These systems actually exist in a region of mean environmental subsidence and negative low level relative vorticity. Weather systems are often referred to as being in a 'coasting' or 'weakening' stage as they move through this subsidence region.

Official best track positions of the National Hurricane Center for the years 1961-1974 were stratified according to the official estimated maximum sustained wind (V_{\max}) to provide the following three data sets:

8. PRE-TROPICAL STORMS: $V_{\max} \leq 35$ kts.
9. TROPICAL STORMS: $35 \text{ kts} < V_{\max} < 65$ kts.
10. TROPICAL STORMS: $V_{\max} \geq 65$ kts.

The observation times 00Z and 12Z for these data sets are within about one hour of 7 PM and 7 AM Local Time, respectively. Diurnal divergence profiles and vertical velocity profiles are shown in Figs. 51 and 52.

There is a marked similarity between these figures and the corresponding Figs. 49 and 50 from the West Pacific. Data sets 6 through 9 can be seen to have every one of the properties a) to f) listed for the Pacific systems. The hurricane data set (data set 10) has properties a), d) and f).

The strong similarity between the diurnal divergence and vertical velocity profiles of the two western ocean regions provides convincing evidence that this variation actually does exist. This is not a trivial point, as divergence is a notoriously difficult atmospheric parameter to measure. The appearance of the six common features a) to f) in these independent data sets shows that they are consistent and realistic features which should be known about in the evolution of tropical convection from satellite information.

GATE Convective Systems. The GARP Atlantic Tropical Experiment (GATE) was performed in the tropical eastern Atlantic Ocean in June through September 1974. Rawinsonde data was taken by ships stationed in the outer hexagon of the GATE network (the A/B-array) as shown in Fig. 53. The GATE array is approximately $3\frac{1}{2}^{\circ}$ latitude radius. The composited divergence and vertical motion can thus be directly compared with the results of the previous section of this study where data are averaged between $2\text{--}4^{\circ}$ radius. The GATE, however, observations on the most convectively active days were taken at 3-hourly intervals; so that much

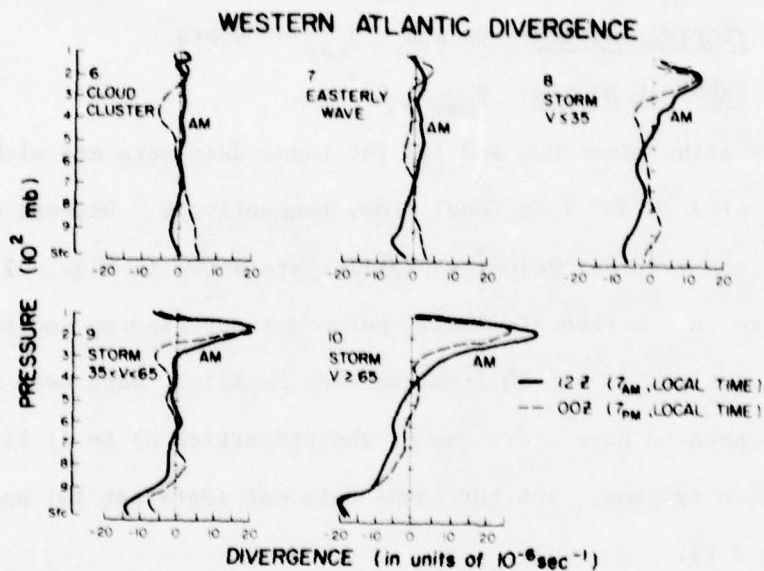


Fig. 51. Mean divergence within the $r = 0-3^\circ$ area for the Western Atlantic composite weather systems.

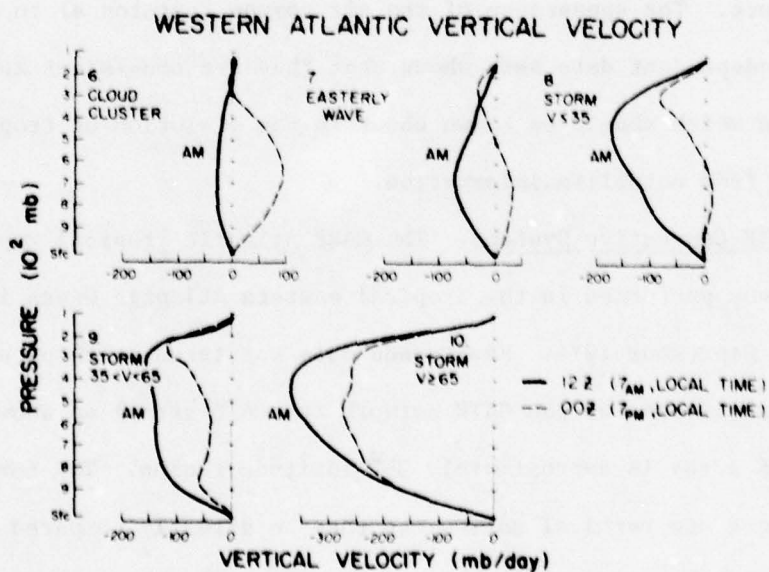


Fig. 52. Mean vertical velocity within the $r = 0-3^\circ$ area for the Western Atlantic composite weather systems.

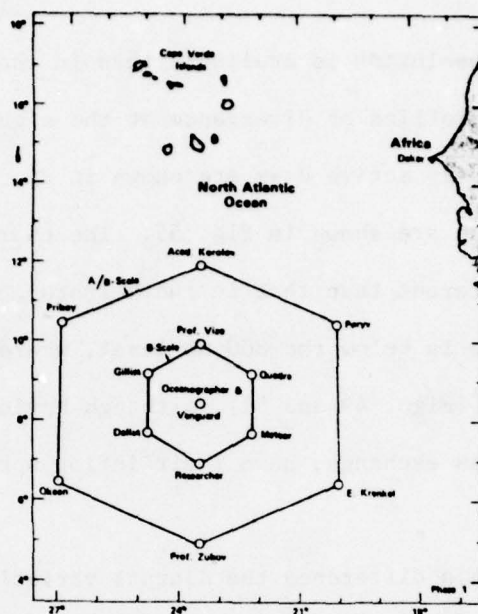


Fig. 53. A/B and B-scale ship arrays for Phase I of GATE.

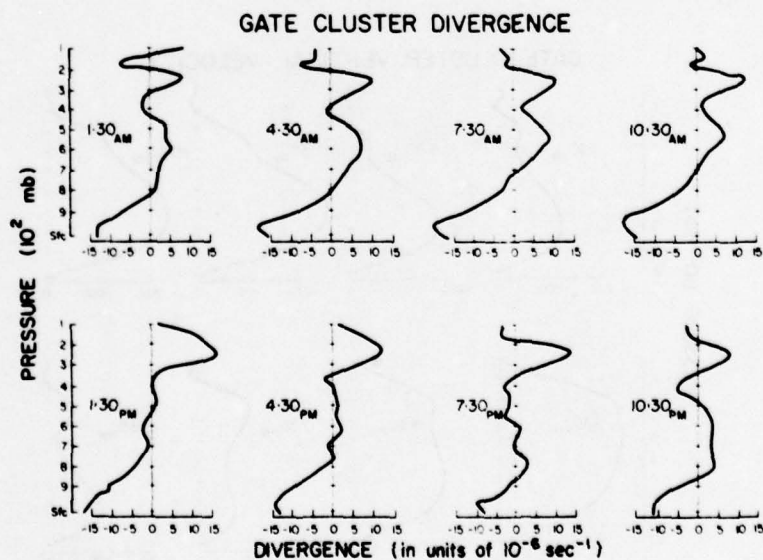


Fig. 54. Mean divergence within the GATE A/B-array for the GATE composite cluster.

greater time resolution is available than in the western oceans.

Vertical profiles of divergence at the eight observation times of these convectively active days are shown in Fig. 54. The corresponding vertical motions are shown in Fig. 55. The character of the divergence profile is different than that in the western oceans. In GATE most of the convergence is below the 800 mb level, whereas the data sets of the western oceans (Figs. 49 and 51), although having a similar total amount of vertical mass exchange, have their inflow spread through a much deeper layer.

Despite this difference the diurnal variation in GATE follows a pattern similar to that in the other systems.

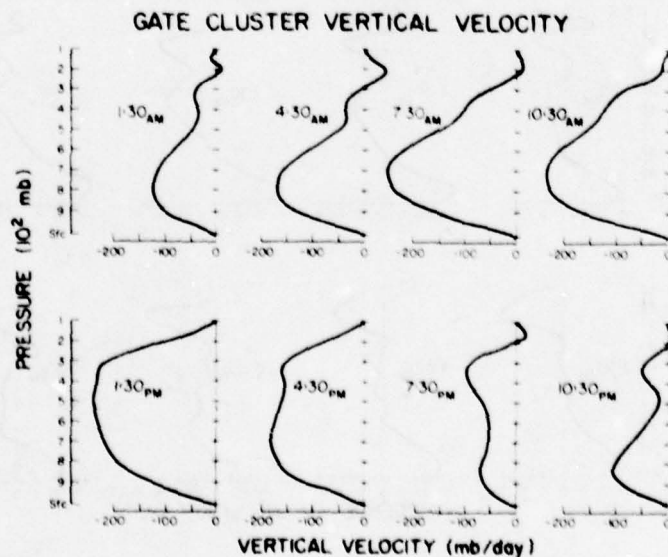


Fig. 55. Mean vertical motion within the GATE A/B-array for the GATE composite cluster.

For a more direct comparison of the data so far presented in this study, Fig. 56 was constructed. This figure shows the GATE vertical motion profiles at the observation times closest to those in the other locations. The left hand side of the figure can be compared directly with Fig. 50, the right hand side with Fig. 52.

Summary. It has been shown above that the diurnal behavior of the divergence profiles of convective systems is very similar in the GATE region, the Western Pacific and in the Western Atlantic. The basic profiles on which this diurnal variation is superimposed are quite different, however, in the three regions. This large diurnal morning maximum and evening minimum in vertical motion appears to be primarily a result of day vs. night difference in tropospheric radiational cooling with a 3-6 hour lag time (see papers by Gray and Jacobson, 1977; Fingerhut, 1978; McBride and Gray, 1978; Dewart, 1978; W. Frank, 1978a and Grube, 1978).

GATE CLUSTER VERTICAL VELOCITY

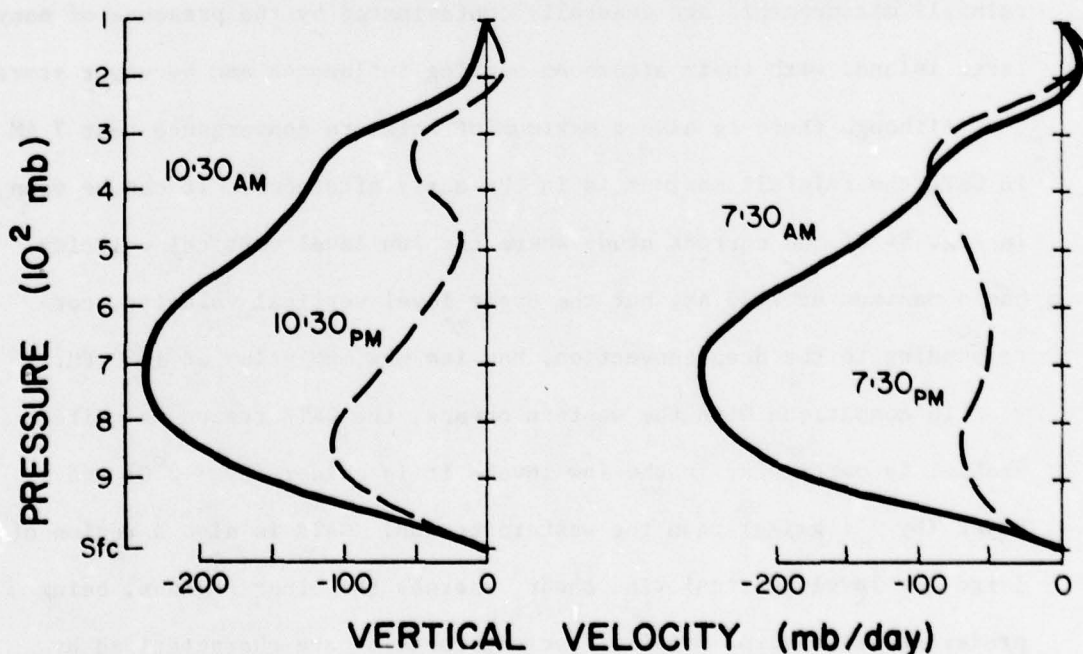


Fig. 56. Mean vertical motion for the GATE cluster at the observation times closest to those in the western oceans. The left side compares directly with Fig. 50, the right side with Fig. 52.

Diurnal Variation of Rainfall. This study has been concerned with the diurnal variation of the wind fields. The variation of rainfall can be quite different to that of vapor convergence if moisture storage and significant convective feedback occur.

It has been shown above that in the three regions under consideration the mass convergence below the 850 mb level is of maximum magnitude near 7 AM local time. In the western oceans this converging moisture is apparently quickly converted to rain. The diurnal variation of heavy precipitation in Western Pacific weather systems has been well documented by Gray and Jacobson (1977). They showed that rainfall has a maximum near 7 AM and a minimum near 9-11 AM. This is in agreement with the low level convergence being driven by the diurnal variation of diabatic heat sources as here discussed. A preliminary analysis of Western Atlantic oceanic rainfall leads to the same conclusion for that region. However, rainfall measurements are generally contaminated by the presence of many large islands with their afternoon heating influences and by vapor storage.

Although there is also a maximum of moisture convergence near 7 AM in GATE the rainfall maximum is in the early afternoon. It can be seen in Fig. 54 of the current study where the low level vertical velocity has a maximum at 7:30 AM, but the upper level vertical velocity, corresponding to the deep convection, has its maximum value at 1:30 PM.

In comparison with the western oceans, the GATE region is quite stable; in particular in the low levels it is colder (by $\sim 2^{\circ}\text{C}$) and dryer (by $\sim 1 \text{ gm/kg}$) than the western oceans. GATE is also a region of large low level vertical wind shear, whereas the other regions, being preferred regions for tropical cyclone genesis, are characterized by quite weak low level vertical shear.

In consequence of this greater stability and greater wind shear, convection takes some time to develop in GATE. In agreement with the diurnal forcing mechanism, the GATE convection is initiated in the morning hours (Weickmann et al., 1977) but appears to take 4-8 hours to organize into the observed cloud lines and squall lines. The line and squall convection can overwhelm the large-scale forcing and cause rain after the forcing mechanism has subsided. The heaviest convection thus comes later than in the western ocean regions where buoyant instability and low vertical shear permit a faster response to the low level mass convergence. One must thus be careful not to too closely associate this large two to one morning maximum and evening minimum in tropical disturbance vertical motion with rainfall.

Conclusion. It is important that this large single cycle in diurnal variation of mass convergence into tropical weather systems be realized and better understood. The implications for the understanding of tropical convection need to be more fully appreciated particularly with the interpretation of cumulus convection as observed from satellite data.

ACKNOWLEDGEMENTS

The author wishes to express his gratitude to William M. Frank, John L. McBride, Johnny C. L. Chan, Edwin Núñez, L/C Charles P. Arnold, and Stanley Kidder for discussion and information concerning these research findings. Mr. Edwin Buzzell has been responsible for the numerical data processing. Thanks are also extended to Mrs. Barbara Brumit for her assistance in manuscript preparation. This work was funded by the Naval Environmental Prediction Research Facility (NEPRF), Monterey, California under work Unit 6.2-14 in the Atmospheric Environmental Support portion of Program Element 62759N.

BIBLIOGRAPHY

- Arnold, C. P., 1977: Tropical cyclone cloud and intensity relationships. Dept. of Atmos. Sci. Paper No. 277, Colo. State Univ., Ft. Collins, CO, 155 pp.
- Chan, J. C. L., W. M. Gray and S. Q. Kidder, 1979: Forecasting tropical cyclone turning motion from surrounding wind and temperature fields. Paper submitted for publication.
- Dewart, J. M., 1978: Diurnal variability in the GATE region. Dept. of Atmos. Sci. Paper No. 298, Colo. State Univ., Ft. Collins, CO, 76 pp.
- Dvorak, V. F., 1975: Tropical cyclone intensity analysis and forecasting from satellite imagery. Mon. Wea. Rev., 103, 420-430.
- Erickson, S. L., 1977: Comparison of developing vs. non-developing tropical disturbances. Dept. of Atmos. Sci. Paper No. 274, Colo. State Univ., Ft. Collins, CO, 81 pp.
- Fingerhut, W. A., 1978: A numerical model of a diurnally varying tropical cloud cluster disturbance. Mon. Wea. Rev., 106, 255-264.
- Frank, W. M., 1976: The structure and energetics of the tropical cyclone. Dept. of Atmos. Sci. Paper No. 258, Colo. State Univ., Ft. Collins, CO, 180 pp.
- Frank, W. M., 1977a: The structure and energetics of the tropical cyclone, I: Storm structure. Mon. Wea. Rev., 105, 9, 1119-1135.
- Frank, W. M., 1977b: The structure and energetics of the tropical cyclone, II: Dynamics and energetics. Mon. Wea. Rev., 105, 1135-1150.
- Frank, W. M., 1977c: Convective fluxes in tropical cyclones. J. Atmos. Sci., 34, 1554-1568.
- Frank, W. M., 1978a: Diagnostic analyses of the GATE A/B scale area at individual time periods. Dept. of Atmos. Sci. Paper No. 297, Colo. State Univ., Ft. Collins, CO, 102 pp.
- Frank, W. M., 1978b: The life cycles of GATE convective systems. J. Atmos. Sci., 35, 1256-1264.
- George, J. E., 1975: Tropical cyclone motion and surrounding parameter relationships. Dept. of Atmos. Sci. Paper No. 214, Colo. State Univ., Ft. Collins, CO, 105 pp.
- George, J. E. and W. M. Gray, 1976: Tropical cyclone motion and surrounding parameter relationships. J. Appl. Meteor., 15, 1252-1264.

BIBLIOGRAPHY (cont'd)

- Gray, W. M., 1962: On the balance of forces and radial accelerations in hurricanes. Quart. J. Roy. Meteor. Soc., 88, 430-458 pp.
- Gray, W. M., 1967: The mutual variation of wind, shear and baroclinicity in the cumulus convective atmosphere of the hurricane. Mon. Wea. Rev., 95, 55-73.
- Gray, W. M., 1968: Global view of the origin of tropical disturbances and storms. Mon. Wea. Rev., 96, 669-700.
- Gray, W. M., 1975a: Tropical cyclone genesis. Colo. State Univ., Atmos. Sci. Paper No. 234; Ft. Collins, CO, 119 pp.
- Gray, W. M. 1975b: Tropical cyclone genesis in the western North Pacific. ENVPREDRSCHFAC Technical Paper No. 16-75, Monterey, CA, 66 pp.
- Gray, W. M., 1977a: Tropical disturbance to cyclone transformation. Paper prepared for the 11th Technical Conference on Hurricanes and Tropical Meteorology, Miami Beach, FL, 8 pp.
- Gray, W. M., 1977b: Cyclone intensity determination through upper tropospheric reconnaissance. Paper prepared for the 11th Technical Conference on Hurricanes and Tropical Meteorology, Miami Beach, FL, 6 pp.
- Gray, W. M., 1977c: Tropical cyclone motion and steering flow relationships in the Western Atlantic and the Western Pacific. Paper prepared for the 11th Technical Conference on Hurricanes and Tropical Meteorology, Miami Beach, FL, 6 pp.
- Gray, W. M., 1979: Hurricanes: their formation, structure and likely role in the tropical circulation. Quart. J. Roy. Meteor. Soc., 105, 155-218.
- Gray, W. M. and W. M. Frank, 1977: Tropical cyclone research by data compositing. NEPRF Technical Report TR-77-01. Naval Environmental Prediction Research Facility, Monterey, CA, 70 pp.
- Gray, W. M. and W. M. Frank, 1978: New results of tropical cyclone research from observational analysis. NEPRF Technical Report TR-78-01, Naval Environmental Prediction Research Facility, Monterey, CA, 106 pp.
- Gray, W. M. and R. Jacobson, Jr., 1977: Diurnal variations of deep cumulus convection. Mon. Wea. Rev., 105, 9, 1171-1188.
- Gray, W. M. and D. J. Shea, 1973: The hurricane's inner core region, II: Thermal stability and dynamic characteristics. J. Atmos. Sci., 30, 1565-1576.

BIBLIOGRAPHY (cont'd)

- Gray, W. M. and D. J. Shea, 1976: Data summary of NOAA's hurricane inner-core radial leg flight penetrations 1957-1967, 1969. Dept. of Atmos. Sci. Paper No. 257, Colo. State Univ., Ft. Collins, CO, 245 pp.
- Grube, P. G., 1978: Convection induced temperature change in GATE. Dept. of Atmos. Sci. Paper No. 305, Colo. State Univ., Ft. Collins, CO, 128 pp.
- Hawkins, H. F., and D. T. Rubsam, 1968: Hurricane Hilda, 1964: II. Structure and Budgets of the hurricane on October 1, 1964. Mon. Wea. Rev., 99, 427-434.
- Hawkins, H. F. and S. M. Imbembo, 1976: The structure of a small, intense hurricane - Inez 1966. Mon. Wea. Rev. 104, 418-442.
- Kidder, S. Q., W. M. Gray and T. H. Vonder Haar, 1978: Estimating tropical cyclone central pressure and outer winds from satellite microwave data. Mon. Wea. Rev., 106, 1458-1464.
- Kidder, S., 1979: Determination of tropical cyclone surface pressure and winds from satellite microwave data. Ph.D. Thesis, Dept. of Atmos. Sci., Colo. State Univ., Ft. Collins, CO.
- Landsat/Nimbus Project, 1976: The Nimbus 6 data catalog, Vol. 2. NASA/Goddard Space Flight Center, Greenbelt, MD, pp. 1-2 through 1-4.
- LaSeur, N. E. and H. F. Hawkins, 1963: An analysis of hurricane Cleo (1958) based on data from research reconnaissance aircraft. Mon. Wea. Rev., 91, 694-709.
- Lawrence, M. B., 1979: Atlantic hurricane season of 1978. Mon. Wea. Rev., 107, 477-491.
- McBride, J. L., 1977: Observational analysis of the differences between developing and non-developing tropical disturbances. Paper prepared for the 11th Technical Conference on Hurricanes and Tropical Meteorology, Dec. 13-16, Miami Beach, FL, 260-267.
- McBride, J. L., 1979: Observational analysis of tropical cyclone formation. Ph.D. Thesis, Dept. of Atmos. Sci., Colo. State Univ., Ft. Collins, CO.
- McBride, J. L. and W. M. Gray, 1978: Mass divergence in tropical weather systems, Paper I: Diurnal variation, Paper II: Large scale controls on convection. Dept. of Atmos. Sci. Paper No. 299, Colo. State Univ., Ft. Collins, CO, 109 pp.
- McGarry, M. M. and R. J. Reed, 1978: Diurnal variations in convective activity and precipitation during phases II and III of GATE. Mon. Wea. Rev., 106, 101-113.

BIBLIOGRAPHY (cont'd)

- Miller, B. I., 1962: On the momentum and energy balance of hurricane Helene (1958). NHRP Rept. No. 53, 19 pp.
- Moncrieff, M. W. and M. J. Miller, 1976: The dynamics of simulation of tropical cumulonimbus and squall lines. Quart. J. Roy. Meteor. Soc., 102, 373-394.
- Moncrieff, M. W. and J. S. A. Green, 1972: The propagation of steady convective overturning in shear. Quart. J. Roy. Meteor. Soc., 98, 336-352.
- Neumann, C. J., 1979: A guide to Atlantic and Eastern Pacific models for the prediction of tropical cyclone motion. NOAA Tech. Memo. NWS NHC-11, National Weather Service, US Dept. of Commerce, Miami, FL, 26 pp.
- Nunez, E. and W. M. Gray, 1977: A comparison between West Indies hurricanes and Pacific typhoons. Paper prepared for the 11th Technical Conference on Hurricanes and Tropical Meteorology, Miami Beach, FL, April 13-16, 528-534.
- Ramage, C. S., 1974: The typhoons of October 1970 in the South China Sea: Intensification, decay and ocean interaction. J. Appl. Meteor., 13, 739-751.
- Riehl, H. and J. S. Malkus, 1961: Some aspects of Hurricane Daisy, 1958. Tellus, 13, 181-213.
- Rosenkranz, P. W. and D. H. Staelin, 1977: Typhoon June (1975) viewed by a scanning microwave spectrometer. To appear in J. Geophys. Res. (Available in manuscript form (44 pp.) from Dept. of EE and Computer Science, M.I.T., Cambridge, MA 02139).
- Ruprecht, E. and W. M. Gray, 1976a: Analysis of satellite-observed tropical cloud clusters, Part I: Wind and dynamic fields. Tellus, 28, 391-413.
- Ruprecht, E. and W. M. Gray, 1976b: Analysis of satellite-observed tropical cloud clusters, Part II: Thermal, moisture and precipitation. Tellus, 28, 414-416.
- Sadler, J. C., 1967a: On the origin of tropical vortices. Working Panel on Trop. Dynamical Meteor., Naval Postgraduate School, Monterey, CA, 39-75.
- Sadler, J. C., 1967b: The tropical tropospheric trough as a secondary source of typhoons and a primary source of tradewind disturbances. Final report, Cont. AF19 (628)3860, AF Cambridge Res. Labs., Bedford, MA, Rept. 67-12, 44 pp.

BIBLIOGRAPHY (cont'd)

- Sadler, J. C., 1974: A role of the tropical upper tropospheric trough in early season typhoon development. Tech. Paper No. 9-74, US Navy Environmental Prediction Research Facility Report, 54 pp.
- Sadler, J. C., 1976: A role of the tropical upper troposphere in early season typhoon development. Mon. Wea. Rev., 104, 1266-1278.
- Sadler, J. C., 1978: Mid-season typhoon development and intensity changes and the tropical upper tropospheric trough. Mon. Wea. Rev., 1137-1152.
- Shapiro, L. J., 1977a: Tropical storm formation from easterly waves: a criterion for development. J. Atmos. Sci., 34, 1007-1021.
- Shapiro, L. J., 1977b: A criterion for the development of tropical storms from easterly waves. Volume of Conference Papers, 11th Technical Conference on Hurricanes and Tropical Meteorology, Dec. 13-16, Miami Beach, FL, Published by AMS, Boston, MA, 9-14.
- Shea, D. J. and W. M. Gray, 1973: The hurricane's inner core region, I: Symmetric and asymmetric structure. J. Atmos. Sci., 30, 1554-1564.
- Sheets, R. C., 1967a: On the structure of Hurricane Janice (1958). National Hurricane Res. Lab. Rept. No. 76, 30 pp. (available from NOAA Weather Bureau, Miami office).
- Sheets, R. C., 1967b: On the structure of Hurricane Ella (1962). National Hurricane Res. Lab. Rept. No. 77, 33 pp. (available from NOAA Weather Bureau, Miami office).
- Sheets, R. C., 1968: On the structure of Hurricane Dora (1964). National Hurricane Res. Lab. Rept. No. 83, 64 pp. (available from NOAA Weather Bureau, Miami office).
- Staelin, D. H., A. H. Barrett, P. W. Rosenkranz, F. T. Bavath, E. J. Johnson, J. W. Waters, A. Wouters and W. B. Lenoir, 1975a: The scanning microwave spectrometer (SCAMS) experiment. The Nimbus 6 User's Guide, J. E. Sissala, Ed., LANDSAT/Nimbus project, NASA/Goddard Space Flight Center, Greenbelt, MD, 59-86.
- Staelin, D. H., A. L. Cassel, K. R. Kunzi, R. L. Pettyjohn, R. K. L. Poon, and P. W. Rosenkranz, 1975b: Microwave atmospheric temperature sounding. Effects of clouds on the Nimbus 5 satellite data.
- Waters, J. W., K. F. Kunzi, R. L. Pettyjohn, R. K. L. Poon and D. H. Staelin, 1975: Remote sensing of atmospheric temperature profiles with the Nimbus 5 Microwave spectrometer. J. Atmos. Sci., 32, 1953-1969.

BIBLIOGRAPHY (cont'd)

Weickmann, H. K., A. B. Long and L. R. Hoxit, 1977: Some examples of rapidly growing oceanic cumulonimbus clouds. Mon. Wea. Rev., 105, 469-476.

Williams, K. T. and W. M. Gray, 1973: Statistical analysis of satellite-observed trade wind cloud clusters in the western North Pacific. Tellus, 25, 313-336.

Wise, C. W. and R. H. Simpson, 1971: The tropical analysis program of the National Hurricane Center. Weatherwise, 24, 164-173.

Zehr, R., 1976: Tropical disturbance intensification. Dept. of Atmos. Sci. Paper No. 259, Colo. State Univ., Ft. Collins, CO, 91 pp.

APPENDIX A

A.4 Pacific pretyphoon versus non-developing clusters

The values of parameters (iii), (iv) and (v) are listed in Table A1 for 18 Western Pacific pretyphoon cloud clusters and in Table A2 for 31 Western Pacific non-developing cloud clusters. The method of obtaining these values from Joint Typhoon Warning Center (JTWC) Guam operational weather maps is described in section 3.3 (Position numbers are the numbers used by S. Erickson (1977).) The latitude, longitude time and date corresponding to each position number are listed in Table A3.

TABLE A1

Pacific Pretyphoon Clusters

System Number	Position Number	(iii) $\Delta U + \Delta V$	(iv) Zonal Zero Line	(v) Meridional Zero Line
1	36-38	8.4	Y	Y
2	39-41,43,45	9.6	Y	N
3	73,75,77,78	15.4	Y	Y
4	150,151,153	13.7	Y	Y
5	159-164	18.0	Y	Y
6	166,168,170,172 175,177	10.0	Y	N
7	174,176,178	13.0	Y	N
8	179-181	7.3	Y	N
9	248-251	10.9	Y	Y
10	284-288	-1.6	N	Y
11	289-293	9.3	Y	Y
12	294-297	14.3	Y	Y
13	298-300	13.3	Y	Y
14	301-303	11.0	Y	N
15	312	9.0	N	Y
16	313-315	- .4	N	N
17	319-321	22.9	Y	Y
18	322-325	20.1	Y	Y

TABLE A2

Pacific Non-developing Clusters

System Number	Position Number	(iii) $\Delta U + \Delta V$	(iv) Zonal Zero Line	(v) Meridional Zero Line
1	20-23	14.1	Y	N
2	24-26	14.2	N	Y
3	27-29	7.3	N	N
4	30-32	19.9	Y	N
5	33-35	15.7	Y	Y
6	42,44,46	0.6	Y	N
7	47-51	-3.3	N	N
8	52-54,56	8.9	Y	Y
9	55,57-59	12.7	Y	Y
10	60,62,64	5.8	N	Y
11	61,63,65-69	2.5	N	N
12	70-72,74,76	0.1	Y	N
13	79-80	-4	N	N
14	121-124	6.9	Y	N
15	125-127	8.8	Y	N
16	128,130,132	14.4	Y	N
17	129,131,133	8.8	Y	N
18	134-136	1.8	Y	N
19	137-139	14.0	Y	Y
20	140-144	1.7	N	N
21	145-149	12.4	Y	Y
22	152,154,155	3.8	Y	N
23	156-158	5.1	Y	N
24	165,167,169, 171,173	9.1	Y	N
25	182-186	2.7	Y	N
26	187-191	9.1	Y	N
27	192-194	11.3	Y	N
28	195-197	7.4	Y	N
29	304-306	-9.3	N	N
30	307-311	0.2	N	N
31	316-318	-6.9	N	N

TABLE A3

Pacific pretyphoon and non-developing cloud clusters (positions from S. Erickson (1977)).

<u>Position Number</u>	<u>Year</u>	<u>Month</u>	<u>Date</u>	<u>Time (GMT)</u>	<u>Latitude (Deg. North)</u>	<u>Longitude (Deg. East)</u>
20	1972	5	7	12	8.0	160.7
21	1972	5	8	00	8.6	159.7
22	1972	5	8	12	7.9	159.4
23	1972	5	9	00	7.8	159.3
24	1972	5	9	00	8.5	146.5
25	1972	5	9	12	7.5	142.5
26	1972	5	10	00	7.5	140.4
27	1972	5	12	00	13.1	158.0
28	1972	5	12	12	12.4	154.5
29	1972	5	13	00	11.7	151.0
30	1972	5	14	00	9.5	161.2
31	1972	5	14	12	9.0	160.0
32	1972	5	15	00	8.2	158.8
33	1972	5	19	00	7.4	156.0
34	1972	5	19	12	8.7	153.0
35	1972	5	20	00	10.0	150.0
36	1972	5	26	00	6.0	169.9
37	1972	5	26	12	6.1	166.6
38	1972	5	27	00	6.3	163.3
39	1972	5	27	00	11.0	140.2
40	1972	5	27	12	13.1	135.7
41	1972	5	28	00	15.2	131.1
42	1972	5	28	00	6.9	142.8
43	1972	5	28	12	15.4	127.6
44	1972	5	28	12	7.5	139.9
45	1972	5	29	00	15.6	124.1
46	1972	5	29	00	8.1	137.0
47	1972	6	06	00	7.8	136.1
48	1972	6	06	12	7.8	135.6
49	1972	6	07	00	7.8	135.0
50	1972	6	07	12	8.4	133.2
51	1972	6	08	00	9.0	131.5
52	1972	6	08	12	9.4	164.2
53	1972	6	09	00	9.0	162.8
54	1972	6	09	12	9.4	161.4
55	1972	6	09	12	13.0	169.5
56	1972	6	10	00	10.0	160.0
57	1972	6	10	00	13.2	169.0
58	1972	6	10	12	14.2	166.0
59	1972	6	11	00	15.2	163.0
60	1972	6	13	00	7.8	150.7
61	1972	6	13	00	14.3	156.9
62	1972	6	13	12	8.0	148.0
63	1972	6	13	12	13.4	153.1

TABLE A3 (cont'd)

<u>Position Number</u>	<u>Year</u>	<u>Month</u>	<u>Date</u>	<u>Time (GMT)</u>	<u>Latitude (Deg. North)</u>	<u>Longitude (Deg. East)</u>
64	1972	6	14	00	8.0	147.0
65	1972	6	14	00	12.5	149.3
66	1972	6	14	12	13.5	146.9
67	1972	6	15	00	14.4	144.5
68	1972	6	15	12	14.4	142.5
69	1972	6	16	00	14.5	140.5
70	1972	6	18	12	10.0	165.7
71	1972	6	18	12	9.9	164.0
72	1972	6	19	12	9.8	162.4
73	1972	6	19	00	9.3	147.3
74	1972	6	19	12	8.9	159.4
75	1972	6	19	12	10.0	146.1
76	1972	6	20	00	8.0	156.4
77	1972	6	20	00	10.7	144.9
78	1972	6	20	12	11.7	141.1
79	1972	6	30	00	5.0	139.6
80	1972	6	30	12	6.0	138.3
121	1972	8	02	12	11.5	141.0
122	1972	8	03	00	12.2	140.0
123	1972	8	03	12	11.7	138.8
124	1972	8	04	00	11.1	137.6
125	1972	8	10	00	15.7	130.9
126	1972	8	10	12	16.6	129.6
127	1972	8	11	00	17.5	128.3
128	1972	8	18	00	11.0	148.0
129	1972	8	18	00	10.3	134.0
130	1972	8	18	12	11.0	145.0
131	1972	8	18	12	10.7	132.2
132	1972	8	19	00	11.0	141.7
133	1972	8	19	00	11.0	130.4
134	1972	8	19	00	7.2	143.2
135	1972	8	19	12	8.1	140.3
136	1972	8	20	00	9.1	136.9
137	1972	8	21	00	7.8	156.0
138	1972	8	21	12	6.9	153.4
139	1972	8	22	00	6.0	150.8
140	1972	8	23	00	7.5	137.8
141	1972	8	23	12	7.2	136.9
142	1972	8	24	00	7.0	135.9
143	1972	8	24	12	7.9	135.0
144	1972	8	25	00	9.7	134.4
145	1972	8	27	00	13.0	145.8
146	1972	8	27	12	13.8	143.1
147	1972	8	28	00	14.5	140.4
148	1972	8	28	12	15.2	138.0
149	1972	8	29	00	15.8	135.5
150	1972	8	29	00	8.7	130.1
151	1972	8	29	12	10.0	127.8

TABLE A3 (cont'd)

<u>Position Number</u>	<u>Year</u>	<u>Month</u>	<u>Date</u>	<u>Time (GMT)</u>	<u>Latitude (Deg. North)</u>	<u>Longitude (Deg. East)</u>
152	1972	8	30	00	5.0	153.0
153	1972	8	30	00	11.3	125.4
154	1972	8	30	12	5.0	151.1
155	1972	8	31	00	5.0	149.1
156	1972	9	01	00	5.0	138.8
157	1972	9	01	12	5.0	137.4
158	1972	9	02	00	5.0	136.0
159	1972	9	05	00	13.9	145.2
160	1972	9	05	12	14.4	143.4
161	1972	9	06	00	14.9	141.6
162	1972	9	06	12	15.2	138.5
163	1972	9	07	00	15.5	135.4
164	1972	9	07	12	14.9	132.9
165	1972	9	08	00	9.0	153.6
166	1972	9	08	00	10.0	139.0
167	1972	9	08	12	9.0	150.6
168	1972	9	08	12	11.3	138.5
169	1972	9	09	00	8.9	147.6
170	1972	9	09	00	12.6	138.0
171	1972	9	09	12	8.7	145.8
172	1972	9	09	12	12.8	138.0
173	1972	9	10	00	8.5	143.9
174	1972	9	10	00	14.3	130.0
175	1972	9	10	00	13.1	138.0
176	1972	9	10	12	15.0	129.2
177	1972	9	10	12	13.2	137.5
178	1972	9	11	00	15.6	128.5
179	1972	9	15	00	13.4	154.5
180	1972	9	15	12	14.5	154.8
181	1972	9	16	00	15.5	155.0
182	1972	9	21	00	8.0	165.5
183	1972	9	21	12	7.6	163.8
184	1972	9	22	00	7.1	162.0
185	1972	9	22	12	7.3	160.3
186	1972	9	23	00	7.4	158.5
187	1972	9	24	00	10.0	168.0
188	1972	9	24	12	9.7	165.5
189	1972	9	25	00	9.5	163.0
190	1972	9	25	12	9.7	162.7
191	1972	9	26	00	10.0	162.5
192	1972	9	27	00	6.0	139.0
193	1972	9	27	12	6.5	136.9
194	1972	9	28	00	7.0	134.7
195	1972	9	29	00	7.0	134.0
196	1972	9	29	12	7.0	132.7
197	1972	9	30	00	7.0	131.3
248	1974	3	11	00	8.2	140.5
249	1974	3	11	12	8.2	141.2
250	1974	3	12	00	8.3	142.0

TABLE A3 (cont'd)

<u>Position Number</u>	<u>Year</u>	<u>Month</u>	<u>Date</u>	<u>Time (GMT)</u>	<u>Latitude (Deg. North)</u>	<u>Longitude (Deg. East)</u>
251	1974	3	12	12	8.4	143.7
284	1974	8	21	00	17.3	171.0
285	1974	8	21	12	17.3	168.8
286	1974	8	22	00	17.4	166.6
287	1974	8	22	12	18.1	164.0
288	1974	8	23	00	18.8	161.3
289	1974	9	07	00	14.0	166.9
290	1974	9	07	12	14.4	166.2
291	1974	9	08	00	14.8	165.5
292	1974	9	08	12	15.9	162.5
293	1974	9	09	00	17.0	159.5
294	1974	10	05	00	10.1	160.5
295	1974	10	05	12	10.1	155.8
296	1974	10	06	00	10.2	151.0
297	1974	10	06	12	10.4	147.0
298	1974	10	18	00	10.1	149.5
299	1974	10	18	12	10.7	146.4
300	1974	10	19	00	11.4	143.3
301	1974	10	21	00	9.2	151.4
302	1974	10	21	12	11.0	150.7
303	1974	10	22	00	12.7	150.0
304	1974	10	23	00	6.2	165.7
305	1974	10	23	12	7.1	163.8
306	1974	10	24	00	8.1	161.9
307	1974	10	28	00	5.1	156.4
308	1974	10	28	12	6.1	155.8
309	1974	10	29	00	7.1	155.2
310	1974	10	29	12	7.3	152.5
311	1974	10	30	00	7.5	150.0
312	1974	10	30	00	10.3	131.0
313	1974	10	31	00	2.3	146.0
314	1974	10	31	12	3.8	144.7
315	1974	11	01	00	5.2	143.3
316	1974	11	06	00	6.4	148.4
317	1974	11	06	12	5.7	145.2
318	1974	11	07	00	5.0	142.0
319	1974	11	12	00	13.0	124.5
320	1974	11	12	12	13.6	122.9
321	1974	11	13	00	14.3	121.2
322	1974	11	18	00	10.0	153.6
323	1974	11	18	12	10.1	150.8
324	1974	11	19	00	10.2	148.0
325	1974	11	19	12	9.8	146.8